COMPENSATING FOR TOPOGRAPHIC INFORMATION FROM SATELLITE IMAGERY IN MOUNTAIN ENVIRONMENTS

Roger Wheate

A Thesis Submitted for the Degree of PhD
at the
University of St Andrews

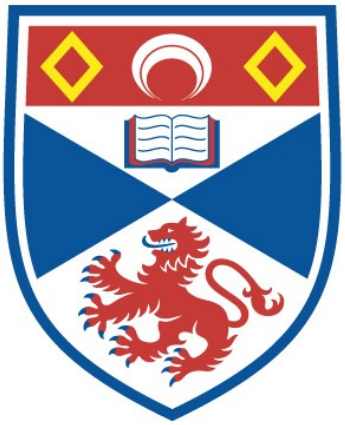

1997

COMPENSATING FOR TOPOGRAPHIC INFORMATION FROM SATELLITE IMAGERY IN MOUNTAIN ENVIRONMENTS

Roger Wheate

Thesis submitted in application for the degree of
Doctor of Philosophy

School of Geography and Geology, Faculty of Science
University of St. Andrews, Fife, Scotland

August 1996

ProQuest LLC.
789 East Eisenhower Parkway
P.O. Box 1346
Ann Arbor, MI 48106 – 1346

ABSTRACT

The use of satellite image data for vegetation mapping and forestry inventory in mountain environments has been greatly restricted by the scene digital values containing a mixture of variations which are due partly to surface cover (albedo) and partly to topography (illumination). Landsat Thematic Mapper (TM) data were selected for a portion of the Rocky Mountains in the Kananaskis Valley, Alberta, Canada and used to derive secondary data channels that sought to compensate for topographic information, by isolating the response due to surface cover.

Two multispectral techniques were used: band ratioing and principal component analysis. In both cases, the generated channels represented the difference between the three spectral groups of bands for TM data: visible, near and middle (shortwave) infra-red. Multi-channel ratio and component combinations were used in an unsupervised clustering procedure that defined homogeneous ground areas. When the original pixel values were replaced by the average brightness for their respective clusters, the resulting image channels represented each of the multispectral bands as if the surface were flat.

Selective principal components proved more successful than band ratioing, being less susceptible to noise and allowing input from more than two bands each. These component channels created a final classification which had a higher overall accuracy than those for studies in adjacent mountain environments using supervised classification and was comparable to those which also incorporated topographic data.

The study was successful in identifying a different approach to topographic correction without having to acquire digital elevation models and considerable ground knowledge. This technique has much potential for expediting forest cover inventory and vegetation mapping in mountain environments and represents a new and promising application for principal component analysis.

DECLARATIONS

(i) I, Roger D. Wheate, hereby certify that this thesis, which is approximately 30,000 words in length, has been written by me, that it is the record of work carried out by me and that it has not been submitted in any previous application for a higher degree.

date: August 7th 1996 signature of candidate:

(ii) I was admitted as a research student in October 1987 and as a candidate for the degree of Ph.D in October 1987; the higher study for which this is a record was carried out in the University of St. Andrews between 1987 and 1996.

date: August 7th 1996 signature of candidate:

(iii) I hereby certify that the candidate has fulfilled the conditions of the Resolution and Regulations appropriate for the degree of Ph. D in the University of St. Andrews and that the candidate is qualified to submit this thesis in application for that degree.

date: August 7th 1996 signature of supervisor:

UNRESTRICTED COPYRIGHT

In submitting this thesis to the University of St. Andrews I understand that I am giving permission for it to be made available for use in accordance with the regulations of the University Library for the time being in force, subject to any copyright vested in the work not being affected thereby. I also understand that the title and abstract will be published, and that a copy of the work may be made and supplied to any bona fide library or research worker.

date: August 7th 1996 signature of candidate:

ACKNOWLEDGEMENTS

My sincere thanks to my supervisor Dr. John Soulsby for his help and advice, his supreme patience in awaiting this document and for giving me the opportunity to spend time in and achieve another degree from St. Andrews University, which I left with great reluctance 20 years ago.

I am very grateful to my local supervisor in Calgary, Dr. Grant Ross, a son of Scotland, for his support and editorial improvements and not least for travelling from Canada for the final stage. I heartily thank Dr. Charles Warren and Dr. Roy Brown for agreeing to serve as my committee at short notice and for their helpful critique and suggestions.

I acknowledge the important roles played by the relevant units at the Universities of Calgary, Northern British Columbia and St. Andrews in providing the facilities necessary for this work. The assistance provided by Richard Batchelor, Colin Cameron and Graham Sandeman during the final lap in St. Andrews was much appreciated.

Some acknowledgement must be made to the tectonic forces that have created our mountain regions, providing both the necessary environments and inspiration for this work and the finest experience that nature has to offer. Many thanks to those who have enjoyed the mountains with me and urged me to finish the thesis: Nancy and Samantha who have suffered most over these years in lost weekends, Dave and Jennie, Ed and Carol, Brian and Anne, and my sister Linda for travel assistance from Canada.

I am indebted to several colleagues who have given support or encouraged me to finish and also provided inspirational role models: Michael Coulson, Steve Herrero, Dave Irvine-Halliday, Nigel Waters, Grant Ross and Joyce Rowden at Calgary, Kevin Hall and Fred Gilbert in Prince George, John Soulsby and Ron Morrison in St. Andrews and Peter Browne in Australia.

Finally to the two people who have enabled me to get all three degrees, my mother Betty Wheate from whom I have inherited a passion for mountains and the outdoors, and my father Donald Wheate, who made everything possible, but was not able to wait for my completion, passing on from this life one month before. If I was more like my father instead of my father's son, I might have finished in time for him to see it.

TABLE OF CONTENTS

Chapter 3. Study area and methodology

Chapter 4. Data processing and analysis I: generation of components and ratios

Chapter 5. Data processing and analysis II: extraction of topography and albedo

List of Figures

List of tables

CHAPTER 1

INTRODUCTION

1.1 Research objectives

The main objective of this thesis is to demonstrate and improve the separability of reflectance due to albedo and topographic variations in remotely sensed data, using multispectral image processing techniques in an area of mountainous terrain. Two techniques which share the ability to distinguish between information that is common across multiple band wavelengths and that is specific to certain wavelengths are principal components analysis and spectral band ratioing. As such, the following is proposed:

1. identify and interpret useful and meaningful components and image ratios, simple and complex, that are most representative of land cover and topographic features;

2. generate new channels from these components and ratios, which best separate the inputs of topography and land cover for mapping and resource information purposes;

3. check these resulting images with existing topographic and vegetation maps, digital elevation data and ground knowledge;

4. determine whether these results are scene-dependent or independent: whether they be applied to other mountain environments;

5. examine how the effectiveness of this approach compares with the procedure of augmenting satellite data sets with topographic variables from a digital elevation model for greater classification accuracy.

1.2 Background

Mapping from satellite data has generally become a cost-effective means of obtaining and updating surface cover information. Boresjo (1989) gives a detailed account of the capabilities of satellite imagery for medium-scale vegetation mapping, while there are numerous examples of updating and monitoring forest change, for example, Fiorella and Ripple (1983) and Vogelmann and Rock (1986). Automated classification procedures using digital imagery in mountainous areas are however greatly complicated by the mixture of illumination, albedo and surface orientation influencing the value of the digital number (DN) recorded for each picture element (pixel) of an image scene. As a result, despite the increasing use and availability of remote sensing, mapping applications in mountainous areas have been limited because remotely sensed data have not been fully effective in the discrimination of land-cover types (Colby, 1991; Leprieur *et al.*, 1988).

Specifically, reflectance contributed by topographic variation (brightness), is mixed with reflectance resulting from surface cover (albedo). While the former is often retrievable from topographic maps, the latter is less easily acquired but is essential for forestry resource management and planning.

The effects of topography significantly reduce the accuracy of land cover classifications in mountainous areas as a result of the differential illumination of surfaces due to slope angle and aspect variations. Topographic effects can be minimised with a high sun angle: near-solstice conditions and scene capture close to the sun's zenithal position at noon.

These conditions do not exist however with Landsat satellites which scan the surface more than two hours before noon; the topographic effect is compounded in temperate latitudes by a relatively low solar elevation, increasing polewards and for imagery dates away from the summer solstice. Conversely this can be used to advantage by selecting non-summer imagery to enhance low relief features with a lower solar elevation (Eyton, 1989).

Digital image classification which fails to take into account the effect of topography produces commission errors in which differing land cover classes with similar topographic positions are grouped together and omission classes where pixels from similar land cover types are classified differently (Naugle and Lashlee, 1992). The effect of topography is to produce a greater apparent degree of heterogeneity within land cover types than there is between cover types. This has long been one of the main problems in forest discrimination and inventory. Multitemporal data sets have failed to overcome the spectral limitations of remotely sensed data as the lower sun angles in non-summer seasons obscure large areas in shadow (Cibula and Nyquist, 1987).

Extreme results may be such that in a supervised classification, north facing shadowed slopes can be classified with water or wetlands, while on illuminated south-facing slopes light forest can be confused with meadow or even bare ground. In an unsupervised classification, the various slope facets in mountainous terrain produce an excessive number of spectral clusters compared to the number of informational classes and an overly partitioned image (Civco, 1989). Potential solutions to this problem have utilised several different approaches:

1. Correcting for the 'topographic effect': with knowledge of the topography, pixel values are adjusted to account for the differential illumination resulting from slope aspect and gradient. The correction however has so far proved to be more complex than can be provided by any single formula.

2. Incorporating ancillary information: particularly topographic variables such as elevation, slope and aspect, which then become additional channels or parameters in a classification procedure. This is known as the 'logical channel method' or multi-dimensional image classification (Avery and Berlin, 1992).

3. Normalisation, band ratioing and other indices: based on the idea that all band wavelengths tend to be equally affected by relief, and hence topography can be isolated or reduced, although the resulting images may be difficult to interpret.

4. Post classification editing: this is based on the observation that a single class of objects can rarely be represented by a single spectral class (Hutchinson, 1982). Classes can be merged into groups which represent object classes, or divided using ancillary data in a process equivalent to an overlay in Geographic Information Systems. This approach has however, proved time consuming and tedious (Naugle and Lashlee, 1992).

The first two solutions require that a digital elevation model (DEM) of appropriate accuracy is available for the area of study and that there is considerable surface-cover information through traditional data sources, such as ground surveys and maps. These techniques have yielded improvement in classification in the order of 5-15%, but after almost two

decades of application, the procedures remain more in the hands of the researcher than being standard among those responsible for managing the inventory of natural resources.

Although DEMs are becoming increasingly available at a variety of resolutions, they are by no means universally present nor affordable. Furthermore the results of their use have met with mixed success, partly because the topographic details of the elevation model may not match the level of detail in the remotely sensed image (Carter, 1992). Introducing an externally produced DEM to account for topography in satellite imagery raises the question of the complete separability of surface albedo and topography as the latter is usually a major contributory factor in determining surface cover, as well as difficulties in registering the two sets of data on mountainous terrain (Erner, 1987).

The relative loadings of the topographic and surface cover contributions to the image pixel DNs are clearly related to the relative complexity of the two elements. In a non-mountainous environment, Karaska *et al.* (1986) used multiple regression to show that the percentage cover of trees and shrubs had the most significant impact on spectral response of eleven environmental variables including terrain factors. In contrast, Bian and Walsh (1993) found that in a mountainous area, the main controlling factors were slope angle and aspect, over cover type, crown size and density.

If topographic variation is minimal, in a flat to gently undulating landscape, regions delineated by surface cover are confused mainly by non-homogeneity, noise and atmospheric variations. Conversely with a homogeneous surface cover, in the absence of albedo and colour variation,

image brightness is mainly a function of topography. In such circumstances it becomes feasible to produce elevations from spectral data as demonstrated by Lodwick and Paine (1985) who used principal components analysis on the uniform surface of an Arctic island ice-cap. Attempts to similarly isolate albedo and topography in the more abundant regions of heterogeneous surface cover have met with mixed success. Local relative relief has been determined directly from Landsat image data by Eliason *et al.* (1981), Wang *et al.* (1984) and Haralick *et al.* (1985) and using a more general 'shape from shading' approach by Carlatto (1986) and Thomas *et al.* (1991). It has long been possible to derive 'synthetic stereo' elevation models using a pair of overlapping images from adjacent tracks (Batson *et al.* , 1976), or if the sensor has a variable viewing angle.

Simple band ratioing has been shown to reduce the topographic effect by up to 83% (Holben and Justice, 1981) but loses the topographic information implicit in the image and further interpretability. Both band ratioing and principal components analysis (PCA) can be effective in separating the combined effects of topography and surface cover on the basis that the contribution from topographic variation is consistent across different band wavelengths while the contribution from surface cover is not. Hence the potential exists to extract topographic information from the satellite image itself and in so doing successfully identify the two major components of the surface reflectance.

Satellite images and aerial photographs display and store a wealth of spatial information about the earth's surface. These comprise many elements which a skilled photo-interpreter can extract and identify, utilising learned and intuitive abilities, one of which is interpreting the

terrain within the area under study, in order to assist in classification processes. Perhaps the most general criticism of digital image processing compared to analogue image interpretation has been that while the latter utilises a range of visual attributes, such as tone, shape, size, site context, shadow, texture and pattern, digital procedures generally use only tone, albeit multiple representations of tone pertaining to the band wavelengths of the sensor data, e.g. Landsat Multi-Spectral Scanner (4), SPOT HRV (3), Landsat Thematic Mapper (7). While advanced algorithms have been written to utilise some of the additional variables, such as texture and context and incorporate elements of expert systems, most procedures still rely primarily on the digital representation of tone, as expressed in band digital numbers.

Image processing of multispectral data offers several specific advantages: understanding the relationship between the spectral bands, compressing the data contained within the bands and extracting physical and scene characteristics (Crist and Cicone, 1984). Band ratioing and PCA offer two procedures that are capable of extracting new information by their multispectral nature. They are further similar in being able to reduce or compress multidimensional space by about a 2:1 scale. The increased number of channels available on Landsat 4 and 5 in the Thematic Mapper and in airborne sensor systems calls for continuing research into their renewed potential (Townshend *et al.*, 1983; Huber and Casler, 1990).

CHAPTER 2

LITERATURE REVIEW

2.1 The topographic effect

The topographic effect has been defined as the variation in radiance from inclined surfaces compared to the radiance from a horizontal surface as a function of the orientation of the surfaces relative to the light source and sensor position (Holben and Justice, 1981). More simply, it is the variation in spectral reflectance that is unrelated to the surface cover and results from differential illumination due to topography (Colwell, 1983). It can be generally given as a function of the angle between the surface and the sun incidence (after Wang *et al.*, 1984):

$$B_{(x,y)} = R_{(x,y)} * (\cos e) + D + H \qquad (1)$$

where:

B (x,y) is the brightness value recorded at pixel x,y

R is the reflectance or radiance of the surface cover at pixel x,y

(cos e) is the angle between the sun incidence and the surface (at x,y)

D is diffuse light and H is haze

For shadowed pixels the digital number is reduced to the additive elements, diffuse light and haze, since there is no direct reflectance (R).

In satellite images of rugged terrain, this effect is manifested by the visual impression of relief, causing a wide range of radiance values for an otherwise homogeneous surface cover type. The effect is most extreme with low solar elevations, high relief variations and slopes oriented

directly towards and away from the solar energy source. In areas of gently undulating forested terrain (slopes less than 15 degrees), the relationship between sensor response and topographic parameters has been found to be weak (Hall-Konyves, 1987), but even in a gently rolling agricultural setting, the technique of spectral band ratioing has been used successfully in minimising topographic effects because terrain-induced changes in red irradiance were accompanied by proportional changes in the near infrared (Pinter *et al.*, 1987).

Attempts to reduce the topographic effect have involved preprocessing the spectral data, by removing some of the signal related to topographic variation. Knowledge of the terrain, namely slope and aspect can be used with the sun zenith and angle to determine sun-surface-sensor geometry. Correction in its simplest form involves dividing the reflectance or radiance values for each pixel by the cosine of the corresponding incidence angle for that pixel, which is the deviation from normal of the angle of the solar illumination striking the surface.

$$R_n = B / (\cos i) \qquad (2)$$

R_n is the normalised radiance, B is the measured brightness (radiance) and i is the angle of incidence. This modification assumes a Lambertian model of reflectance which corrects only for differences in illumination caused by surface orientation. That is, regardless of viewing angle, reflected radiance is proportional to the cosine of angle of incidence. This assumption has generally proved unsuccessful as it leads to overcorrection of the topographic effect and further increases the variance in spectral signatures associated with a cover type. Proposed models are based on the assumption that vegetation remains uniform regardless of

slope and aspect and therefore they fail in mountainous areas, because there is a strong relationship between vegetation cover and terrain factors (Barry and Wie, 1974; Thomson and Jones, 1990). The correction is considered inappropriate for forest vegetation with the exception of high solar elevations (Ekstrand, 1996).

The failure of Lambertian models has also been attributed to the variation in the bidirectional-reflection distribution function (BRDF) of the surface, which defines the magnitude of reflected flux for all elevations and azimuths and may be related to surface texture (Colwell, 1983). Such behaviour is best described by a non-Lambertian model which corrects for variations in the orientation of the surface relative to the sun and sensor (Smith *et al.*, 1980). Non-Lambertian models incorporate an empirical constant, Minnaert's k, which indicates the extent to which the surface exhibits Lambertian behaviour (Jones *et al.*, 1988). Minnaert (1941) actually developed this as an index of surface roughness for lunar applications. The equation is given as:

$$\log (B * \cos e) = \log R_n + k * \log (\cos i * \cos e) \qquad (3)$$

where e is 'exitance' which is the angle between the normal to the surface and the sensor; this is the same as the angle of slope for nadir pointing (vertical) sensors such as Landsat. B, R_n, i are the same as in equations (1) and (2).

The Lambertian model is actually a special case of this reflectance model when k = 1. However different surface cover types are shown to be best described by varying values of k and hence extensive prior knowledge of the scene area would be required for it to be correctly modelled. In addition, the value of k is wavelength specific, so for a given cover type

using TM data, each class will have six to seven values of k. Hence in order to apply the best correction for each different surface type in an inventory mapping scenario, one must already know where these occur, thereby making redundant the need to map them.

The complications of applying corrections to remote sensing data in mountain environments is illustrated by the volume of publications on atmospheric effects in mountainous terrain (Horn, 1981; Hugli and Frei, 1983; Sjoberg and Horn, 1983; Woodham, 1989; Woodham and Gray, 1987) and possible correction strategies (Itten and Meyer, 1993; Kimes and Kirchner, 1981; Meyer, 1993; Teillet *et al.*, 1982).

2.2 Incorporating topographic variables as ancillary information

Digital image processing has generally relied on one image attribute alone, that is gray level, albeit n-dimensional, where n equals the number of channels or bands available. The other traditional air photo interpretation elements such as size, shape, pattern and association are not readily available from digital data, nor can an automated procedure utlise cues like proximity or context. Using ancillary data, such as digitised map themes is one way of replacing this 'lost' information.

Incorporating topographic data as additional 'logical' channels has become a conventional method for using knowledge of the topographic surface to enhance surface cover classifications for almost two decades, (Strahler *et al.*, 1978). The most commonly used topographic elements are elevation, slope and aspect, although secondary derivatives such as slope convexity, concavity and relative relief have also been used. In the time since Hutchinson (1982) commented that the hoped-for improvements

have generally not materialized, numerous studies have nevertheless demonstrated considerably improved vegetation classification with the inclusion of topographic channels, for example Frank (1988), Moulton (1989) and Niemann (1991).

This approach however is not without its drawbacks:

1. New samples are required to describe the association (covariance) with other observations (bands) and ensure a full range of surface cover-topographic site sampling. In other words considerable *a priori* knowledge of the area is required.

2. Extra cost in data acquisition, data storage and processing is incurred. Data storage has become cheaper and more accessible at an ever-increasing rate, but this is associated with challenges in data management and processing particularly with databases for large geographic areas.

3. Additional channels place extra constraints on the classification algorithm which may result in a higher percentage correct among those pixels that are classified but also a lower percentage overall classified. This occurs because pixels must satisfy more criteria before being assigned to a class, as the number of channels increase.

4. Digital terrain data, although becoming more available and in some cases at cheaper cost than previously, may not be accessible for a desired area at reasonable cost, at a suitable scale or acceptable data quality.

5. Digital elevation data can be derived from cartographic or photogrammetric sources but co-registration with satellite data can induce potential problems of registration modelling, compatibility and

artificial landscape artifacts. The quality of DEM accuracy resulting from the interpolation of a continuous grid from either a discrete set of points or contour lines remains an ongoing research question.

2.3 Spectral band ratioing

A. THE THEORY OF BAND RATIOING

Image arithmetic consists of combining the digital numbers for any band with those of another or using the standard mathematical operators to create a more complex equation. The basic operators are addition, subtraction, multiplication and division. New data channels are created by arithmetically combining the pixel values for two or more bands.

Bands may be added to yield averages or reduce noise or subtracted to create an image that represents change between the two original bands. Multiplication is used most often with a binary mask to separate major classes such as land and water and might be considered as much a 'GIS' operation. It is division however that is by far the most common arithmetic combination in image manipulation to create a band ratio image, by dividing the radiance value in one channel by the corresponding value in a second channel.

The resulting digital number can either be retained as a real decimal number or more usually 'automatically' scaled by a multiplicative factor to fit an 8 bit data range (0-255), which takes up substantially less storage space. In theory, ratio values could range from zero to infinity (if either the numerator or denominator is equal to zero), but because bands tend to be at least moderately correlated, in practice most values lie between 0.25 and 4.0 (Siegal and Gillespie, 1980). These values which

are initially real rather than integer numbers, can then be scaled to fit the available range of display values.

Ratios are useful for several reasons (Rowan *et al.*, 1977):

1. The differences between slopes of reflectance spectra between two bands can be displayed in a single image;

2. Brightness variations caused by topography can be reduced or removed and the responses from like materials normalised;

3. The width of the distribution of image brightness values is reduced so that a greater contrast stretch can be applied.

Ratioing in general may perform one or both of two functions:
a. enhance certain aspects of the ground surface and
b. remove or reduce undesirable effects on recorded radiances, such as the effect of variable illumination resulting from topography (Mather, 1987).

The general principle is that the act of ratioing will cancel out what is common between the numerator and denominator bands, while enhancing what is unique to them. It is usually assumed that the depiction of topography is fairly consistent across bands; hence band ratios will minimize the effect of slope and aspect and highlight albedo differences in reflectivity between bands which are diagnostic of various surficial materials (Colwell, 1983). Figure 2.1 illustrates this principle in an environment where illumination differences are stronger than variations due to surface cover (albedo). If illumination changes across a scene but colour (surface cover) does not, ratio images will stay constant (Siegal and Gillespie, 1980).

Figure 2.1: Using band ratios to remove the effects of topography.

In this example, a topographic feature contains three different surface cover types on two slopes, one illuminated, the other in shadow. The raw reflectances have more contrast due to illumination than albedo. Ratioing isolates the three classes, producing three distinct values. However it should be noted that another example could produce identical ratio values for two quite different surface cover types; for example if band 1= 80 and band 2 = 100, the ratio value is the same as that for the 'treed class'. Figure adapted from Campbell (1987).

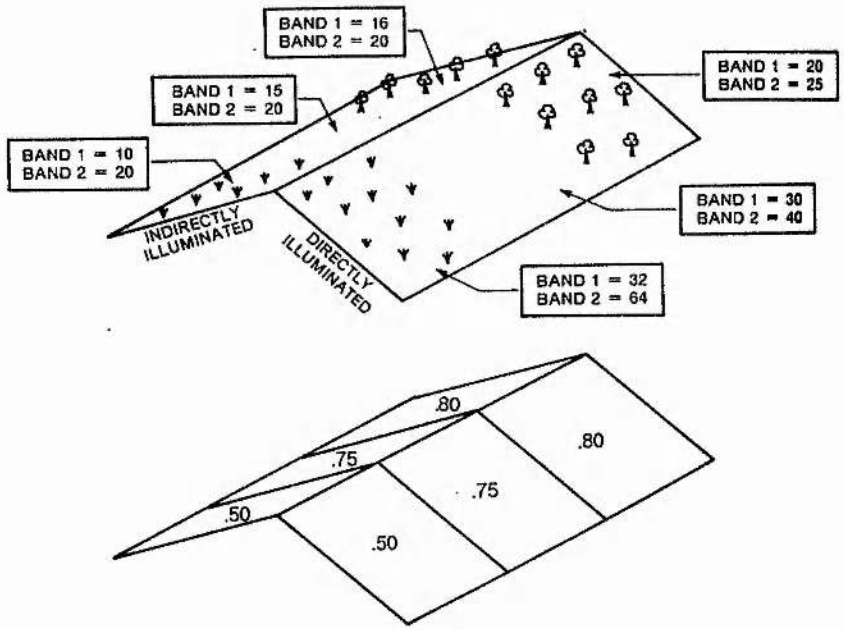

Thus, ratios while 'suppressing' topographic effects can also enhance colour differences. For this reason, ratios have been used extensively to enhance minor differences in vegetation and rock discrimination by reducing the topographic effect , which masks these subtler variations (e.g. Rowan *et al.*, 1977, Walsh *et al.*, 1990); it has also been used specifically to investigate the reduction of the topographic effect (Holben and Justice, 1981). However ratioing may also enhance noise or unmeaningful variations due mostly to sensor miscalibration, since noise is not correlated between bands.

The use of band ratios requires a certain rationale to prevent an overwhelming number of ratios and potential colour composites. The number (p) of possible ratio combinations for a multispectral sensor with n bands is:

$$p = n (n-1)$$ (Avery and Berlin, 1992)

Hence for Landsat MSS, n = 12 (p=4) and for Landsat TM, n = 30 (p=6, disregarding the lower resolution thermal channel), although in each case half of the ratios are reciprocals of others e.g. 4/3 and 3/4 etc.. The potentially more useful ratio combinations can be identified by following these guidelines (Walsh *et al.*, 1990):

a. There should be a low correlation between the bands: high correlation results in little information being contained in a ratio;

b. The researcher should consult with the published literature documenting specific channel combinations;

c. The hypothesised relationships or fields of application should be first established to determine the usefulness of derived ratio channels.

Lower between-band correlation would imply that the most meaningful ratios would be found for MSS data between one of the visible bands (4 or 5) and one of the infrared bands (6 or 7). For TM data, more useful ratios would be created by drawing one band from two of the three different band groupings in the visible (1,2,3), near infrared (4) and middle infrared (5 and 7). However for both sensors, there has also been found some utility in geological applications for ratios between two bands in the same portion of the electromagnetic spectrum, e.g. 5/4 for MSS and

3/1 for TM. Expressed another way, ratios using bands from different broad areas of the spectrum help distinguish between major groups, such as water, rock, bare soils and coniferous or deciduous vegetation while ratios using bands within adjacent wavelengths might help distinguish within major groupings, such as soil or geologic types.

Band ratioing was used widely with MSS data following the first launch of Landsat in 1972, but curiously has been less used with TM data despite the potential for many more combinations. This may be a result of a far greater range of image processing options with more sophisticated software that has been developed over the last 25 years.

B. RATIO COLOUR COMPOSITES

A three channel colour composite can be formed from any combination of any original bands or derived channels for the purpose of visual examination and interpretation. Using original bands alone, there are 4 possible combinations with MSS data and 20 for TM, excluding band 6. When ratio combinations are considered but excluding reciprocal ratios, there are 20 possible permutations for the 6 MSS ratios and 455 (!) for the 15 nonthermal TM ratio images (Avery and Berlin, 1992). These numbers can be calculated using the equation :

$$p = n\,(n-1)\,(n-2) / 6$$

where p is the number of permutations and n is the number of channels.

Gillespie *et al.* (1986, 1987) demonstrated a number of procedures including band (channel) ratios to enhance colour displays for interpretation and analysis.

C. BAND RATIOS AND RADIOMETRIC CORRECTION

The radiance recorded by the sensor consists of a multiplicative term and an additive term. The multiplicative term is direct radiance attenuated by quantifiable environmental factors, dependent on target reflectance and sun-sensor-ground geometry and as such is quantitive information (Holben and Justice, 1981). The topographic effect as a function of surface incidence of sunlight is contained within the multiplicative term and can thus be reduced by ratioing assuming that the multiplicative effect is the same for all wavelengths.

Before ratioing can be performed, it first requires preprocessing to remove 'additive' terms that results from two sources: diffuse light scattered into the path between the target and sensor by the atmosphere and diffuse light scattered into the sensor by the environment. These additive effects can often be ignored for imagery captured from low altitude aircraft, but should be removed for high altitude aircraft and satellite data (Holben and Justice, 1981). If they are not dealt with, additive terms affect the ratios derived: surface features with similar reflectance response will retain higher values on brightly illuminated surfaces, where the ratio has the longer band wavelength as the numerator (Kowalik *et al.*, 1983).

The simplest method of removing the additive term is known as 'dark object subtraction'. This involves subtracting the smallest radiance value in each spectral channel from the radiance value for each pixel. Ratioing cannot be effective on shaded surfaces as they are illuminated only by scattered light, but ratioing can enable discrimination between shaded

surfaces and other dark surfaces such as water, which may be equally dark on raw band images. More complicated techniques have been developed, such as the utilisation of linear regression between bands and variance-covariance matrices, but in general these produce very similar results to the simpler method (Crippen, 1988; Kowalik *et al.*, 1983; Switzer *et al.*,1981).

D. BAND RATIOING IN VEGETATION STUDIES

In vegetation studies, the most commonly used ratio has been one that compares an infrared and a red band. Such a ratio is strongly related to attributes of vegetation cover, particularly biomass production and green leaf area index (LAI). This results from the contrast between high reflectance by healthy vegetation in the infrared wavelengths and high absorption in the red wavelengths. By inference, vegetation interpretation is enhanced by the reduction of the topographic effect, as the relative difference between the two bands, rather than the absolute radiance values, are recorded in the ratio, which using MSS bands would be 7/5, and with TM data 4/3. Attempts to use these ratios may be thwarted with high sun altitude and maximum growth conditions as these combine to produce low variance in the red image, creating an almost constant denominator (Justice *et al.*, 1981).

The greater range of TM bands enables vegetation studies using any ratio comparing an infrared band and a visible band, such as 5/2, 7/1; vegetation discrimination between coniferous and deciduous types is always superior when an infra-red band is included because the difference in leaf morphology causes significant reflection differences that are not apparent in the visible wavelengths (Karaska *et al.*, 1986).

Thomson and Jones (1990) have alternatively suggested the 'green minus red' calculation (TM2-TM3) as a quantitative measure related to the physiological activity of a vegetated surface. Near infrared minus red (TM4 - TM3) is used as a measure of 'greenness' (Pinter *et al.*, 1987) or more commonly is standardised as the Normalised Difference Vegetation Index (NDVI) given as (TM4 - TM3) / (TM4 + TM3) to produce a measure of biomass. Any ratio difference can be similarly normalised, such as between TM bands 2 and 5: (2-5) / (2+5) is used in snow analysis and known as the 'NDSI', where S is snow. Wolter *et al.* (1995) equally describe the Normalised Difference Green Index (NDGI) as (4-2) / (4+2).

E. BAND RATIOING IN GEOLOGIC INTERPRETATION

Whereas vegetation studies rely mostly on ratios comparing an infra-red and a visible band, geologic applications of band ratioing more commonly utilise ratios of bands that are within the same spectral region, such as 7/6 and 5/4 with MSS data, 3/2 and 7/5 with TM data.

Rowan *et al.* (1977) used the MSS ratios 5/4, 6/5, 7/6 to create a color composite for mineral enhancement. Hydrothermally altered rocks containing increased abundance of certain minerals were undetectable in any individual bands or colour composites. These MSS ratios greatly enhanced the mineral occurrences, by minimizing the influence of topography and overall albedo, but partly because the MSS spectral bands were not the best for discriminating between altered and unaltered rocks. The inclusion of longer wavelengths, particularly band 7 in the Thematic Mapper of Landsat 4 and Landsat 5 were specifically designed to alleviate such sensor shortcomings. With TM data, the ratios 3/1, 5/4 and 5/7 have been recommended for geologic interpretation by Crippen *et al.* (1988).

Kowalik *et al.* (1983) used all six ratios with MSS data (5/4, 6/4, 6/5, 7/4, 7/5, 7/6) to enhance the classification of limonite quartz monzonite, further increasing classification accuracies from 87 to 97% by removing additive radiance terms. Further examples of the use of band ratios in geological applications are provided by Knepper and Rames (1985), Qari (1991) and Siegal and Gillespie (1980).

F. BAND RATIOING TO REMOVE TOPOGRAPHY

Holben and Justice (1981) used band ratioing to reduce the topographic effect by up to 83% in a controlled study using a ground-based radiometer recording in the red and infrared wavelengths over a variety of slope and aspect conditions. The greatest reduction occurred where the effect was most pronounced, i.e. on slopes parallel to the principal plane and least on slopes perpendicular to the principal plane. They concluded that satellite data results would be less successful due to greater additive factors, such as atmospheric haze as well as sensor calibration. Overall, removing the topographic effect is a complex procedure dependent on a number of interrelated factors: sun angle, distribution of slope and aspect, surface reflectance and sensor characteristics.

Eliason *et al.* (1981) attempted to separate topographic and spectral albedo information using MSS data for a Colorado River canyon scene and also a Viking Orbiter image of Mars. In the technique they developed, they first performed a clustering analysis using three ratio images: 6/5 which best distinguished the major types- rocks, vegetation, water; 5/4 to separate within major soil and rock types and 7/6 for classifying vegetation types. Storage and processing restrictions at that

time forced them to modify the procedure such that an intermediate variable was generated that took on the value of 7/6 in vegetated areas and 5/4 in non-vegetated areas. The original pixel values were then replaced by the average value for the homogeneous cluster in the three-dimensional space defined by the ratios. The result was an estimate of average scene brightness if there were no topographic effect; the pixel values for this channel were then divided into the original brightness values to create an image with albedo or colour eliminated, resembling a shaded relief map of the scene.

The image of Mars was solved more simply given the apparent lack of vegetation, but the authors recognised difficulties in separating the two components in scenes where topographic effects are large. They proceeded to generate relative height information and thence synthetic stereoscopic display from slope values. They concluded that their technique as a 'closed system' employing only multispectral data, could be applied to any data set.

G. DIRECTED BAND RATIOING

Band ratioing has been used to reduce the topographic effect in order to enhance surface reflectance information. However topographic expressions can be a valuable indicator of geological attributes. In general in colour composite images, band correlated information (particularly topography) is expressed as brightness and band variant information as colour. Crippen *et al.* (1988) elaborated a technique they refer to as directed band ratioing, which retains topography in a controlled manner while distinguishing its effect on the scene from surface reflectance which is portrayed by hue, itself almost perceptually independent of intensity (brightness).

This technique is designed primarily to enable more effective image display for interpretation but at the same time to enhance understanding of the relationship between the two image components: topographic brightness and surface cover reflectance. It consists of four preliminary stages to produce (directed) ratio images, determined by examining the bispectral data distributions between the two bands used in each ratio. The final stage involves adding a constant to each band value, the size of which determines the degree of topographic expression. In other words, the additive value that is usually carefully calculated and subtracted in order to enable the removal of topography, is here deliberately manipulated to enhance topography.

2.4 Principal Components Analysis (PCA)

Principal components analysis (PCA) was first designed in the 1930's, received wider use in the 1960's during the 'quantitative revolution' in the natural and social sciences, but it required more recent computing capabilities to enjoy its full exploitation (Mackiewicz and Ratajczak, 1993). It has also been called 'Hotelling', after its first inventor, and the Karhumen-Loeve transform and is described in detail for applications in geography and geology respectively by Gould (1967) and Davis (1986).

A. THE THEORY OF PRINCIPAL COMPONENTS

Where band ratioing requires a careful choice of band combinations to emphasize specific spectral characteristics, the use of principal components analysis (PCA) requires no such *a priori* information. PCA is a mathematical transformation of multi-band data, which rotates the

axes of a multi-dimensional image space in the direction of maximum data variance (PCI Manual, 5.1). A new multichannel data set is created, with its origin at the mean of the original data distribution and new channels orthogonal to each other (figure 2.2). The relative orientation of the observations is maintained, only the coordinate system has changed.

Figure 2.2 PCA Transformation shown for two dimensions.

The figure on the left depicts raw data. On the right, the lines PC1 and PC2 which are orthogonal represent the new axes, with more variance along PC1 than PC2. Subsequent dimensions can be calculated but cannot be illustrated graphically. Figure adapted from PCI User's Manual (1995).

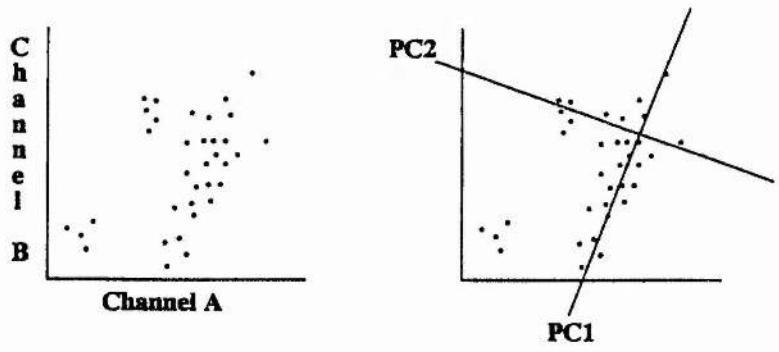

In contrast to the original contributing bands, which are usually highly correlated, the resulting components are not correlated with each other, being orthogonally offset in n-dimensional space. The first component accounts for the greatest scene variance, with each succeeding component accounting for progressively less variance. Weightings, expressed in the form of eigenvectors indicate how the original bands contribute to the principal components.

Principal components analysis has been used for the following purposes:

1. PCA can be used initially to first establish and then reduce the dimensionality of multispectral data, which are usually highly correlated between adjacent bands in the electro-magnetic spectrum. Data reduction is useful both in computer storage and data processing limitations, given a relatively high degree of data redundancy, since the ground features being sensed are common to all wavelengths. The intrinsic dimensionality of both 4-band MSS and 3-band SPOT (MLA) data can be reduced to two significant components, which are essentially the contributions from visible and infrared bands (Crist and Ciccone, 1984), while Thematic Mapper data usually yields three major components from the six reflective bands (Horler and Ahearn, 1986), or four components if the thermal channel is included.

2. PCA can reduce datasets to the three most important components for RGB displays and technically this can display more information than using any three original bands. The information not available (for display) in lower components is usually less than that lost from the original channels. A three band display utilising principal components will exhibit greater colour than one using original TM bands, which are correlated to some degree. However, although such color composites may hold more information and colour contrast than composites using original bands, they are less easy to interpret. Principal component images should be superior to the individual bands since noise is eliminated in the higher components as it is unlikely to be correlated between bands (Chavez and Kwarteng, 1989).

3. Surface change detection studies utilise PCA since the first component will identify the common elements in a time series analysis (what has not changed), while lesser components show the difference between sets of image data. These changes may be either cyclical (seasonal), directional (particularly in urban studies) or irregular (such as forest health and clearance). Respective examples include Ingebritsen and Lyon (1985), Fung and LeDrew (1987), and Collins and Woodcock (1996). In change detection studies, it may be desirable to use standardised principal components if the individual band variances are significantly different, causing eigenvector loadings to be biased by bands with large variances (Fung and LeDrew, 1987).

4. A fourth reason for utilising PCA procedures lies in deriving new channels that may provide different information about the sensed surface, made visible by separation from the more dominant signals recorded in higher component channels. This comprises the chief interest in this technique in this thesis. Several studies have shown that a principal component transformation creates one component that isolates vegetation details better than any individual TM band (Walsh *et al.*, 1990; Wheate and Franklin, 1991). The PCA transform can also allow the operator to define training bitmaps to enhance specific selected classes. Sidjak and Wheate (1996) used this aspect of PCA to display details on glacier surfaces which were not visible on TM bands where they were overwhelmed by saturated reflection and topographic variation.

B. STANDARDISED PRINCIPAL COMPONENTS

In remote sensing, it is most common to calculate principal components from the variance-covariance matrix generating 'unstandardised

components'. The components can be standardised by dividing them by the band standard deviations, thereby reducing the covariance matrix to the correlation matrix and the variables (bands) to having equal weighting. Retaining the unequal variance of the bands can normally be justified as an indication of their relative amount of useful signal and impact on the scene. In this case the first component usually has all reflective bands positively weighted on the size of their standard deviations (Singh and Harrison, 1985).

Standardising is required if the variables (bands) are measured on incompatible scales, (e.g. MSS band 7 against bands 4,5 and 6), but if they are in the same units, standardisation is unnecessary or even undesirable as it removes the effects of changes in variability between the bands (Mather, 1987). Singh and Harrison (1985) advocated using standardised components to improve image enhancement and signal to noise ratios and more significantly where images are compared as in change detection studies. Eastman and Fulk (1993) used standardised components in a long time series evaluation of monthly NDVI images for Africa over a three year period.

C. MSS DATA AND PCA

With Landsat MSS data, the four bands can be reduced to two principal components which in some environments may retain over 95% of the original variance. In an earlier study in the Kananaskis area the first two components accounted for over 99% (Paine, 1984); the component scores are shown in table 2.1. In other environments, this figure may be considerably lower (see Lodwick and Harrington, 1985).

Table 2.1. Principal component eigenvectors for Kananaskis Lakes area, from MSS bands 4, 5, 6, 7 (Paine, 1984).

Band	PC1	PC2	PC3	PC4
4	.49	-.42	.69	.32
5	.59	-.41	.41	-.56
6	.50	.31	.47	.65
7	.39	.75	-.36	-.39
%variance	95.4	4.0	0.4	0.2

The first principal component (PC1), termed 'brightness' represents what is common in all the original bands, particularly the topographic surface and basic land-water distinctions. Factor loadings are therefore positive and high for all bands. Where vegetation is absent or uniform, brightness information is primarily related to topographic variation. Lodwick and Paine (1985) used this premise to derive contour heights for the Barnes Ice cap on Baffin Island (Canada) from slope values contained in the first component which accounted for over 95% of scene variance.

The second component (PC2) is termed 'greenness' and represents the difference between the visible and infra-red channels. It is therefore a more useful channel for distinguishing vegetation types despite the greater total variance in PC1, and more directly related to surface cover. The difference is normally noted in vegetated scenes by positive loading values for the infra-red channels and negative loadings for the visible channels as a result of high reflectance by vegetation in the infrared wavelengths (Ingebritsen and Lyon, 1985).

The third component and fourth components (PC3 and PC4) each represent the difference between the two visible bands or the two infra-

red bands, which have been termed 'yellowness' and 'nonsuch' respectively (Lodwick,1981). Which is third or fourth (PC3 or PC4) seems to be dependent on the nature of the scene: urban, rural, agricultural or forested. In a study in an agricultural landscape, the first two components are reversed in their relative importance, i.e. the first component appears to be 'greenness' detailing the visible-infrared difference, at least in summer, while in spring the components conformed to the more conventional pattern (Fung and LeDrew, 1987).

In change detection studies between two image dates, Ingebritsen and Lyon (1985) found the first and second components to represent brightness and greenness respectively and the third and fourth to be changes in brightness and greenness. Fung and LeDrew (1987) came to a similar conclusion but with 1 and 2 reversed and 3 and 4 reversed.

These differences have led some researchers to conclude that principal component analysis may be a "scene dependent technique that requires visual inspection of images to assign specific landscape elements to specific components" (Fung and LeDrew, 1987). However the general features shown in component images and the eigenvector loadings remain consistent with most satellite data.

D. THEMATIC MAPPER DATA AND PCA

With a larger number of contributing channels, the number of useful principal components likewise increases. Despite TM data having been available for over a decade, the components have not been as clearly defined as they were for MSS data due perhaps to the increased number of bands, the question of scene-specifity, concentration on developing

other classification techniques, the reluctance of some researchers to include the thermal channel and the increasing complexity of interpreting the resulting images.

PCA requires understanding of the band correlation matrices for TM scenes, which usually show high correlation between bands 1, 2 and 3, and between bands 5 and 7. Band 4 has only medium correlation with the other infra-red bands, but it appears to be higher in urban scenes than in forested and alpine scenes (Wheate, pers. obs.). In any case, the maximum scene contrast and general information displayed in a three band composite will consist of a combination of one band from each of these three groups, such as 3,4,5 or 1,4,7 (Horler and Ahearn, 1986).

PC1: 'Brightness'

The first principal component - PC1 contains the largest amount of variance in any image, though it may vary from over 90% in a sparsely vegetated, high alpine environment (Huber and Casler, 1990) to around 50% in urban scenes which are typically highly heterogeneous (Forster, 1985). PC1 receives positive loadings from all bands, with the possible exception of the atypical thermal channel (TM6). PC1 maps surface features that dominate spectral response in all bands: topography and large-scale land-cover patterns, but not the discrimination between forest classes. Lakes and shadows may be difficult to discriminate and low order streams are poorly represented (Walsh *et al.*, 1990).

Within a forest class, the main source of scene variation in mountain regions results from differential illumination as a consequence of topography. Conese *et al.* (1988) found an average correlation of 89% (range 84-95%) between PC1 and the cosine of the incidence angle (of illumination) for each forest class. The removal of PC1, or some variant

thereof, should reduce the topographic effect, leaving the remaining lower components to reveal land-cover qualities. The elimination of PC1 inevitably leads to the loss of potentially useful information, but is considered bearable given the remaining high quantity of spectral information provided by seven TM bands (Conese *et al.,* 1988).

PC2: 'Greenness'

Since PC1 identifies the common elements across the bands and contributes to the overall tone of an image, PC2, as the first difference between bands, has also been referred to as 'colour' (Forster, 1985). The second principal component, as with MSS data is referred to as 'greenness' and represents the contrast between the visible bands (1,2,3) and the near infra-red band, 4. Its characteristics result from the high absorption by vegetation in the visible wavelengths and high reflection in the infra-red. Crist and Cicone (1984) postulate moderate to high correlation between this component and canopy closure, leaf area index and fresh biomass. Depending on the scene however, in some cases the second and third component are switched, perhaps a function of whether band 4 is more highly correlated with bands 5 and 7. This component has been found to depict some features better than any individual TM band *e.g.* avalanche slopes (Walsh *et al.,* 1990) or roads (Mather, 1987).

PC3: 'Wetness'

It is in the third principal component that Thematic Mapper data differs from MSS data through the addition of the two middle or short-wave infra-red ('swir') bands 5 and 7, (as well as the blue band TM1). Crist and Cicone (1984) have described PC3 as a measure of 'wetness', related to forest canopy and soil moisture. However, since this new component mostly highlights the difference between the short-wave infra-red bands

and the three visible and one near infra-red bands, Ahearn and Horler (1986) have preferred the term 'swirness' since 'wetness' may oversimplify the sensitivity of the short-wave infra-red region to shadowing, leaf water content and possibly other effects. The remote sensing community however has not widely adopted this term.

PC4

Since the thermal band 6 is quite different in character to the six reflective bands, if included, it loads most of PC4, though many studies choose to omit TM6 on the grounds of its lower resolution (120 metres versus 30 metres) and poor contrast resulting from daytime sensing in thermal wavelengths giving a mixture of incoming solar radiation that is transmitted and outgoing terrestrial radiation that is emitted from the earth's surface. Nevertheless the thermal channel has been seen to have some importance. Mather's 1987 study of the Derbyshire High Peaks area, had TM6 primarily loading PC2, which accounted for 11.4% of scene variance. The raised importance of the thermal channel contribution here is partly attributed to Mather's use of standardised components.

Lower components (some texts refer to these as the 'higher' components):
While the first three components correspond to structures observed in Thematic mapper three-dimensional space (excluding the thermal channel), the remaining components reflect 'low-level' contrasts between highly correlated bands. They may be dominated by noise, and have also been described as 'leakage' from higher components (Crist and Cicone, 1984). Indeed in most cases they do seem to repeat features seen in PC's 1 to 4, albeit with more visual noise, and hence most studies have discarded the lower components 5, 6 and 7 as primarily noise, rarely accounting for more than one percent of scene variance.

However they are consistent between studies: if all seven bands are used, components 5, 6 and 7 represent respectively the differences between band 1 and bands 2 and 3 ('blueness'), between bands 2 and 3 ('redness') and between bands 5 and 7 (the two short-wave infra-red bands: perhaps the closest to 'nonsuch' for MSS data).

Very few studies have found an application for these lower components. Townshend (1984) working with simulated TM data from an airborne scanner emphasised the additional discriminatory power of the lower components even though they accounted for less than 1% of the total variance. The seventh component revealed two features not visible on any of the original bands, distinguishing between peat and silty clay, and apple and plum orchards in an agricultural study. These results might be explained by the difference between simulated and actual TM data: among the factors causing noise in TM principal component images are lack of calibration between band detectors, differences in response between the forward and reverse scans of the scanner and the narrow range of recorded values for some bands. For bands 1 to 3, the range of values relative to the available 256 counts is particularly narrow. For the simulated airborne data, with five-metre resolution and broader distribution of digital values, these problems were absent or much reduced (Townshend, 1984). He concludes that more than three bands should be retained for maximum discriminatory power .

Sidjak and Wheate (1996) found that lower components in a high alpine environment contained considerable details on glacier surfaces, especially when they had been created using a binary mask for glaciers, rather than using the whole scene variance. This was partially attributed to the pixel saturation that occurs on highly reflective surfaces; its removal through PC1 left more details in the remaining components.

Table 2.2 is a summary of selected studies using PCA with TM data:

Table 2.2: Studies using PCA on TM data in a variety of environments

Study	PC1	PC2	PC3	PC4	PC5	PC6	PC7	Env.
Bernstein et al (1984)	IR	G	Swir	Th	5 v 7	B	R	U
	84.6	9.4	3.6	1.2	0.6	0.3	0.1	
Conese *et al.* (1988)	All	Swir	G	Th				F
	70	17.5	8.5	3.5				
Horler and Ahearn (1986)	IR	G	Swir		B	R	5 v 7	F
	63.6	28.0	4.6	-	2.3	0.9	0.4	
Huber and Casler (1990)	All	G	Swir					M
	91.4	6.4	2.2					
Jensen (1986)	IR	G	Swir	Th	5 v 7	B	R	U
	85.0	11.0	3.0	0.6	0.3	0.2	0.1	
Mather (1987)	All	Th	G	Swir	B	R	5 v 7	M
	79.0	11.4	5.5	2.8	0.8	0.4	0.3	
Walsh *et al.* (1990)	IR	Swir	G		5 v 7	B	R	M
	80	10.7	7.8	-	1.2	0.1	0.1	
Wheate and Franklin (1991)	Vis	Swir	G	Th	B	R	5 v 7	M
	69.5	24.1	5.0	0.8	0.4	0.2	0.1	

The first row for each study gives the sequence of components; the second the percentage of total variance explained by each component.

PC1 is a weighted average of all bands, with either all approximately equal (All) or visible (Vis) or infrared (IR) loading more heavily. Column 4 is left blank if the authors chose to exclude the thermal band 6.

G = *Greeness*
Swir = *Swirness (wetness)*
Th = *Dominated by band 6*
B = *Blueness*
R = *Redness*
5 v 7 = *The contrast between the shortwave infrared bands 5 and 7*

Environments: M = Mountain, F = Forested, U = Urban

E. SELECTIVE PRINCIPAL COMPONENTS

The various between-band differences expressed in all but the first principal component (PC 2-7) can also be extracted by utilising 'selective or directed' principal components. These are produced by examining only pairs of correlated bands and using the second principal components, thus identifying what is unique between two adjacent bands, rather than what is common. Comparison of low to medium correlated pairs should produce more substantial results than highly correlated pairs. The second component of a pair is highly correlated to their ratio, a pointer to the similar principle underlying the two techniques. Visually the images look similar, but while the PC2 image represents the absolute difference between the two images, the ratio is directly related to the slope between the two spectral regions represented by the two images.

Chavez and Kwarteng (1989) used selective PCA in an arid environment, to enhance iron and hematite deposits, vegetation differences, standing and running water and the presence of gypsum, which has higher moisture retention than the surrounding soils and rocks. The first component will map the information that is common to both bands (typically topography and albedo information) while the second component will show the contrasts between the two images, e.g. visible versus infra-red would show vegetation contrast, visible versus mid-infrared would show the contrast in moisture content. This makes it easier to 'see' the unique differences between bands, which would otherwise be overwhelmed in a colour composite by what is common to all bands. The combinations they selected were 2-4, 2-7, 4-7, 1-2, and 5-7. They recommended viewing the second component of bands 5 and 7 since unlike the first 5 bands, they are not immediately adjacent in the electromagnetic spectrum.

Loughlin (1991) used an adaptation of this procedure using 'Feature Oriented Principal Components Selection' (FPCS). The detection of hydroxyl-bearing minerals was more reliable if only one visible band was used and only one middle infra-red band for iron-oxide.

Directed or selective principal components have also been applied to band ratios by Fraser and Green (1987) whose target of information, geological discrimination, was confused or interfered with by vegetation cover. They chose two ratios that would maximise information on these two factors: 4/3 for vegetation and 7/5 for geological features (but affected by vegetation). The first principal component of these two ratios displayed the vegetation, leaving the second component to more clearly display non-vegetation: ferric oxides and clays.

Another variation of PCA was used by Fontanel *et al.* (1975) by first applying an unsupervised classification to create subsets within the scene. They then performed PCA on each of the groups to transform the multispectral data on a more selective basis and delineate mapping units. A similar procedure was applied using PCA for individual classes following a supervised classification of land use classes by Townshend *et al.* (1983), and of vegetation classes by Conese *et al.* (1988) and Horler and Ahearn (1986).

Two further techniques closely related to principal components analysis have also been used in image analysis; these are canonical analysis and the tasseled cap technique.

F. CANONICAL ANALYSIS

Canonical analysis, also known as multiple discriminant analysis is similar to principal components analysis in that an orthogonal linear transformation is performed such that the first new axis accounts for the greatest amount of variance, but it is based on two component parts of the covariance matrix where principal components analysis uses the total covariance matrix. For example, the two parts might be the TM bands and a set of topographical variables. The data transformation is based on the maximum separation of a set of identified targets, to determine the transformation, which in PCA is based on the entire image. Examples of canonical analysis applied to geologic enhancement are given in Siegal and Gillespie (1980) and Siegal and Abrams (1976).

Moulton (1989) used canonical analysis in mountainous terrain to summarise the shared variance between the following sets of data: surface cover variables and the TM bands, topographic variables and the TM bands, surface cover and topographic variables combined and the TM bands. Results showed that surface cover variables and the TM data shared 46% of the variance, compared to 64% for topographic variables and the sensor data, leading to the conclusion that the incorporation of ancillary topographic variables should improve vegetation classification. Had the two variable sets shared the same variance, an opposite conclusion would be derived. This indicates the importance of some knowledge of terrain in the interpretation and classification of satellite data in mountainous areas.

G. THE TASSELED CAP

This technique was developed by Kauth and Thomas (1976) and has been further elaborated by Crist and Ciccone (1984) and Crist and Kauth (1986). These studies have focused on agricultural landscapes, using first MSS and later TM data. Coefficients of brightness, greenness and yellowness with decreasing percentages of variance explained are determined as with PCA, where yellowness has been described as either senescence or scene noise. These same terms applied to PCA have been adopted from this technique.

The tasseled cap technique is so named because when data are plotted with two of the coefficients (components) as the axes, the distribution of points resemble a tasseled cap. The prime difference with PCA is that the coefficients are determined *a priori* by the pixel values for all contributing bands, while principal components transformations are defined by the statistical relationships between the bands for the whole scene. The tasseled cap method claims to be scene-independent, a point disputed by Mather (1987). Nevertheless it has only been applied to limited agricultural scenes in the US east and mid-west, where topographic variations are relatively small.

With TM data, the brightness coefficient is similar but not identical to that for MSS data due to the influence of the mid-infrared bands. Since the technique has been applied only to agricultural scenes, brightness is dominated by soil reflectance. Greenness is also very similar as the two longer infrared bands in TM data, tend to cancel each other out and the blue band (also absent from MSS data) is highly correlated to the other visible bands. The third feature equivalent to wetness contrasts the sum of the visible and near infrared bands with the longer infrared bands.

CHAPTER 3

STUDY AREA AND METHODOLOGY

3.1 Introduction

The Front Ranges of the Rocky Mountains commence about 80 kilometres (50 miles) west of the city of Calgary and provide the mountain environments necessary for this study (figures 3.1 and 3.2). The topographic effect on satellite data commences midway between Calgary and the study site in the Foothills, which mark the eastern extreme of the northwest-southeast trending ranges resulting from the orogenic overthrust associated with the collision of the North American continental and the Pacific tectonic plates. Correspondingly, precipitation and moisture decrease eastwards as the predominantly westerly winds deposit their moisture on windward slopes. Two hours' drive west from Calgary, the continental divide separates the provinces of British Columbia and Alberta, and the Rocky Mountain National Parks of Kootenay and Yoho, Banff and Jasper respectively.

The study area chosen encompasses the Kananaskis Lakes in the upper reaches of the Kananaskis Valley, located in the front ranges of the Rockies but adjacent to the continental divide with Banff National Park to the northwest, and British Columbia to the south and west. The valley lies within the 'Kananaskis Country' management area that has been developed since the 1970s as an integrated multi-recreational area by the province of Alberta and is used heavily by Calgarians as an alternative to the adjacent and internationally visited National Parks. Activities such as hunting, camping, golfing, hiking, skiing and cycling make use of developed facilities and interpretive centres (figure 3.3).

Figure 3.1 Study area, Kananaskis Lakes, Alberta.

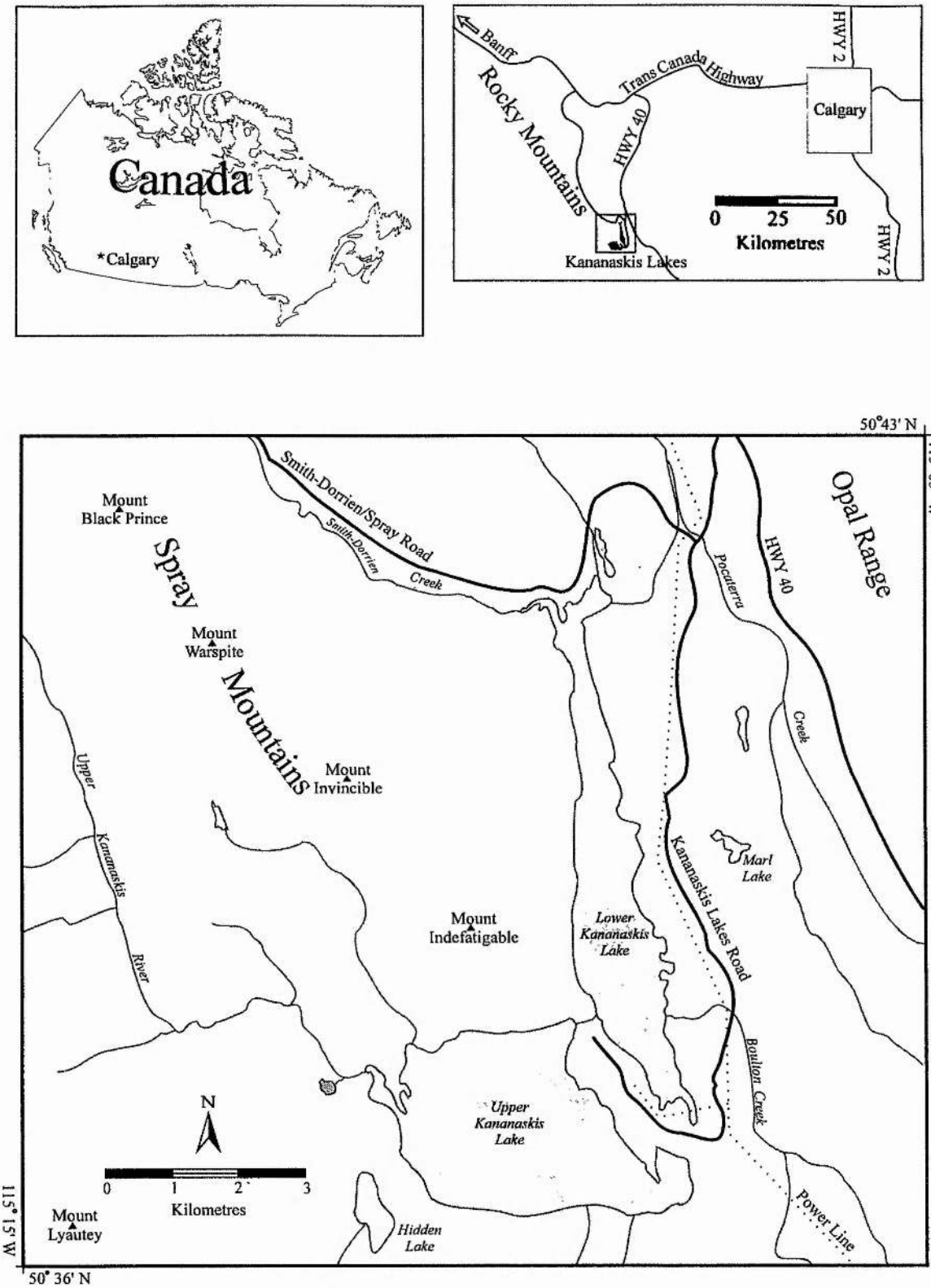

Road access is provided by Highway 40, which connects to the Trans-Canada Highway where the tributary Kananaskis Valley enters the main Bow Valley connecting Calgary and Banff (figures 3.1 and 3.2). The University of Calgary Field Station is located close to the entrance to the valley at Barrier Lake, approximately 50 kilometres (30 miles) north of the selected study site. This has helped contribute to substantial related research in this area (Lodwick *et al.*, 1986; Lodwick *et al.*, 1991).

Resource management of such an area is essential to safeguard a substantial provincial investment. Fire management and suppression are particularly important programs which require up to date spatial databases. Fire has been actively suppressed in the area for several decades as a function of its recreational use. Forest cover data is used in fire management and the Kananaskis Valley contains a network of fire lookout stations, three of which border the study area. However, effective use of satellite data has been hampered as in other mountainous areas by the confusion of topographic and land-cover information. The proximity of the area to Calgary, the University Field Station and its research interest has resulted in several theses utilising satellite data for this area (Paine 1984, 1987; Connery, 1992; Williams, 1992; Smart, 1992).

The particular scene portion, captured on August 5 1984, which was selected for this study is comprised of 512 x 512 pixels, covering an area of 12.8 x 12.8 kilometres (8 x 8 miles). It fulfills a number of criteria, including available satellite and digital elevation data, hardcopy vegetation maps, existing research data in ground surveys and known sites, an appropriate variety of environments, particularly a mixture of forest, alpine and wetland communities within sub-alpine and alpine ecosystems and as cloud-free an area as possible. The inclusion of the Kananaskis Lakes was deliberate for local context and as a control.

Figure 3.2 Regional satellite image and study area window
Above: Regional setting from an enhanced TM 1-2-3 colour composite satellite image. City of Calgary is at top right on the west edge of the Canadian Prairies, and Kananaskis Lakes are at bottom left in dark blue. *Below:* TM 3-4-5 colour composite of study area.

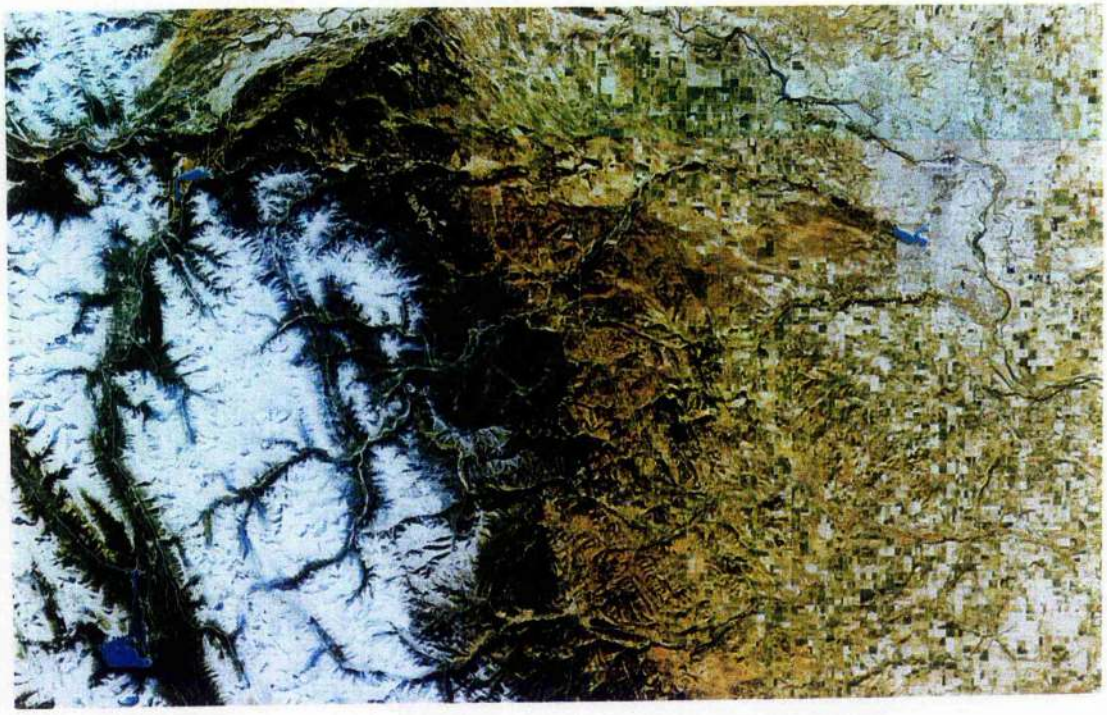

Figure 3.3 Portion from Kananaskis Country recreational map covering the study area and a shaded relief image for the same section.

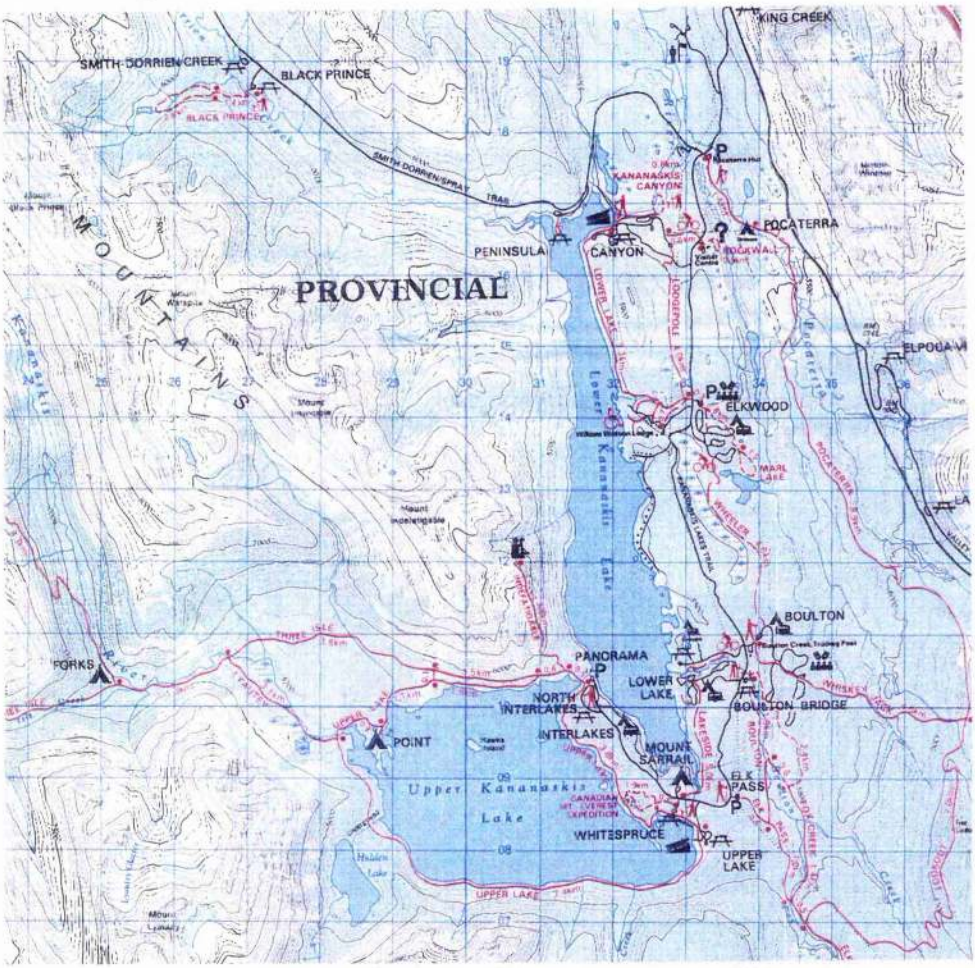

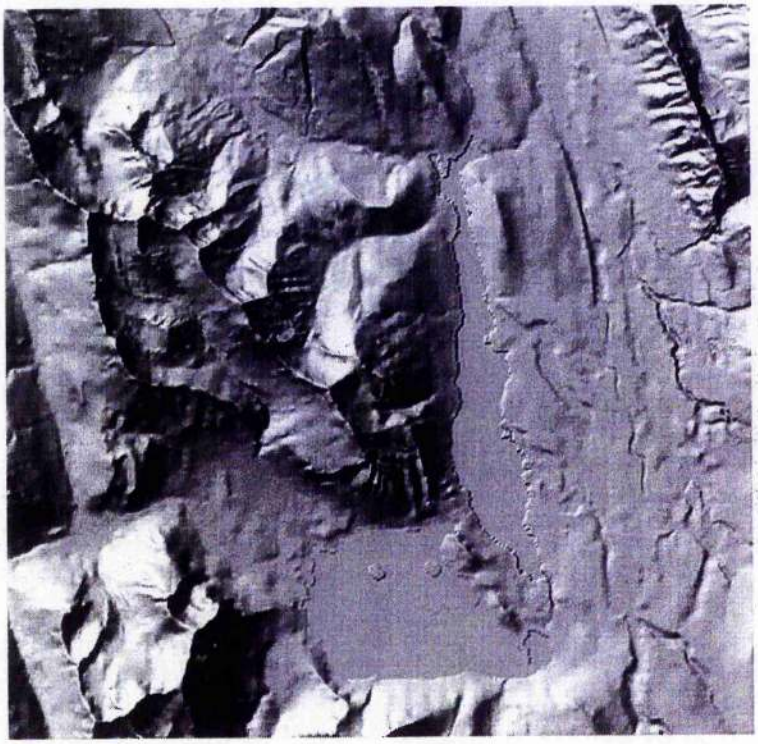

3.2 Data sources and image processing

A variety of satellite data for the Kananaskis Valley were available as a result of wide research interests in the area. A Landsat Thematic Mapper data tape was available for August 1984 (and also for October 1991). The scenes were largely cloud-free with the exception of isolated cumulus clouds. Summer imagery is preferred over autumn in land cover and vegetation studies owing to the greater range of spectral values for vegetation during the growing season, as well as excessive shadow in non-summer seasons due to the low sun angle.

The Thematic Mapper (TM) data channels of Landsat 4 and 5 were designed primarily for vegetation discrimination with a subsequent addition, band 7, for geologic applications in response to demand from potential users (Townshend, 1984). The spectral bands are summarised in table 3.1:

Table 3.1. Characteristics of the Thematic Mapper sensor

TM Band	Resolution	Wavelength (micrometers)	Spectrum region
1	30 metres	0.45-0.52	Blue (Visible)
2	30 metres	0.52-0.60	Green (Visible)
3	30 metres	0.63-0.69	Red (Visible)
4	30 metres	0.76-0.90	Near Infra-red
5	30 metres	1.55-1.75	Shortwave infra-red
6	120 metres	10.4-12.50	Thermal infra-red
7	30 metres	2.08-2.35	Shortwave infra-red

These spectral bands were selected to take advantage of distinctive characteristics of the spectral response of vegetation: bands 1, 2 and 3 for

chlorophyll absorption, band 4 is controlled by the mesophyll layer of leaves, band 5 is on a shoulder between two water absorption bands and band 7 was chosen for identification of minerals with application to both soils and rocks. Band 6 records emitted radiation in the far infrared; digital values are related to temperature but reduced in utility for natural resource mapping by its lower resolution. Generally only the first three bands are affected by atmospheric scattering. This number of bands gives many advantages to Thematic Mapper data for multispectral studies.

SPOT multispectral data was also available. Despite its higher spatial resolution (20 metres), it was considered inferior for the purposes of this study due to the fewer spectral bands and hence accepted lower information content (Chavez and Bowell, 1988). In particular, SPOT lacks any information in the middle infrared portion of the electro-magnetic spectrum. The multispectral SPOT image was also adversely affected by widely distributed low clouds.

Digital elevation data was acquired from the federal and provincial government mapping agencies at scales of 1:250,000 (100 metre pixels) and 1:20,000 (25 metre pixels) respectively. It was expected that these would be used to correlate actual with derived topography in the thesis.

The satellite image and digital elevation data were processed primarily on UNIX workstations: IBM RISC/6000 and later on Silicon Graphics Indy workstations, and also on personal computers (386/486 clones). All platforms were used to run 'EASI/PACE' image processing software from PCI, Toronto and the PCs alone ran 'IDRISI' GIS software from Clark University, Worcester, Massachusetts. The PCI software is one of the

world's most complete digital image processing systems, based initially on code written at the Canadian Remote Sensing Centre, Ottawa. The IDRISI GIS software contains a considerable repertoire of GIS and image processing options, some not available in more expensive systems.

Initially extra routines were written to enable file transfer between the two systems, but this aspect of data processing (along with many others) has been subject to considerable expansion from the 1980s rendering many previous in-house algorithms obsolete (see Wheate, 1988). Recent additions enabled the speedy transfer of files which could be ASCII or binary format and .TIF image or Postscript files. High resolution screens allowed initially a file size of 512 x 512 and either 8 bit or 256 shades of gray for single band images or 24 bit, up to 16.7 million colours for multi-band colour composites. While a larger image area could have been used, this would have slowed data processing and display and encumbered data storage.

Output was sent as Postscript files to monochrome laser jet and colour ink jet printers, along with photographic screen capture where necessary.

3.3 Methodology

(i) A sample image window from the 1984 (August 5) scene was extracted and corrected to fit the Canadian National Topographic System (NTS) based on the Universal Transverse Mercator (UTM) grid which enables co-registration with Alberta provincial digital elevation data based on 25 metre pixels. The latter was used mainly to compare efforts to extract topographic information from the satellite imagery, rather than as an element to be integrated within the analysis.

(ii) Landsat seven band Thematic Mapper data were used to generate image channels that were in principle 'topography free' to enable optimal vegetation and land cover discrimination without the conflicting topographic information present in the original bands. Eliason *et al.* (1981) pioneered one procedure with Landsat MSS data, which subsequently received little attention. Since then there have been two major developments:

a. TM data has seven bands compared to four in MSS (and three in SPOT); this provides for much greater selection of channel generation possibilities.

b. Computer storage and operating speeds have multiplied manyfold in the intervening fifteen years, releasing the restrictions they encountered in data processing and the number of channels used in procedures they had developed.

New sets of image channels were produced for the generation of surface cover images in which the topographic effect has been reduced or eliminated. These was performed using the two parallel techniques of spectral band ratioing and principal components analysis. In the case of ratioing, the number of ratio combinations has increased from six with MSS data to 15 with TM data. PCA was hardly a viable option with MSS data as only one principal component (PC2) could have been described as not dominated either by topography or noise.

(iii) These two sets, one composed of ratios, the other of principal components, could then be used as input in a clustering algorithm (unsupervised classification) to generate clusters that represent

homogeneous ground cover areas from which the effects of topography have been removed. The pixel values for each TM band under consideration were replaced by the average value calculated for the pixels in each homogeneous cluster. In this case, it has been determined that TM bands 3, 4 and 5 were the most representative. The resulting image, either as individual bands or as a colour composite represent the image area effectively if there were no topographic effect (i.e. if it were flat).

(iv) The difference between this image and the original TM band should represent the topographic component in the studied area; it could be compared with the digital elevation model, and should be correlated to the cosine of the incidence angle.

(v) The homogeneous clusters derived in stage (iii) were used towards a classification procedure in a hybrid approach to determine surface cover type. This might be compared to traditional supervised and unsupervised classification procedures. The results were checked against known vegetation classes derived from existing surveys, maps and ground truthing procedures, carried out previously.

3.4 Physiography

The sedimentary layers, mostly sandstones, limestones and shales date from the Devonian to the Cretaceous (380 million to 155 million years ago) and were overthrusted and folded in the Laramide Orogeny that created the Rocky Mountains 60 million years ago. The whole region has been subsequently glaciated in the Quaternary, leaving a heavily incised landscape with steep valley sides, U-shaped troughs, cirques, glaciers and pointed peaks. Erosion continues by local scouring and subaerial weathering, evident in numerous rock and snow avalanches (Gadd, 1990).

Figure 3.4 Geology of study area, adapted from McCechan, 1988.

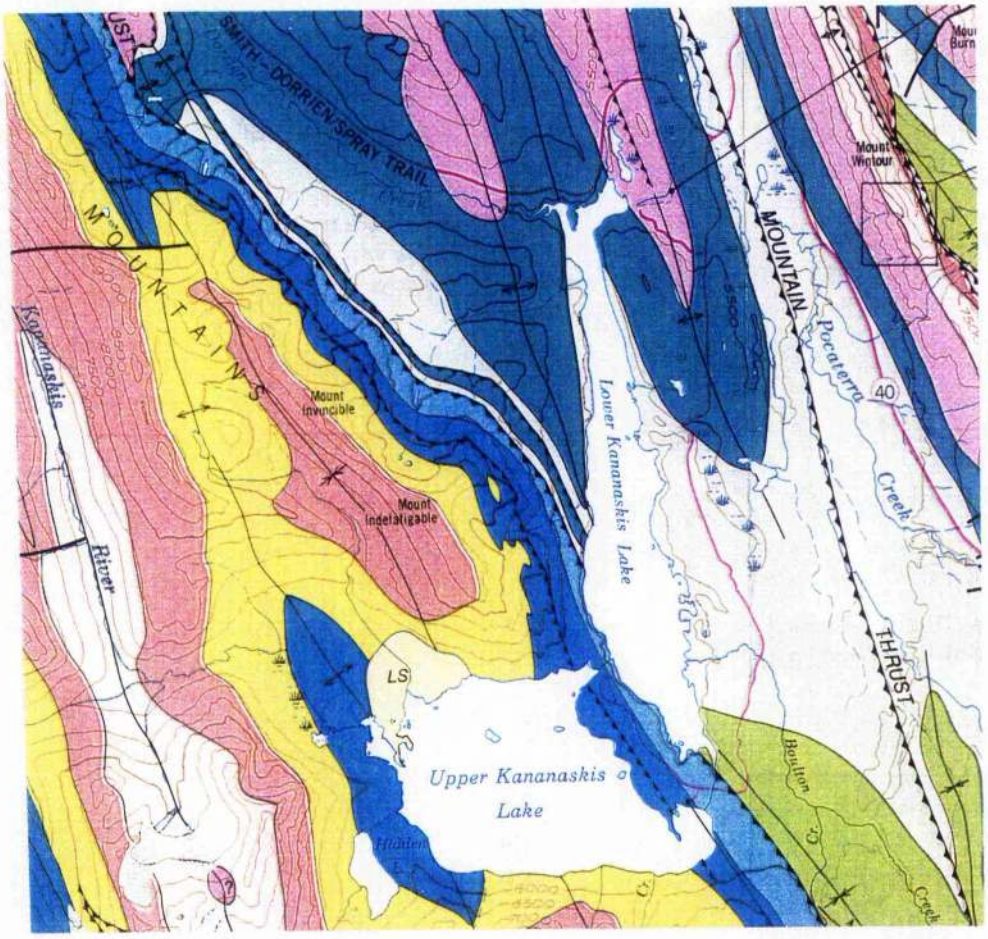

Rock types:

- Conglomerate
- Chert
- Coal
- Dolomite
- Limestone
- Sandstone

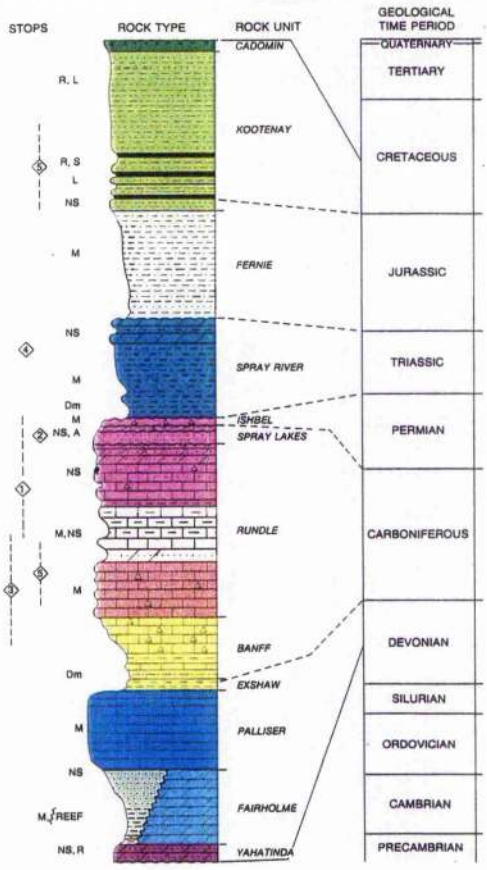

Figure 3.5 Fire history, Alberta Provincial Government map .

Dates are given for the most recent fire at each site.

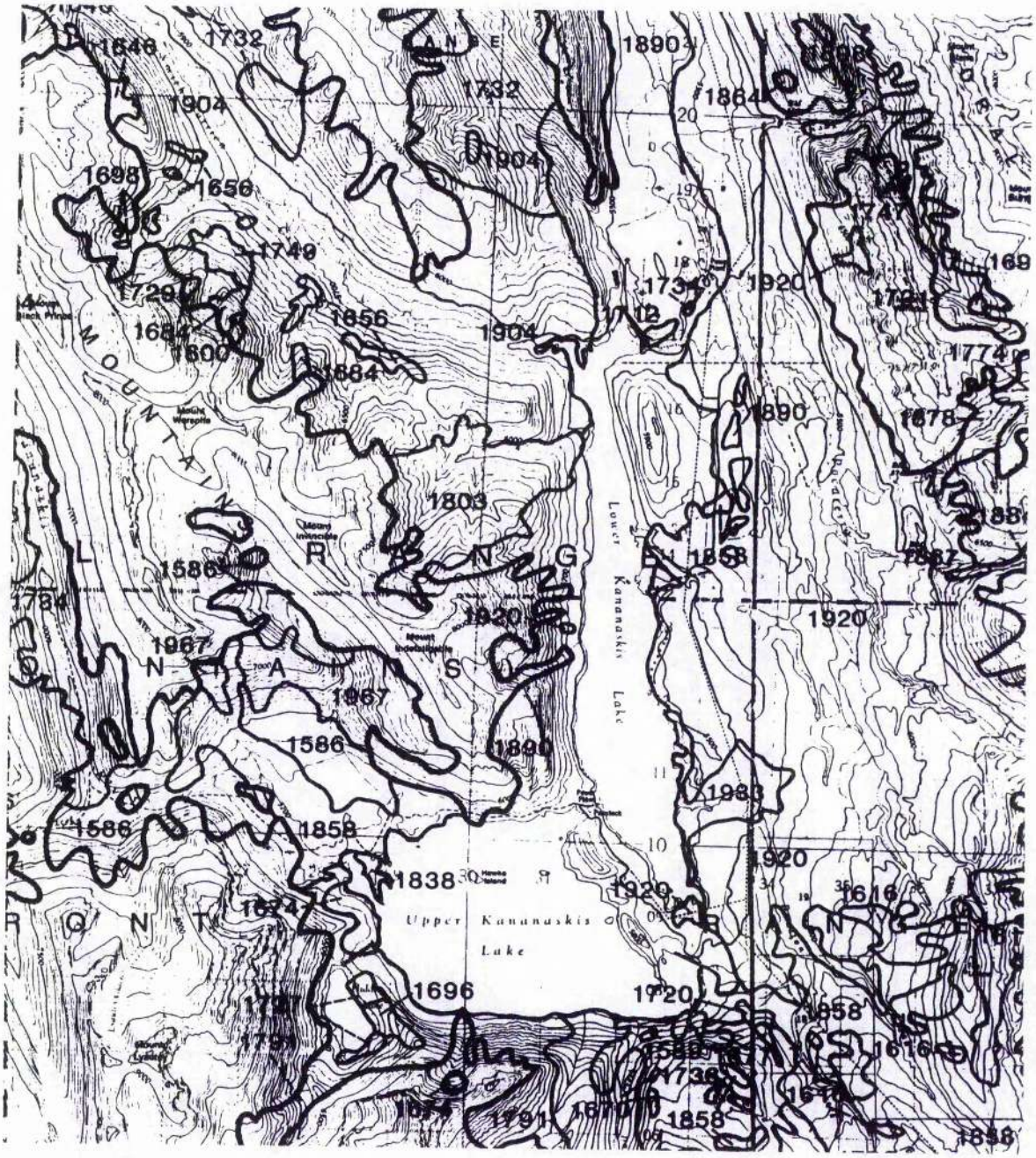

Figure 3.6 Vegetation communities, from Williams, 1990

(legend on next page)

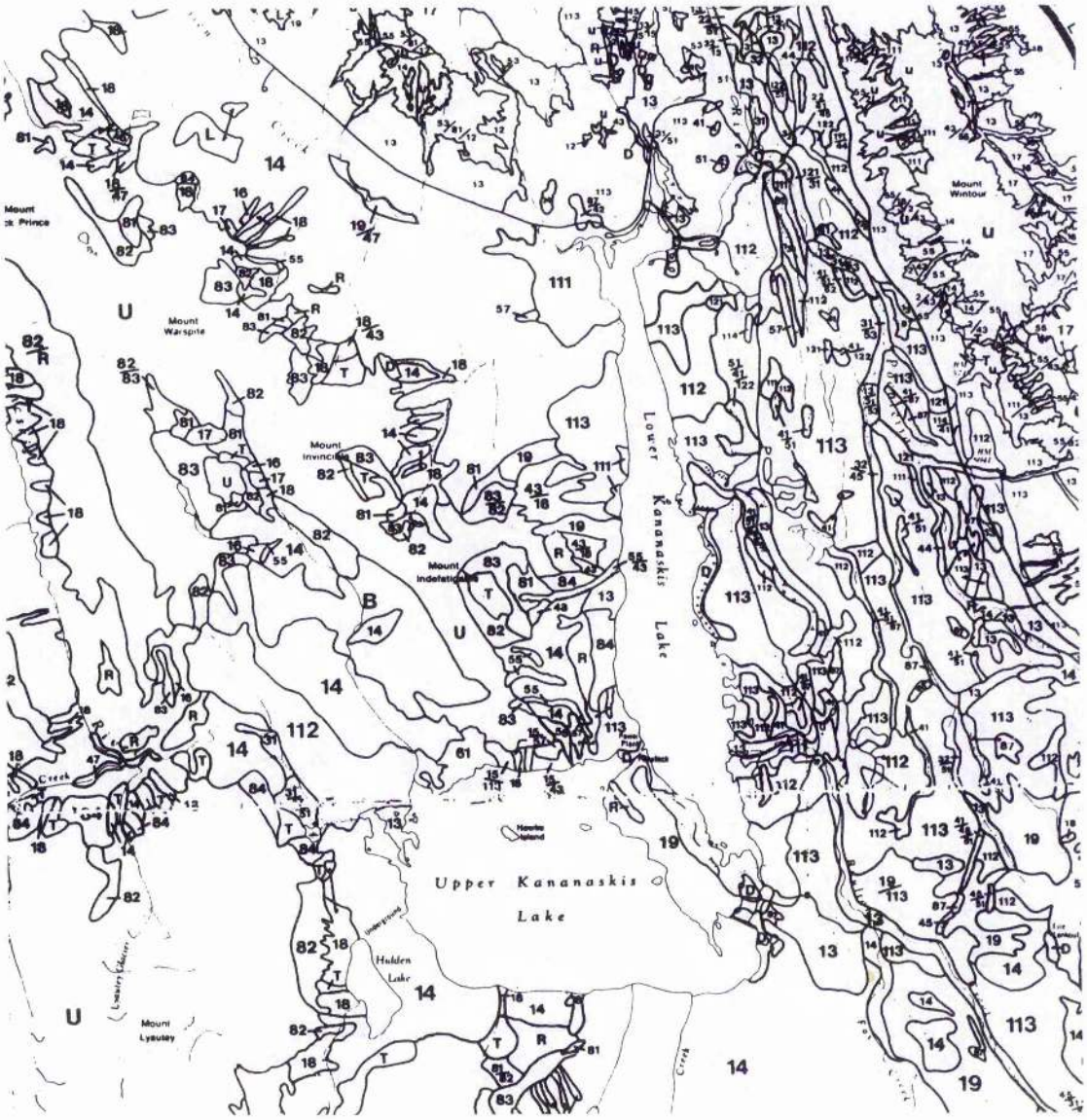

Figure 3.6 (continued) Vegetation communities: legend.

1 CONIFEROUS FOREST
- 11 Lodgepole Pine forest
  - 111 Open Lodgepole Pine forest
  - 112 Moderately Dense Lodgepole Pine forest
  - 113 Dense Lodgepole Pine forest
  - 114 Lodgepole Pine / Sphagnum - Labrador Tea bog
- 12 Spruce forest
  - 121 Spruce / Feathermoss forest
  - 122 Spruce / Sphagnum - Labrador Tea bog
  - 123 Spruce / Willow alluvium
- 13 Spruce - Pine forest
- 14 Spruce - Alpine Fir forest
- 15 Douglas Fir forest
- 16 Alpine Larch forest
- 17 Alpine Fir - Spruce - Larch forest
- 18 Alpine Fir avalanche track or slope
- 19 Spruce - Pine - Alpine Fir forest

2 DECIDUOUS FOREST
- 21 Aspen Poplar forest
- 22 Balsam Poplar forest

3 TALL SHRUB DOMINATED
- 31 Riparian Willow
- 32 Wetland Willow
- 33 Willow - Sedge alluvium

4 LOW SHRUB DOMINATED
- 41 Birch fen and bog
- 42 Birch - Willow fen
- 43 Willow avalanche track or slope
- 44 Buffaloberry - Herb slope
- 45 Willow fen
- 46 Alpine Willow
- 47 Streamside Willow

5 HERB DOMINATED
- 51 Wet Sedge fen
- 52 Dry Sedge fen
- 53 Grassland
- 54 Dryas
- 55 Herb avalanche track or slope
- 56 Horsetail - Moss
- 57 Dry forb - grass mixture

6 LICHEN / BRYOPHYTE DOMINATED
- 61 Lichen dominated
- 62 Bryophyte dominated
- 63 Earth hummocks

7 UNVEGETATED TYPES
- R Rock outcrop complex
- T Talus slope complex
- U Rock, Snowfields, Glaciers

8 ALPINE
- 81 Subalpine tree islands with Heath - Herb clearing
- 82 Alpine complex
- 83 Alpine meadow heath
- 84 Alpine slope complex
- 87 Conifer dominated wetland

9 DISTURBANCE
- B Burn (79 = date of burn
- L Logged (cc = clearcut; pc = partial cut; 76 = date cut)
- D Other (gravel pit; trail; powerline, facility, etc)

Relief is largely related to a series of thrust faults with NNW-SSE strike (figure 3.4). These have produced the upthrust of the Spray, Kananaskis and Opal ranges, while smaller transverse faults further complicate the relief. Resistant Paleozoic limestones and dolomites tend to form the peaks and ridges, while the less resistant Mesozoic shales and sandstones are found on the lower slopes and valleys. The main valley represents the remnants of an eroded anticline, set between the opposite folds on the east and west sides (McCechan, 1988).

The predominant strike of 330-340 degrees associated with overthrusting is extremely evident, including several longitudinal thrust faults, as these mountains represent the front ranges of the Rocky Mountain system. The general trend is apparent in the mountain ranges present in the scene, as well as some geologic boundaries, notably on the west side of Hidden Lake, which is just to the southwest of the Upper Lake (figures 3.4 and 3.2b).

Depositional features occur in the valley bottoms as coarse colluvial and alluvial deposits, hummocky moraine containing ablation till, some kame deposits and deltaic gravels. These are largely camouflaged by a veneer of vegetation except where surface drainage prevents the development of climax coniferous forest, broken up by poorly drained fens and bogs.

3.5 Vegetation

The area covers the Subalpine and Alpine ecoregions. The lower subalpine forests in the valleys are dominated by coniferous species: Englemann Spruce (*Picea englemanii)*, White spruce (*Picea glauca*),

hybrids of the two species and Alpine Fir (*Abies lasiocarpa*). Drier sites include some Douglas Fir (*Pseudotsuga menziesii).* Subclimax stands of Lodgepole Pine (*Pinus contorta*) are indicative of fire disturbance with little regeneration of spruce or fir (Williams, 1992). These show on aerial photographs as smoother texture areas as a result of homogeneous younger age compared to the older growth climax stands, which show coarser texture of varying canopy density and height, reflecting several centuries of growth and lack of disturbance.

On the colour composite (figure 3.2b), the older stands dominated by spruce appear as darker green, especially on the south and west shores of the Upper Lake, the west side of the Lower Lake, dating back to 1803, and the very north centre part of the image, dating back to a 1732 fire (figure 3.5). The area burned by the most recent fire in 1967, north of the Upper Lake, on the west side of Mount Indefatigable, is clearly visible on aerial photographs and satellite images due to the lack of regrowth.

Deciduous species (yellow-green in the colour composite), include aspen (*Populus tremuloides*), balsam poplar (*Populus balsamifera),* white birch (*Betula papyrifera)* and various willows (*Salix spp.*) which are confined to disturbed sites, particularly avalanche slopes, rockslides and river banks. Scattered throughout the area are numerous wetlands and on steep south facing slopes are grasslands of rough fescue, spear grass, wild rye, oat and wheat grasses (Williams, 1992).

With increasing elevation, alpine fir is more successful until the treeline at about 2000 metres is marked by occasional stands of alpine larch (*Larix lyallii)* and more rarely limber pine (*Pinus flexilis*) and whitebark pine (*Pinus albicaulis).* Above the treeline is the alpine tundra. Here, the

effect of topography creates countless topoclimates in response to slope and aspect effects (Barry and Van Wie, 1974). There are several alpine-heath and meadow communities, dominated by woody perennials such as mountain heathers *(Phyllodoce, Cassiope),* sedges, grasses and alpine flowers. Steeper and higher slopes degrade into rock talus, colluvial veneers and exposed bedrock, perennial snow and ice in the form of cirque glaciers, which have been retreating for much of this century.

3.6 Vegetation classes in the study area

The vegetation cover classes of the Kananaskis Valley have been described and mapped in considerable detail by Williams (1990, 1992) and are briefly summarised here, with reference to the colour composite of bands 3, 4 and 5 (figure 3.2b). Forty-nine vegetation community types have been identified in the area and can be initially grouped into four main categories: coniferous forest, wetlands, alpine, and non-forested slopes and meadows. The last category consists of non-forested communities that can be found at all elevations, as a function of drainage, parent material or disturbance through avalanche activity.

All four categories contain rich diversity and high variation in composition within small distances, making classification complex and often subjective. While the coniferous areas have some commercial significance, the other three categories contain communities that are mostly small in size, sensitive to disturbance, and contain ecologically unique or significant plant and animal species. Much of the alpine zone is considered crucial for its use by grizzly bear while wetlands provide important habitat for moose and threatened species such as the river otter and long-toed salamander (Williams, 1992). Not all of the forty-

nine community types are present in the study window selected or large enough to warrant discussion. They have been regrouped to provide the following recognisable classes.

A. NON-VEGETATED

1. Snow and ice

Located at higher elevations, the extent of snow cover varies with the time of year an image is captured and the annual precipitation and temperature patterns. Remnant snow can be distinguished from bare ice, but not from snow-covered ice. Snow and ice appears as light blue on the composite image (figure 3.2b).

2. Water

Lakes and ponds are found mostly at lower elevations in the valley floor and in some higher basins. Most rivers and streams are not wide enough to be visible or to be analysed with Thematic Mapper 30-metre pixel resolution. Deep water appears as black in the image, while shallow and sediment laden water may have some colouration from the green and blue wavelengths, see for example the southern end of Marl Lake (located on the east side of the Lower Lake). Lakes vary in width and depth annually according to water supply and seasons, having greatest volume after periods of snowmelt. The Kananaskis Lakes are subject to additional fluctuating levels as a result of water use and release, as both are dammed. This creates a gravel strip, devoid of vegetation along the shores, which is similar in appearance to bare rock.

3. Rock

Bare rock is found on a variety of sites and over a wide range of elevations, continuously above the tree-line, as well as in talus slopes

and some small sites within the forested valley bottom and sides. It appears in the composite as a purple to white colour, depending on aspect and geologic composition. Road beds and lake shorelines exposed by low water have similar spectral characteristics.

Note: there are some isolated cumulus clouds, one towards the upper right corner, and a few in the left edge, which along with their respective shadows need to be accounted for in any image processing.

B. FOREST

4. Pine forest

Lodgepole pine (*Pinus contorta*) is dominant on the lower slopes and valley bottoms (about 1600-1950 metres) where they have been disturbed by fire in the last 150 years. Crown closure varies from dense to moderate to open, depending on fire history. The forest floor may be covered with a variety of shrubs and herbs, particularly Canada buffaloberry (*Shepherdia canadensis*), grouseberry (*Vaccinium scoparium*), bilberry (*V. myrtillus*) and Labrador tea (*Ledum groenlandicum*) but these are not distinguishable on imagery of this resolution.

5. Spruce and spruce-fir forest

White spruce (*Picea Glauca*) dominates the pine in the valley bottoms when undisturbed by fire, giving way to Engelmann Spruce *(Picea engelmanii)* at higher elevations, up to 2150 metres, with moderate to densely closed forests. On the composite image these stands appear as darker green and are evident on the south and eastern shores of the Upper Lake; the contrast with pine dominated sites is particularly striking on the western side of the Lower Lake towards the northern end, where a more recent fire in 1890 was contained by a ridge separating slopes facing east (burned) and slopes facing north (last burned in 1803).

6. Spruce-pine and spruce-pine-fir

Pine and Spruce are co-dominant with larch either absent or as an understory component, and canopies moderately open to moderately dense. This is found here in the 'Interlakes' area between the Upper and Lower Lakes, which has seen fire as recently as 1920, and in the southeast corner of the image. The herb layer is lush, but there is more bare soil and less deadfall than the other coniferous types.

Note: Within the study area, some other forest types are represented but not in large enough stands to warrant mapping using satellite imagery. These include Douglas fir on the north shore of the Upper Lake, alpine larch on the east slopes of Mount Indefatigable and some deciduous forest of aspen and balsam poplar in the very north of the area, increasing in frequency further down the valley with decreasing altitude.

C. SHRUB DOMINATED

7. Riparian willow

Dense stands of willow over two metres in height occur in wetlands below 1750 metres along the edges of rivers and streams and in marshy environments and up to 1825 metres as lower shrubs averaging one metre in height. As deciduous cover, they are yellow-green on the image but not always with the distinct linear shape seen in the fens and bogs.

8. Fens and bogs

The valley floor is littered with linear wetlands dominated by a mixture of birch, low willows, sedges and sphagnum mosses. Drainage is very slow due to low gradients, high water table and peat substrate. They appear as yellow and yellow-green ribbons within the pine and spruce forests.

9. Alpine fir avalanche slopes

Slopes with a lower avalanche frequency support a cover of alpine fir, particularly on east and north facing slopes, where melting is less variable (see below). They are most noticeable on the western slopes of Hidden Lake, on the east slopes of Mount Invincible and in two tracks on the south shore of the Upper Lake.

10. Buffalo-berry herb slope

Avalanche slopes at lower elevations (1850-2050 metres) dominated by Canada buffalo-berry shrubs and various grasses. Occasional saplings of fir, spruce or pine and patches of willow, birch and bearberry. The herb layer is low in cover, including wild rye, wild strawberry and fireweed.

D. HERB DOMINATED

11. Herb-dominated avalanche slopes

These occur at higher elevations in alpine and sub-alpine zones (1950-2250 metres). They are more common on slopes generally facing south due to greater acceleration of melting to lubricate avalanches and on steeper slopes, but not so steep as to inhibit snow collection, up to a maximum of 42 degrees (Connery, 1992). There are limited amounts of shrubs such as ground juniper and shrubby cinquefoil, but slopes are dominated by fireweed, grasses and herbs including hedysarum, common paint-brush, cow parsnip, wild strawberry and many other flowering species. They are easily detectable on images which include band 4 as narrow (yellow) strips running from bare rock areas through the forests below, such as here on the east side of Mount Indefatigable .

12. Heather-dominated meadow heath (alpine complex)

These communities on alpine slopes, are dominated by white mountain heather (*Cassiope tetragona*) or mountain heather (*Phyllodoce empetriformis*) covering 50% of the site. They occur between 2300 and 2450 metres, with alpine and snow willow *(Salix reticulata)* as co-dominants at some sites. There are some krummholz spruce, larch and fir and about 20% lichen ground cover.

13. Dryas-dominated alpine meadow heath

Exposed alpine meadows, on relatively flat or gently sloping terrain above 2300 metres, with around 50% white mountain avens (*Dryas octopetala)* and secondary cover of cinquefoil, alpine willow, moss campion, sedges and patches of krummholz Engelmann spruce. Lichens cover about 30% of the ground, mosses up to 15%.

E. DISTURBED

14. Burns

Burns can occur on a variety of slopes and elevations. They are species poor, dominated by fireweed, grouseberry and a number of herbs until lodgepole pine regenerates. The spectral signal is strongly influenced by deadfall, standing dead trees and bare soil. The main example is the 1967 burn on the south-east slopes of Mount Indefatigable.

15. Logged areas

These include areas that were predominantly spruce-fir forests which were cut before 1978. There is sparse regrowth of pine and some spruce (less than 5% cover) and soil erosion along old logging roads. These are species poor sites dominated by grouseberry, false azalea and occasional alpine fir. Common herbs include fireweed, arnica, felwort and wild strawberry. There is one logged patch north of Mount Warspite.

Figure 3.7 LAND COVER ILLUSTRATIONS : Forest communities

(Photographs on following page)

Top: View looking south from eastern slopes of Mount Indefatigable over the interlakes area and Elk Valley, May 1992. In late afternoon, the topographic effect is most pronounced on the rock complex hill which forms the spine of the interlakes and on 'Blueberry Hill' in centre above it. The interlakes area is covered by spruce-pine-fir, while the valley behind is dominated by pine except for darker areas of spruce-fir, which have escaped fires this century. The distinct linear feature is the power line.

Middle: An infra-red photograph from July 1989, looking north from the same viewpoint as the top photograph. Healthy forest is shown in red, with heavier shadowing than on normal colour photographs. The contrast with non-vegetated areas is stronger also, highlighting the rock/gravel shoreline exposed by varying lake levels.

Bottom: Looking north from south of the study area across the lakes and valley, September 1991. The 1967 burn is clearly visible on the north shore of the Upper Lake towards the top left corner, though similar in colour to the alpine meadows and slopes on the northeast side of Mount Indefatigable (top centre). The lichen dominated landslide can be seen below the burn adjacent to the lake, the rock layers having collapsed down the slopes of Indefatigable along tilted bedding planes. In the foreground the autumnal colours of alpine larch occur just below the treeline.

Figure 3.7 Land cover illustrations : Forest Communities

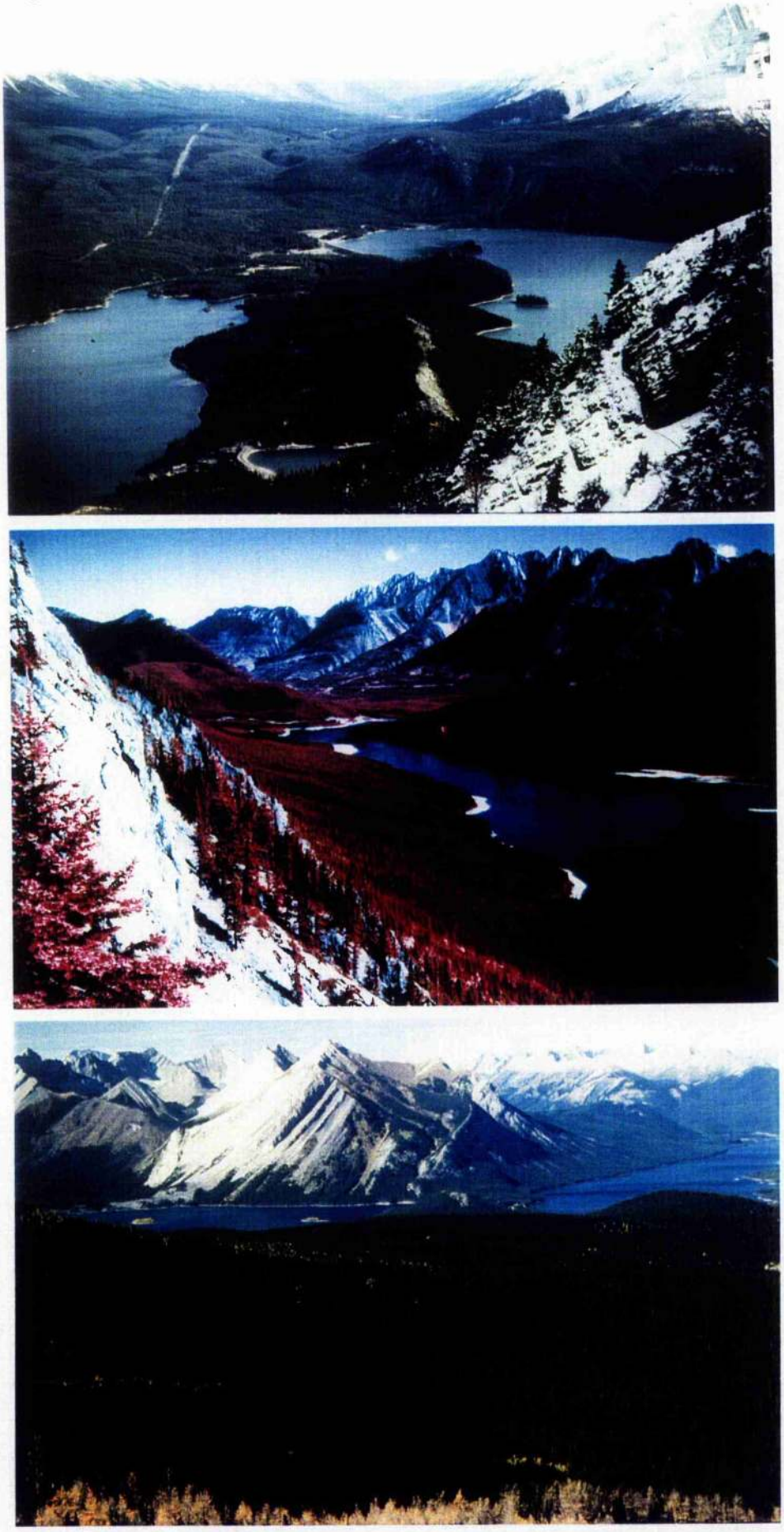

Figure 3.8 LAND COVER ILLUSTRATIONS: Wetlands
(Photographs on following page)

Top: fen wetland in autumn (September 1990), dominated by willow and birch; early snow lingers in the shade of spruce-fir stands.

Bottom: aerial photograph, taken on August 16, 1984, within two weeks of the satellite image used in this study, shows northern part of Lower Lake. It has been reduced to 66% from an original 1:20,000 scale to 1:30,000 or 1 cm to 300 metres (approximately 1 inch to half a mile). Some detail has been lost in reproduction, but the figure still gives an indication of the complexity of vegetation patterns.

On the western side (left), numerous herb-dominated avalanche tracks run from alpine meadows through the pine dominated forest. Near the top left of the photo is the very marked boundary, where the 1890 fire was stopped by the northeast running ridge. North of it, the spruce-fir presents a much coarser texture, resulting from uneven canopy density, compared to the smooth lodgepole pine canopy to the south and east. On the eastern side of the lake, wetlands stand out among coniferous stands, and small lakes give a mixed signal depending on water level. Hidden Lake, not shown here, can dry up completely (hence its name!).

Figure 3.9 LAND COVER ILLUSTRATIONS: Alpine
(Photographs on second following page)

Top left: alpine meadow heath, dominated by mountain heather, some snow willow and assorted herbs (August 1990).

Top right: infra-red photo of herb dominated avalanche slopes, containing assorted herbs and some ground juniper (August 1989). The richness of the herb layer makes these sites attractive travel routes for grizzly bear.

Bottom left: riparian willow community along river edge (July 1984).

Bottom right: talus slopes south of Upper Lake (July 1987).

Figure 3.8 Land cover illustrations: Wetlands

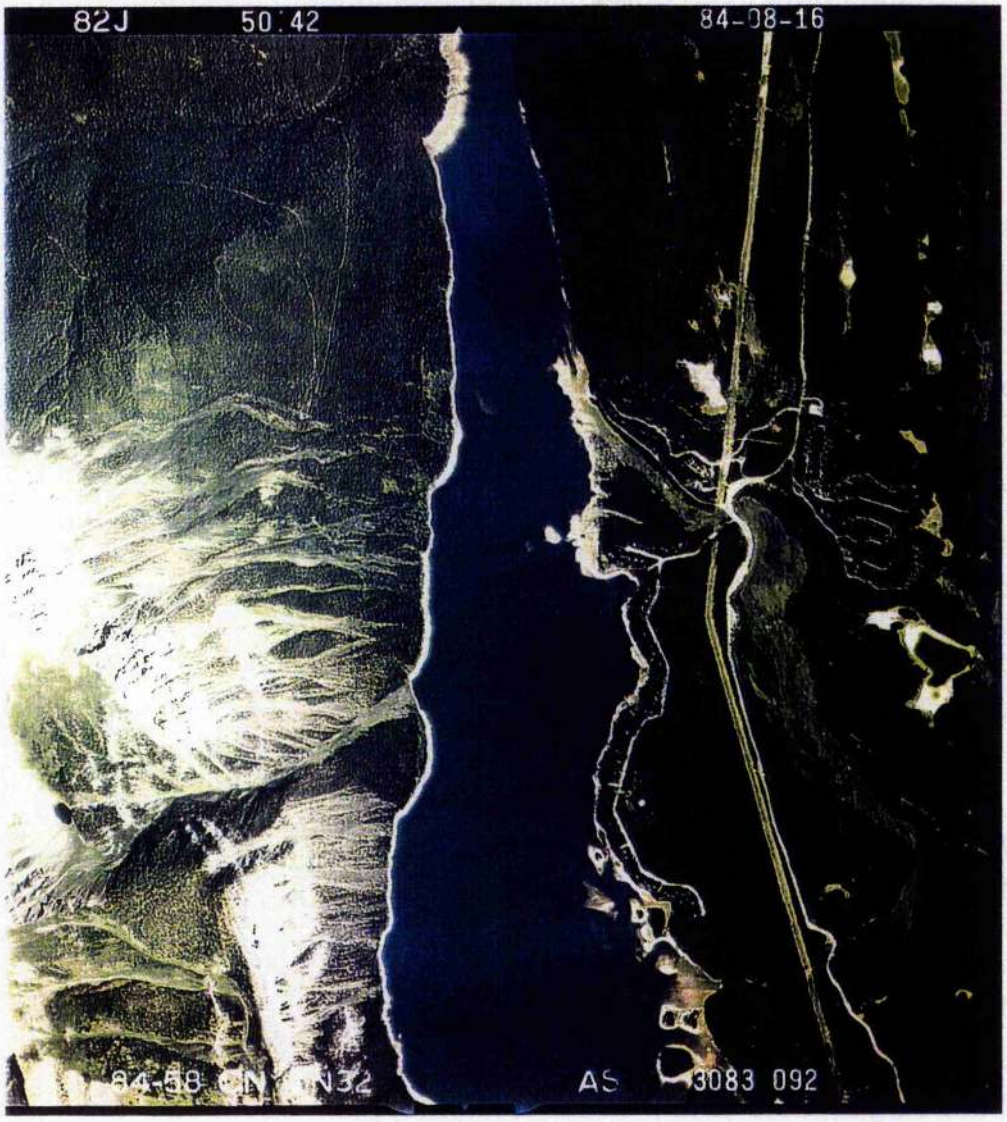

Figure 3.9 Land cover illustrations: Alpine communities

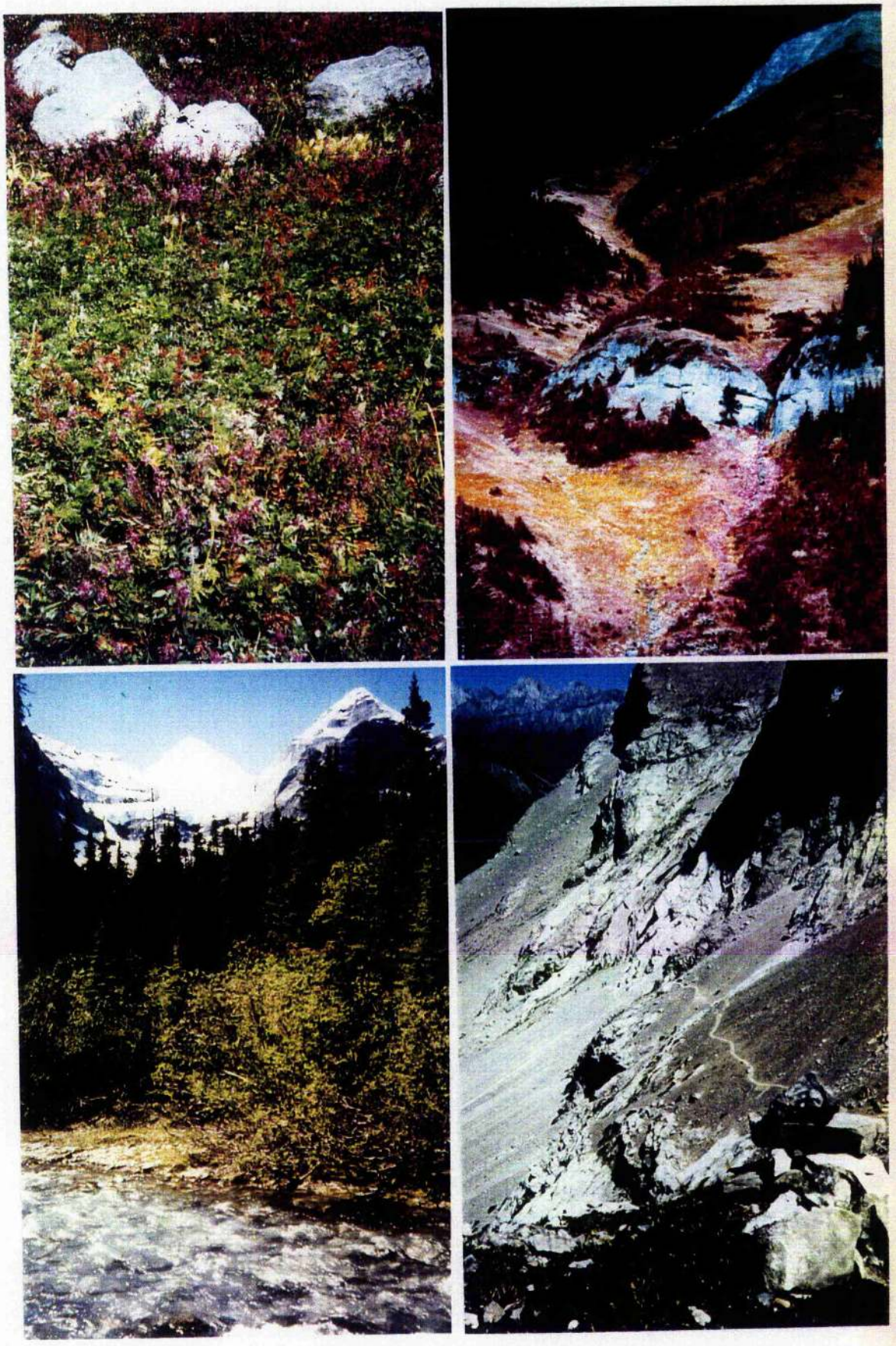

3.7 Relationship of topography and vegetation

While it is necessary to be able to separate the mixed effects of topography and surface cover, something we accomplish through experience with analogue models (aerial photographs), the surface cover in mountainous areas is causally linked to topographic variation. Most plant species are controlled by altitude as well as favouring areas of either lower or higher slope and illuminated or shaded aspects, with the associated drainage conditions. The darker north facing slopes result not only from shadows but also a preponderance of coniferous vegetation that enjoys or endures the cooler moister conditions compared to those on south facing slopes.

The effect of rugged topography is to create countless topoclimates which differ widely in slope and aspect effects (Barry and Van Wie, 1974). In addition to these components, there is a direct relationship on a larger scale between elevation and air temperature, ultraviolet radiation, length of growing season, snow cover duration and cloud cover. Other environmental factors controlling vegetative cover and dependent on topography include soil type and drainage conditions, available moisture, prevailing winds and avalanche events.

Slope and aspect (the vertical and horizontal components of terrain) affect the radiance recorded by a sensor in two ways: direct effects on the geometry of illumination and reflectance (the topographic effect) and indirect ecological effects. These effects have been described for an upland area in Wales by Thomson and Jones (1990). Differences in radiation receipts from slope and aspect affect precipitation received and held, soil moisture and soil temperature which consequently affect the distribution of vegetation.

Aspect is of great importance to vegetation growth patterns in mountainous areas with its direct link to the micro-climate of the steep sided terrain and connection with the reflectance angles of the sensed energy (Teillet *et al.*, 1982). Areas of adequate moisture supply typically show a pattern of forested slopes especially with northerly exposure, contrasting with grassland meadows on warmer dry south facing slopes.

On slopes of 50% (26.72 degrees) at 50 degrees latitude (the approximate latitude of this study area) the radiation received on south facing slopes is more than double that received on north facing slopes, rising to over quadruple on slopes of 100% or 45 degrees (table 3.2). Such contrasts are manifested in soil temperature differences and consequently in favoured vegetation species.

The effect of aspect through snow cover is equally significant, as snow accumulation provides protection from environmental extremes in winter and a moisture source well into summer. There is a close relationship between exposed ridges and severely restricted vegetation cover, which contrast with lusher growth in more sheltered sites.

Table 3.2 radiation index as a function of slope and aspect at 50 degrees north, expressed as a % of the radiation index for a horizontal surface (from Barry and Van Wie, 1974).

Aspect	10% (5°43')	50% (26° 43')	100% (45°)
N	90	56	33
NNE	91	59	38
NE	93	69	54
ENE	96	84	76
E	100	100	98
ESE	104	114	117
SE	106	125	130
SSE	108	131	139
S	109	133	142

3.8 Analysis of topography and its potential effect

Advances in digital image processing over have produced readily accessible software that enables the generation of several useful derived (GIS) layers from a digital elevation model (DEM), containing elevation values. These can be used both in analytical work and in topographic representation on cartographic products (Wheate, 1996). They include slope, aspect, incidence, and three dimensional perspectives views.

A. ELEVATION

Elevation ranges from 1600 metres (5300 feet) in the main Kananaskis Valley to peaks above 3000 metres (10000 feet), with a distinct treeline at an average height of 2200 metres (7000 feet), which fluctuates according to local slope, aspect and surface materials. Almost two-thirds (65%) of the area lies below 2000 metres, less than 7% above 2500 metres (table 3.3).

Table 3.3 Study area, analysis of elevation

Height Range (metres)	% of total
1600-1700	13.83
1700-1800	27.49
1800-1900	14.58
1900-2000	9.02
2000-2100	6.99
2100-2200	6.17
2200-2300	5.90
2300-2400	5.23
2400-2500	4.04
2500-2600	2.95
2600-2700	1.90
2700-2800	1.19
2800-2900	0.59
2900-3000	0.11
3000-3100	0.01

Figure 3.10 Distribution of slopes and aspects in the study area

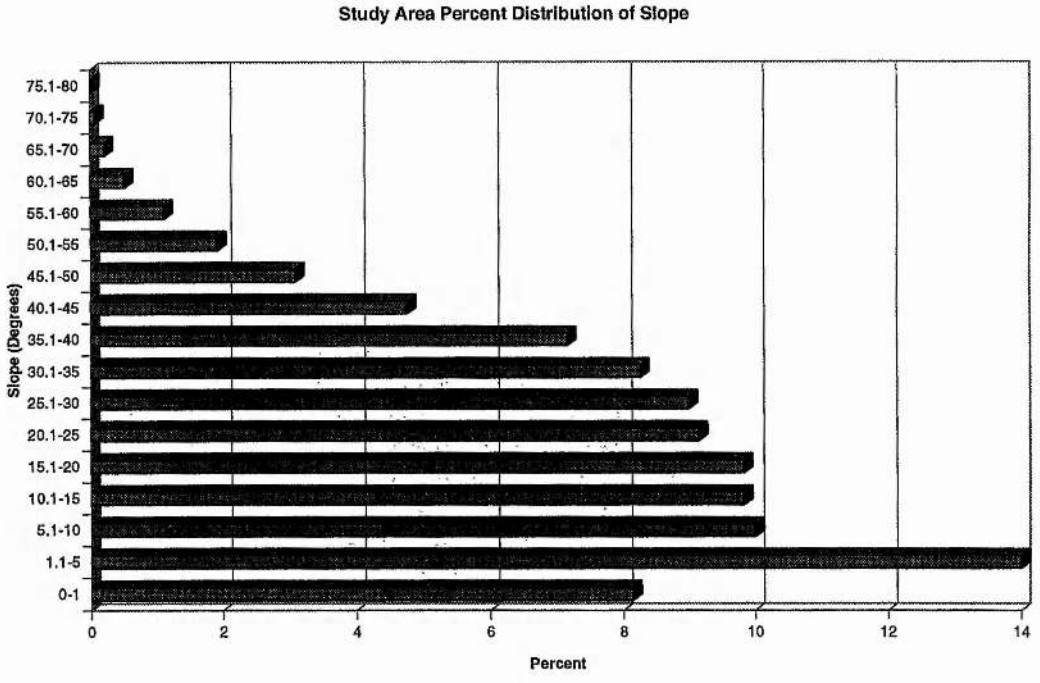

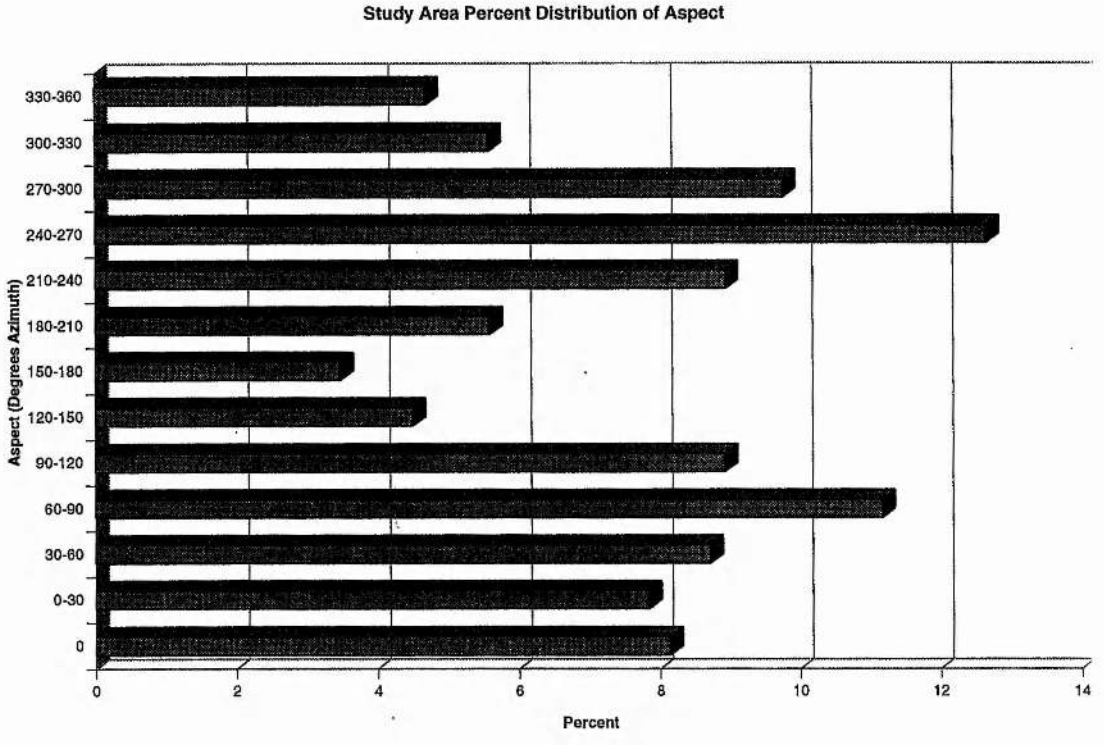

Figure 3.11 DIGITAL ELEVATION MODEL PRODUCTS
(Illustrations on following page)

Top left: elevation channel; pixel brightness is directly related to the elevation value it stores. Higher elevations are brighter, lower (valley) are darker. The two lakes differ in elevation by about 30 metres.

Top right: Steeper slopes show as brighter bands, which typically in mountains present semi-linear patterns associated with side walls.

Centre right: aspect (flat - no aspect is white; otherwise gray shades increase from black for azimuth 1 to near white for azimuth 360.

Centre left: incidence, digital numbers stored from 0-90 depending on angle between the sun and the surface in degrees.

Bottom: aerial view in winter (March 1994) taken from a plane looking at the study area from the northwest. Lakes are frozen and whole landscape is snow-covered but the snow is hidden by the forest canopy. The line in the foreground running into the scene is the Smith-Dorrien Road, connecting with Highway 40 in the left middle edge.

Figure 3.12 PERSPECTIVE VIEWS
(Illustrations on second following page)

Top: View from northwest, similar to photograph on the previous page.

Middle: View from the northeast. Avalanche tracks on the east slopes of Mount Indefatigable and Invincible are now apparent, and the spatial distribution of the alpine zone between the forested valley floors / lower slopes and bare rock above.

Bottom: View from southeast looking northwest, initially along the power line and towards Mount Indefatigable. The landslide (pink) and burn (orange-brown) can be seen on the north side of the Upper Lake and the geologic boundary on the slopes west of Hidden Lake is quite evident.

Figure 3.11 Digital elevation products (see legend on preceding page)

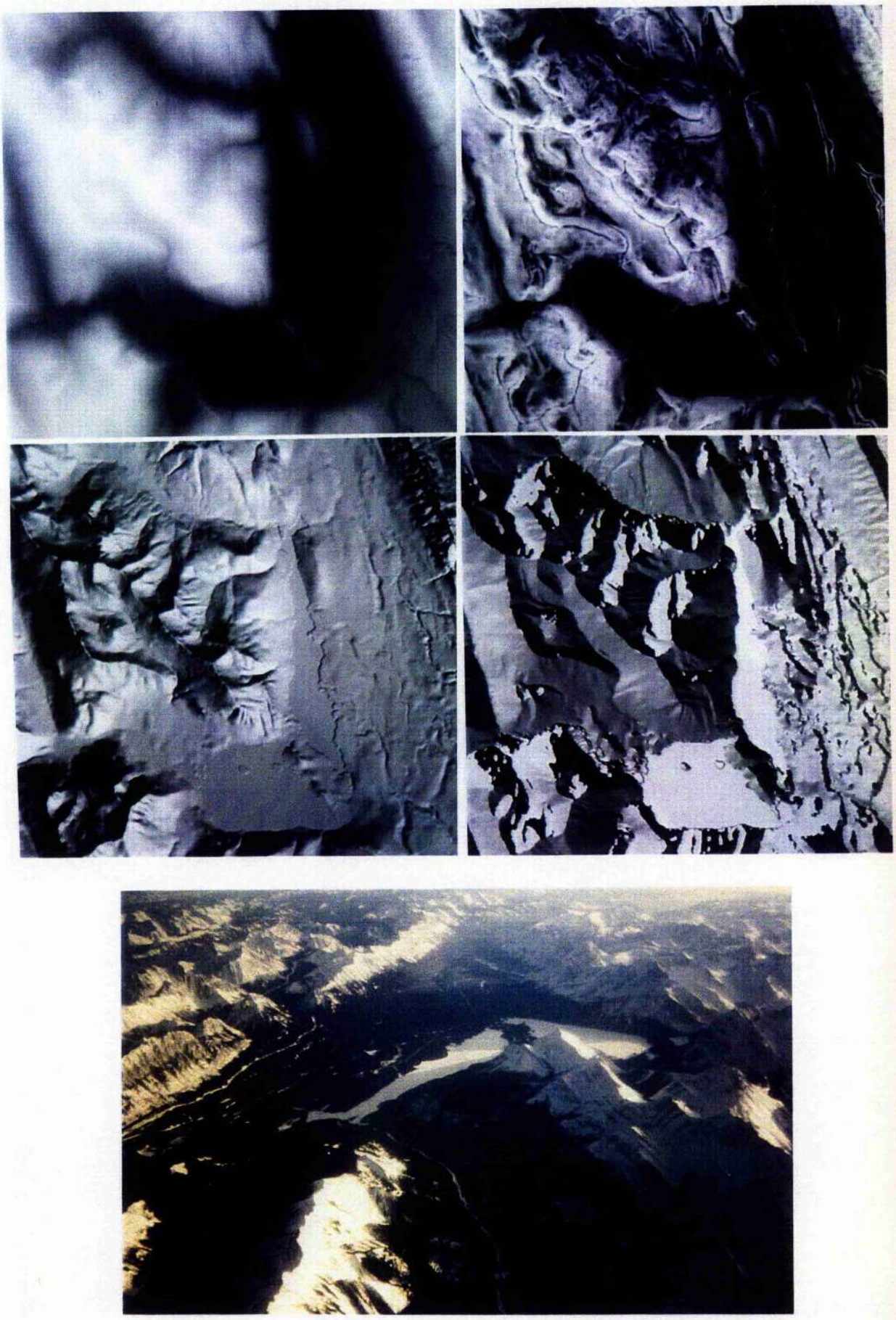

Figure 3.12 Three-dimensional perspective views

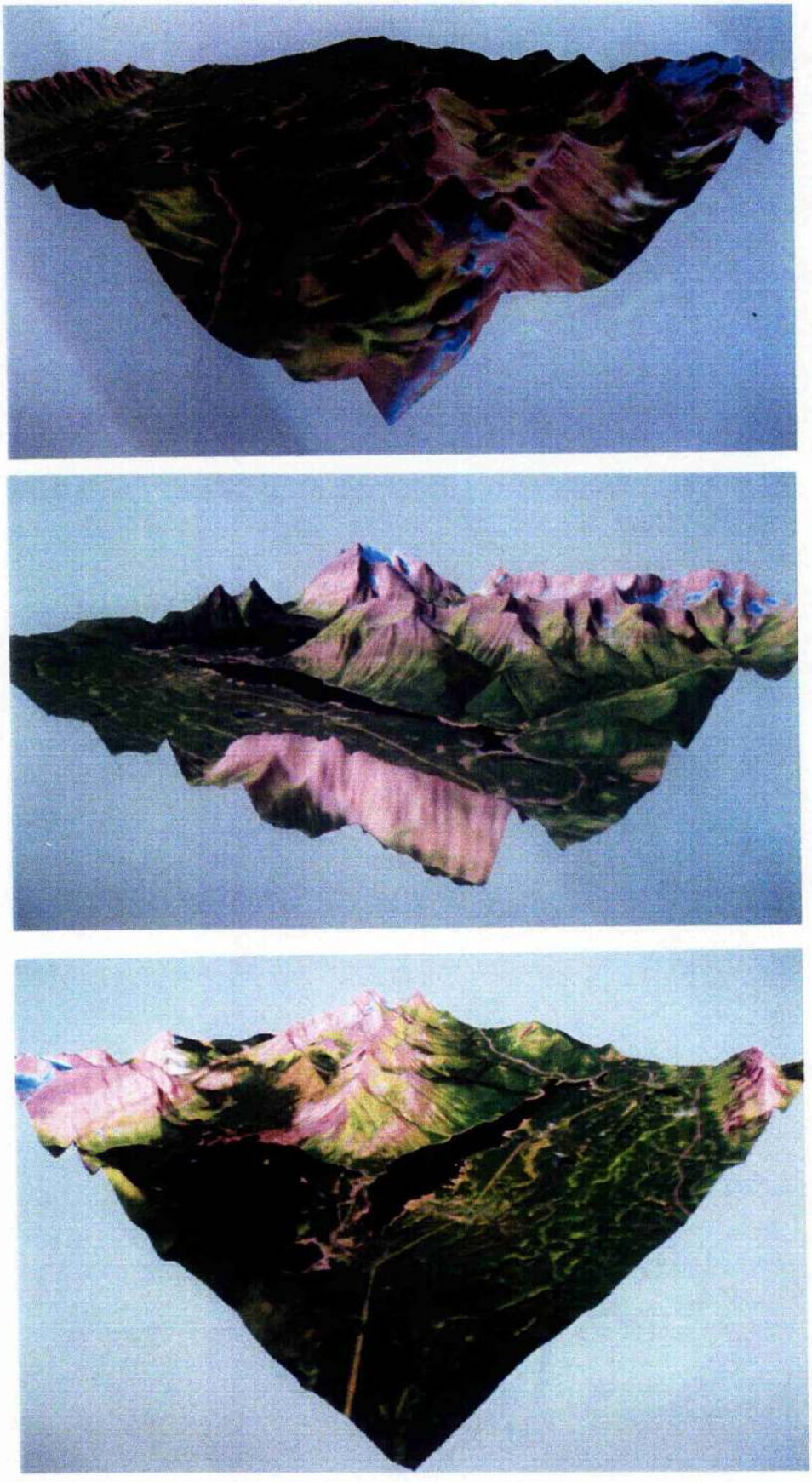

B. SLOPE

The average slope is around 20 degrees, with steeper slopes abundant at higher elevations and lower slopes associated with valley floors more common at lower elevations. About 8% of the area is covered by lakes and hence is completely flat, while a further 14% is under 5 degrees. The distribution of slopes and aspects is shown graphically in figure 3.10.

Table 3.4 Study area, analysis of slope

Degree of Slope	% of total
0-1 (flat)	8.14
1- 5	14.00
5-10	10.00
10-15	9.83
15-20	9.93
20-25	9.15
25-30	9.00
30-35	8.26
35-40	7.15
40-45	4.76
45-50	3.09
50-55	1.92
55-60	1.11
60-65	0.57
65-70	0.21
70-75	0.07
75-80	0.01

C. ASPECT

There is a marked maximum of slopes facing WNW and ESE, over double in frequency compared to slopes facing SSE and NNW as a result of the dominant mountain range trend. This has a significant impact on vegetation cover, since both temperature and moisture are influenced by

local aspect. In a randomly distributed landscape, one would expect each 30 degree sector of the compass to contain one-twelfth or 8.33% of all slopes; here however the percentage of slopes ranges from 3.3% for 150-180 azimuth or SSE, to 12.5% for 240-270 azimuth or WSW (table 3.5 and figure 3.10).

The solar azimuth in Landsat imagery for the northern hemisphere is always approximately southeast (as it is captured in the morning). It therefore is more normal than perpendicular to this bimodal distribution of slopes, and so one could surmise that the 'topographic effect' is actually less than it might be later in the day or on an equal landscape with different orientation. However this is true for most of western North America given the general consistent trend of the Rocky and Coastal Mountains, corresponding to the tectonic plate boundaries.

Table 3.5 Study area, analysis of aspect.
(Zero degree slopes are given an aspect of '0').

Aspect (degrees azimuth)	% of total
Flat (no aspect)	8.14
0- 30	7.84
30- 60	8.72
60- 90	11.17
90-120	8.93
120-150	4.50
150-180	3.48
180-210	5.59
210-240	8.94
240-270	12.65
270-300	9.76
300-330	5.58
330-360	4.69

D. INCIDENCE

In GIS and remote sensing analyses, a problem with using aspect lies in its circular scale, that is the two extreme values of 0 and 360 in fact represent identical slopes, not the most dissimilar. As a result, a more practical layer for analytical work can be found in 'angle of incidence' or a measure of the actual amount of solar radiation reflected from a surface based upon the geometry between the surface orientation (topography) and the angle of the sun, a function of height (zenith) and direction (azimuth). Incidence can be calculated as follows (Richards, 1984):

$$\text{Incidence} = \cos(S) + \sin(S) * \cot(E) * \cos(A)$$

where S is the angle of slope, E is the solar elevation angle and A is the difference between the slope aspect and solar azimuth.

Values will range from 0 (shadowed slopes) to 90 (slopes normal to the sun's rays). Incidence can be calculated for any possible combination of values for 'E' and 'A', based on the suns's azimuth and zenith, but it is usually desirable to replicate the conditions at the same moment that the imagery was captured. For Landsat imagery, time of day is always between 9.30 and 10 am local time, so that azimuth is almost constant with only the zenith varying with the seasons. For this scene, captured on August 5, 1984, the recorded sun azimuth was 138.1 degrees and zenith 49.3 degrees. Effectively the recreated incidence image reflects a function of the topographic input to the image. The majority of values are clustered around the mean but with sufficient variance to significantly impact on pixel DNs (table 3.6).

Table 3.6 Study area, analysis of incidence

Degree Range	% of total
0-10	1.73
10-20	3.81
20-30	8.49
30-40	13.80
40-50	39.88
50-60	20.67
60-70	7.49
70-80	3.24
80-90	0.89

The incidence image is virtually the inverse of a conventional shaded relief image (figure 3.3b) , which would be illuminated from the north-west (315 degrees azimuth). Consequently the incidence image may appear inverted to some viewers, with valleys showing as ridges and vice versa. In contrast to an incidence image, a shaded relief image is purely cartographic in that the values are scaled to fit an 8-bit range and only represent illumination in a relative sense.

E. THREE-DIMENSIONAL PERSPECTIVE VIEWS

An interesting consequence of having co-registered multispectral imagery and a digital elevation model is the possibility of generating perspective views (Jones *et al.*, 1988). These can be used for landscape assessment and planning, general educational tools and to visually assess the interaction of topography and vegetation. The views generated are based on several parameters, including the viewer's position in x, y and z, the desired field of view, horizontal and vertical angle of view in azimuth and zenith, and the degree of vertical exaggeration (figure 3.12).

CHAPTER 4

DATA PROCESSING AND IMAGE ANALYSIS I: GENERATION OF COMPONENTS AND RATIOS

4.1 Preprocessing

Certain steps must first be completed before Landsat data can be subjected to detailed analysis and for co-registration with ancillary data such as digital elevations and thematic maps. These are generally referred to as geometric and radiometric correction.

A. GEOMETRIC CORRECTION

Landsat image data upon collection is oriented along path track lines, offset from north-south and at a resolution of 30 metres on the ground. Conventionally this data is resampled to match a planimetric mapping system and at a 25 metre pixel resolution.

A portion of the 1984 TM scene quadrat was downloaded and geocorrected to the Universal Transverse Mercator (UTM) projection co-ordinates, which form the basis of the Canadian National Topographic Series of maps at 1:50,000 and 1:250,000. The geometric correction utilised the bilinear resampling method as a compromise between the jagged appearance of nearest neighbour corrections and the more complex radiance value modification of cubic convolution.

The pixels were resampled from their original 30 metre size to 25 metres both to better fit the UTM system and to conform with the provincial

digital elevation model data, which would be used in part to check the results obtained in this study. The Root Mean Square (RMS) error during the resampling process was less than half a pixel in X (0.46) and Y (0.47). A 768 x 768 pixel geo-corrected 7-band data set was created from which a 512 x 512 window was subset for ease of display on all systems. This represents a ground area of 12.8 x 12.8 milometres (8 x 8 miles) or about 164 square kilometres (64 square miles).

B. RADIOMETRIC CORRECTION

TM bands are differentially affected by atmospheric scattering, which is represented in images as haze. While some image analysis procedures can ignore this contribution which lightens pixels (or increases their DN), the procedure of band ratioing is extremely sensitive to this additive factor. Using the black-box pixel subtraction method described in chapter 2, the minimum digital number recorded is subtracted from each pixel in the area of study. For this area, values were as follows:

Table 4.1 Radiometric corrections to TM bands for haze

TM Band	**Min DN**	**Max DN**	**Correction**
Band 1	51	255	51
Band 2	15	255	15
Band 3	10	255	10
Band 4	4	251	4
Band 5	0	255	0
Band 6	87	146	n/a
Band 7	0	174	0

Hence 51, 15, 10 and 4 were subtracted from the digital numbers of bands 1 to 4 respectively. No correction was necessary for bands 5 and 7 and is inappropriate for band 6, since digital numbers are related to temperature rather than reflected energy.

The values derived were checked against those resulting from more sophisticated methods based on linear regression and covariance matrices, as described by Crippen (1988). The values thus derived were virtually identical to those using the simpler method, the same conclusion reached by Switzer *et al.* (1981). For example, the regression offset method utilises the offset value in a linear regression between two bands as the difference in value between the two bands to be subtracted for haze correction. If one of the bands has a zero correction, then the offset value becomes the amount to be subtracted. Hence these regression equations were derived between bands 7 and 3, between bands 1 and 3 and between bands 7 and 1 (independent variable listed first):

$y = 52.4 + .82x$ (1 - 7)

$y = 41.4 + 1.09x$ (1 - 3)

$y = 9.98 + .76x$ (3 - 7)

These confirm that the difference in correction between 1 and 3 is 41, between 3 and 7 is 10 and between 1 and 7 is between 51 and 52.

4.2 Preliminary data analysis

Prior to further analysis, a first step is to calculate the correlation between TM bands. As one would normally expect, there is a high correlation between the three visible bands, and between bands 5 and 7 in the middle infrared (table 4.3). Other correlations are medium, although the thermal band (6) is almost completely uncorrelated with the visible bands. One may conclude that TM data is essentially three-dimensional among the reflected bands and four dimensional when the thermal band is included. Band 6 is also distinguished by substantially

higher mean values and low variance, both indicative of its fundamentally different nature. These tables are used further both in interpreting the results of principal component analysis and in assessing appropriate spectral band ratios.

Table 4.2 TM band statistics

Band	Mean	Standard Deviation
1	27.27	30.36
2	18.67	19.18
3	23.95	26.78
4	51.91	23.62
5	60.58	43.17
6	119.05	7.21
7	28.26	27.34

Table 4.3 Between band correlations for TM bands (significant in bold)

TM Band	1	2	3	4	5	6
1						
2	**.972**					
3	**.976**	**.993**				
4	.468	.564	.568			
5	.637	.603	.658	.629		
6	-.059	-.025	.012	.423	.466	
7	.720	.663	.720	.484	**.968**	.356

4.3 Band ratios

With six TM bands, it is possible to generate 15 different ratios and their reciprocals but ratios between bands that are highly correlated such as 1, 2 and 3 yield little useful information, leaving the eleven ratios in table 4.4 . All ratios were calculated first using the 8-bit digital numbers of the TM bands and secondly their raw radiance values, as

some authors claim this is important for 'true' ratio values. However no significant difference was found either in the visual appearance of the ratio images, nor in the statistical distribution of their pixel values. As a result, it was not considered necessary to look any further into the radiance values.

Table 4.4 Main band ratios products examined

Band ratio	Mean	Std. deviation
4/1	39.72	25.75
4/2	68.19	37.37
4/3	70.10	42.29
5/1	48.65	22.16
5/2	54.74	19.57
5/3	101.05	36.75
7/1	52.77	20.08
7/2	33.52	12.60
7/3	76.44	22.94
7/4	22.31	11.49
5/4	24.14	11.93

Table 4.5 *Class Correlation Matrix for selected band ratios*

Ratio	4/1	4/2	4/3	5/1	5/2	5/3	7/1	7/2	7/3	5/4
4/1										
4/2	.96									
4/3	.96	.96								
5/1	.88	.85	.80							
5/2	.67	.75	.63	.90						
5/3	.84	.86	.85	.94	.90					
7/1	.53	.52	.42	.89	.84	.76				
7/2	.06	.14	.001	.46	.72	.45	.83			
7/3	.34	.38	.32	.66	.82	.72	.90	.90		
5/4	-.70	-.70	-.74	-.40	-.14	-.38	.074	.50	.26	
7/4	-.72	-.72	-.75	-.46	-.22	-.46	.026	.46	.22	.97

This still leaves a possible 165 combinations of three ratios (11*10*9/ 6), which can be reduced since while all band ratios eliminate the topographic effect to some degree, many are highly correlated, displaying the same features as other ratio channels. It is possible to find the best 3 ratio band combination in terms of non-redundancy and information content by determining the 'Optimum Index Factor' (OIF) for potential combinations. This is given for any 3-band combination as the sum of their three standard deviations, divided by the sum of the three correlations between each pair, added absolutely, without regard to positive or negative sign (Sheffield, 1985). It can be written thus:

$$OIF_{abc} = \Sigma (s_a + s_b + s_c) \; / \quad | \Sigma (r_{ab} + r_{bc} + r_{ac}) |$$

The optimum then is likely to result from a combination that provides a high numerator and/or a low denominator. Ratios which tend to have larger variance will reduce the need to stretch the data values which can induce more noise. Ratios which are not highly correlated to each other will contain different information. Logically, similar ratios which combine bands from the same two of the three spectral groups (1-2-3, 4 and 5-7) will be highly correlated, for example 7/1 , 5/2 and 7/3. An optimum combination would thus consist of three ratios, where each one represents a ratio between two of the three groups, *e.g.* 4/1, 7/1 and 5/4.

The possibilities can be further reduced by ackowledging the similarity of 4/1, 4/2 and 4/3 and also 5/4 and 7/4. We will accept 4/3 given its importance in vegetation discrimination as a ratio and vegetation index, and also because in this instance both 4/1 and 4/2 appeared to retain some topographic effect. We will also accept 5/4 over 7/4 as it has a higher variance, and because band 5 has greater application than band 7

in vegetation sensing. In this case 5/4 is also visually less noisy than 7/4. OIF scores are tabulated below for the resulting possible combinations:

Table 4.6 Optimum Index Factor scores for 3-ratio combinations

Ratio 1	Ratio 2	Ratio 3	∑Num	∑Denom	OIF
4/3	5/1	5/4	76.38	1.94	39.37
4/3	5/2	5/4	73.79	1.47	50.20
4/3	5/3	5/4	90.97	1.97	46.18
4/3	7/1	5/4	74.30	1.23	60.41
4/3	7/2	5/4	66.82	1.26	53.02
4/3	7/3	5/4	75.73	1.29	58.71

On this basis, it can be concluded that the best 3 channel band ratio combination containing the most information is 4/3, 5/4 and 7/1. These are displayed in figures 4.1 and 4.2. Ratio images of this landscape, while clearly differentiating between vegetated and non-vegetated areas, generally appear to be inherently noisy within forested areas, in that they contain random variations in pixel intensity. The 4/3 ratio however contains a particularly useful feature, in that it naturally separates land cover into four general groupings, if the process truncates the real numbers generated by dividing the digital numbers in band 4 by band 3. These appear in increasing lightness from black to near white, although the distinction may not have reproduced as clearly in figure 4.2b:

DN	Shade	Vegetation cover
0:	black	no vegetation- rock and water
1:	dark gray	alpine tundra and grassland, including roadsides
2 :	light gray	coniferous forests
3+:	white	deciduous shrubs and trees

These groups can potentially be further refined to separate vegetated and non-vegetated surfaces by setting more precise threshold boundaries or by using the normalised ratio, also known as the normalised difference vegetation index or 'NDVI' (figure 4.3a). Small 'outliers' can be eliminated by using a 'filter' or 'sieve' that removes those below a selected threshold size (figure 4.3b). This can also be performed using similar operations in a raster geographic information system (GIS), that recognise contiguous groupings of similar pixels and allows the user to select desired groupings by number.

Bare rock and water surfaces, while similar in lacking vegetation are obviously fundamentally different in surface type; bare rock is strongly influenced by the effects of topography, while water surfaces have zero slope and aspect. They can be separated by combining the above 'density slice', with a density slice of an infra-red band, in which water surfaces have very low or zero reflectance. Band 4 is often the best in mountainous environments as ice and snow also have low reflectance in bands 5 and 7. By overlaying this image with the 4/3 ratio, water can be separated from bare rock since water is low or zero in both, while bare rock has zero values in the ratio but high values in band 4 (figure 4.4).

Figure 4.1 Band ratios: 5/4 (above) and 7/1 (below)
Note that undesirable striping on the lakes can be removed by overlaying the ratio with a binary mask for water (see figure 4.4b)

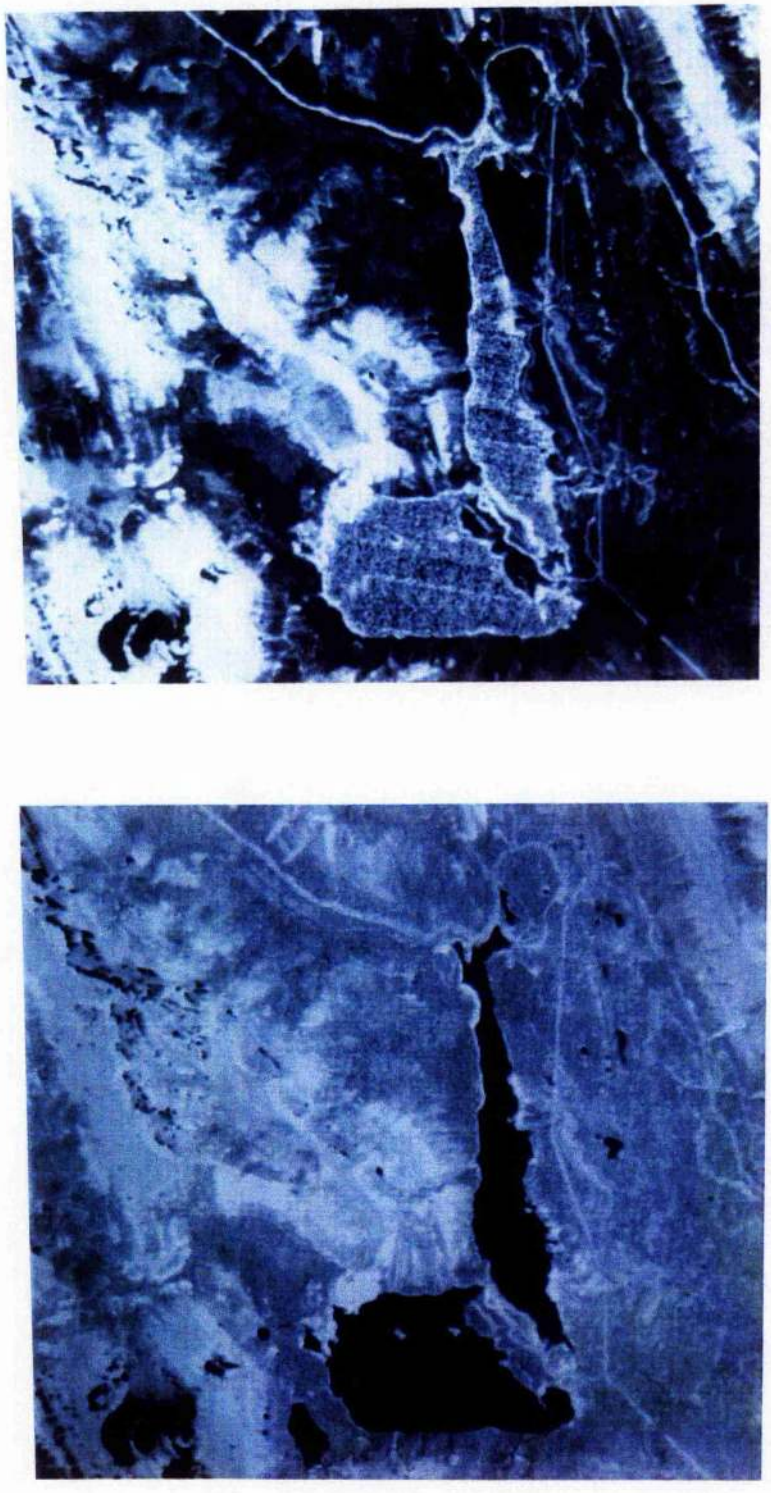

Figure 4.2 Band ratios 4/3:
8-bit stretched values (above) and unstretched values 0-4 (below)

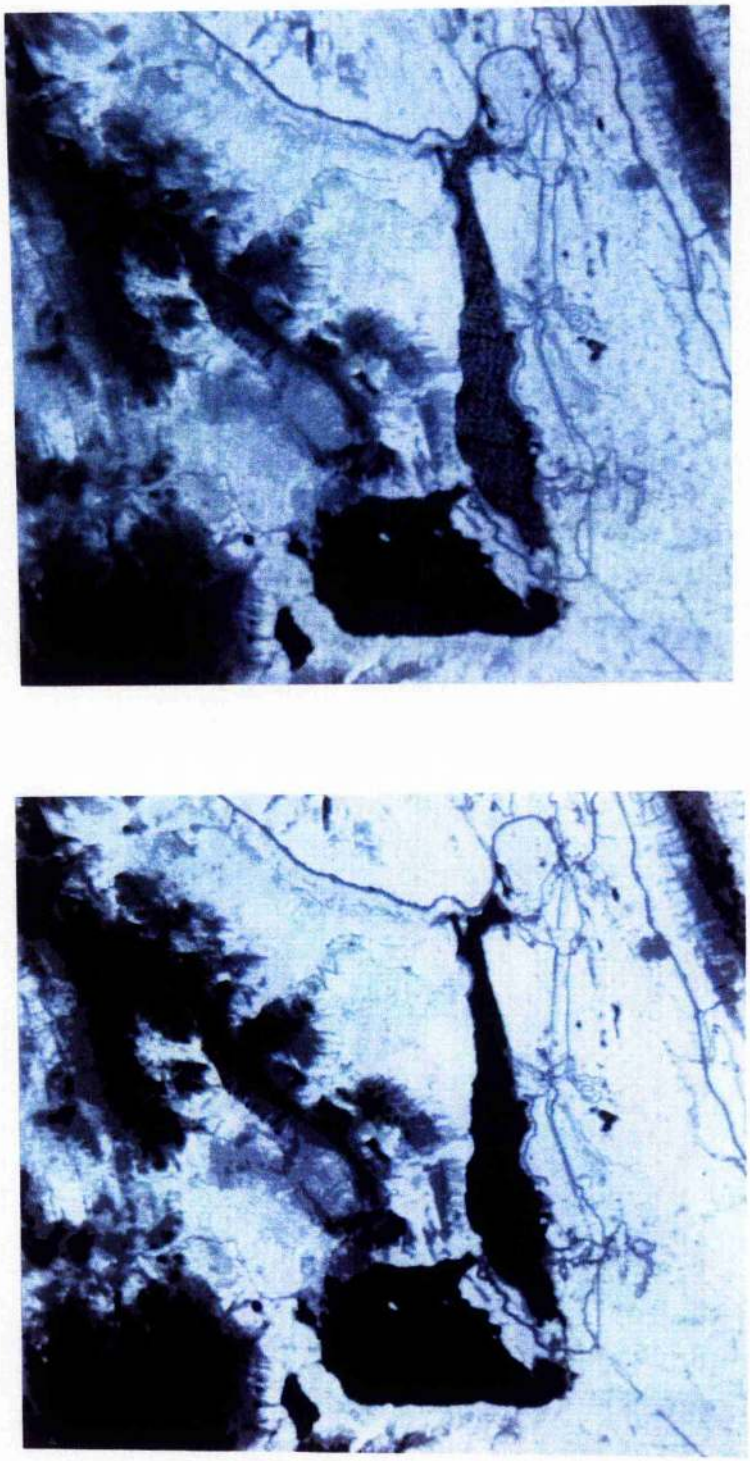

Figure 4.3 Binary mask from 4/3 separating vegetation from non-vegetated, initial image (above) and 'sieved' (below): black = vegetated

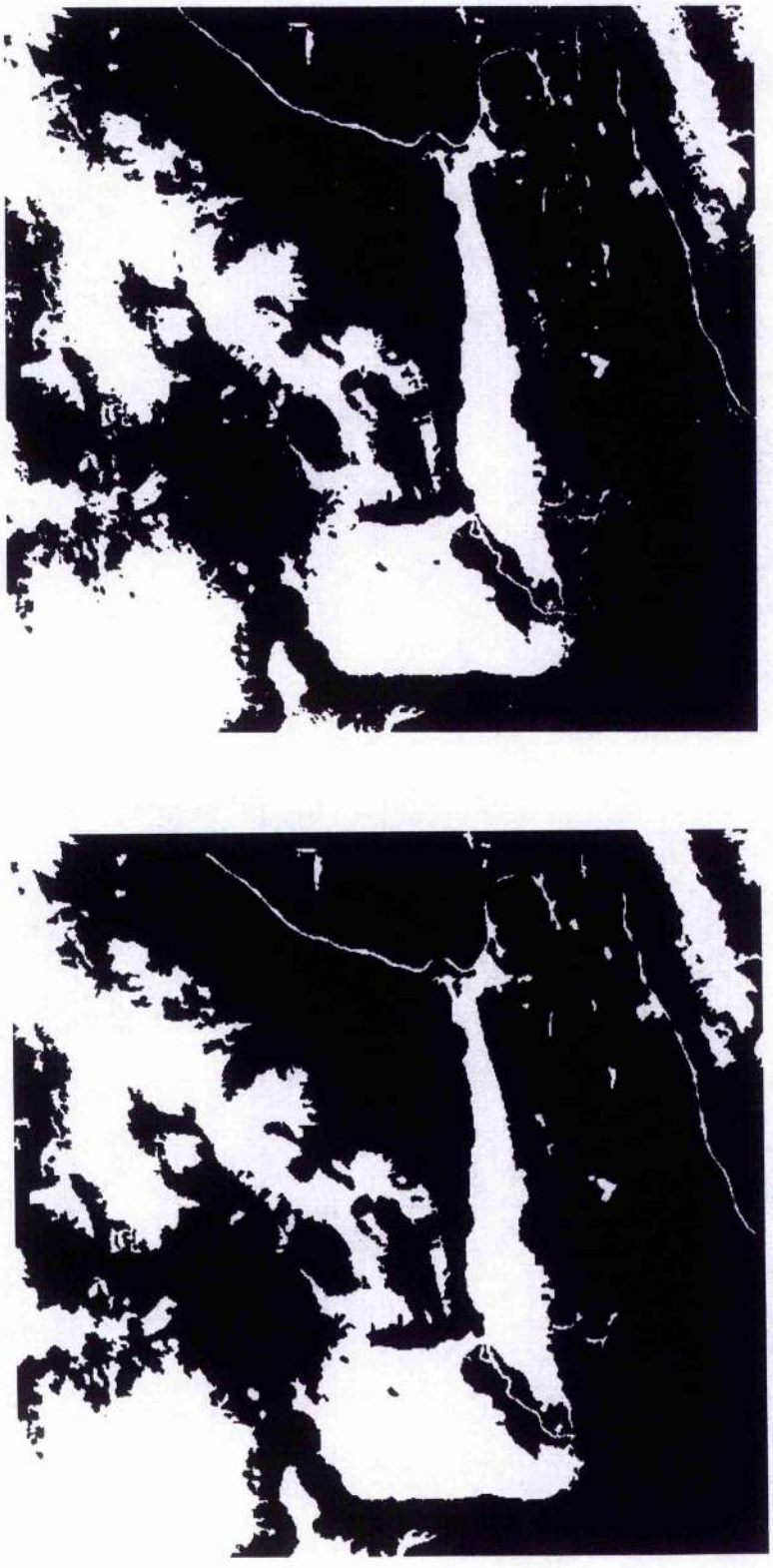

Figure 4.4 Binary mask for vegetation (above) and water (below)
above: Black is water and bare rock; hence vegetated = white
below: water = black

4.4 Principal Component Analysis (PCA)

A. INITIAL PCA PROCESSING

The first three components account for over 99% of total scene variance, from which one might surmise that components 4 to 7 contain little useful information. This figure is consistent with other studies in similar alpine and forested area, as listed in table 2.2.

Table 4.7 PCA eigenvalues and variances

Eigenchannel	Eigenvalue	Standard Deviation	%Variance of total scene
1	4051.15	63.65	77.51
2	768.22	27.72	14.70
3	357.87	18.92	6.85
4	27.75	5.27	0.53
5	14.37	3.79	0.27
6	5.52	2.35	0.11
7	2.03	1.42	0.04

Table 4.8 Eigenvectors of covariance matrix

Band	PC1	PC2	PC3	PC4	PC5	PC6	PC7
TM1	.413	-.529	-.154	-.118	.712	.061	.048
TM2	.256	-.357	.061	.133	-.304	-.234	-.799
TM3	.372	-.441	-.035	.209	-.535	-.068	.576
TM4	.249	.080	.916	-.138	.068	.262	-.012
TM5	.632	.561	-.096	-.116	.050	-.508	.055
TM6	.033	.154	.099	.944	.272	.003	.002
TM7	.404	.234	-.337	.034	-.185	.781	-.153

The eigenvectors indicate the extent to which each TM band affects each component channel, but do not take into account the overall variance of the eigenvalues, which decreases steadily from PC1 down to PC7, with a standard deviation about 50 times smaller. For example while bands 2 and 3 appear to be the main influence on PC7, this channel accounts for only .04% of total scene variance. It is generally more informative to convert the eigenvectors to 'loadings' so that we can see directly the influence of bands on components and their role in the scene as a whole. This is performed by making the following conversion, which effectively computes the correlation of each band k with each component p as described by Jensen (1986):

$$L_{kp} = E_{kp} * sd_p / sd_k$$

where:

L_{kp} is the loading for band k on component p

E_{kp} is the eigenvector for band k on component p

sd_p is the standard deviation for eigenchannel p

sd_k is the standard deviation for band k

For example, TM1 on PC1, the new loading = .413 * 63.65 / 30.36 = .867

The resulting table shows that this procedure greatly reduces the value of the lower component loadings; indeed many are close or equal to zero. These values are also depicted graphically in figure 4.5 in an attempt to clarify the relationship between the TM bands and the components. The original Thematic Mapper bands and the resulting component images are shown in figures 4.6 and 4.7.

Figure 4.5 PCA loadings from TM bands 1-7.
(above) as 'flat' graph, (below) as 3D graph

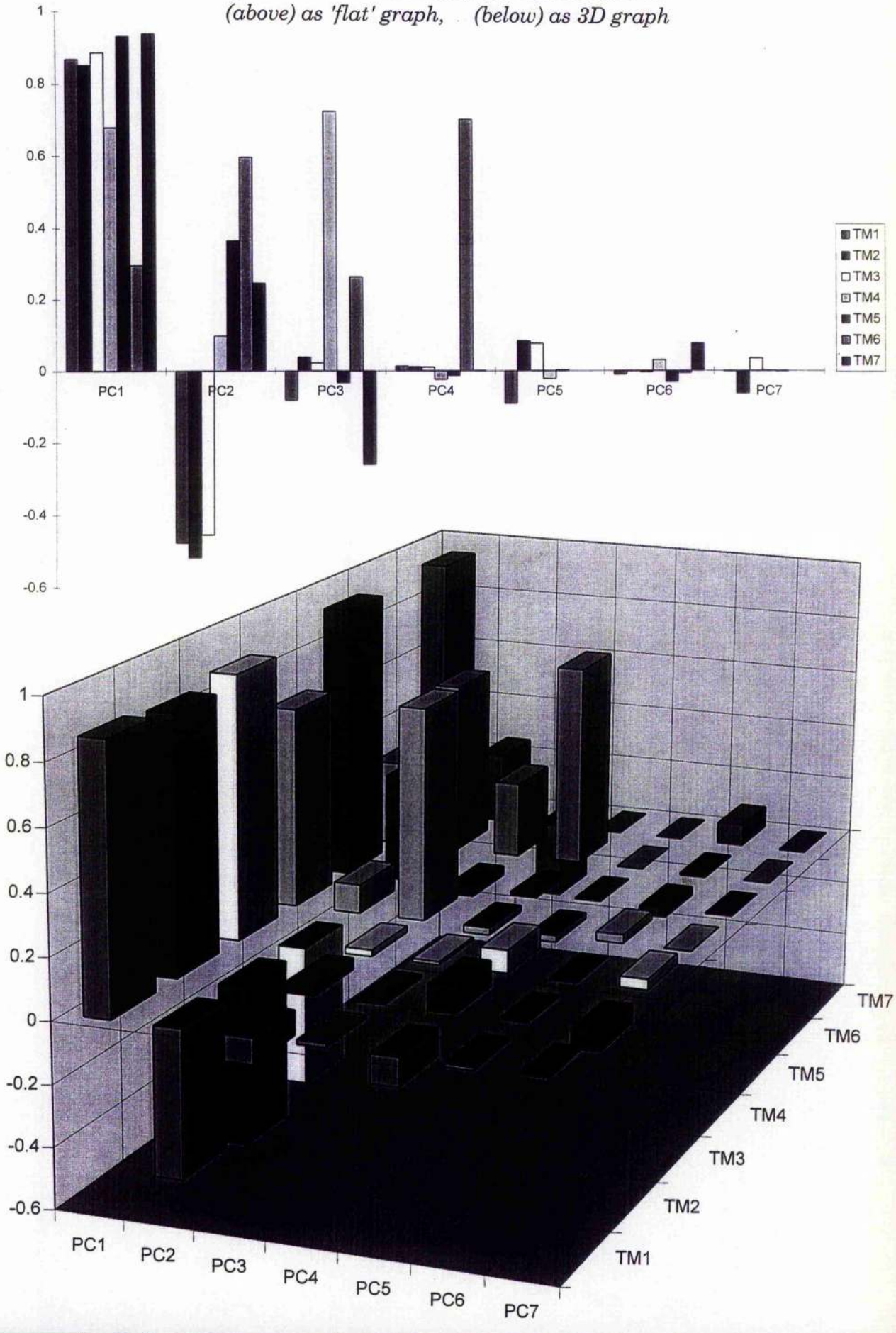

Figure 4.6 TM bands and principal components
Top: bands 3 and 4, Middle: bands 5 and 6, Bottom: PC1 and PC2

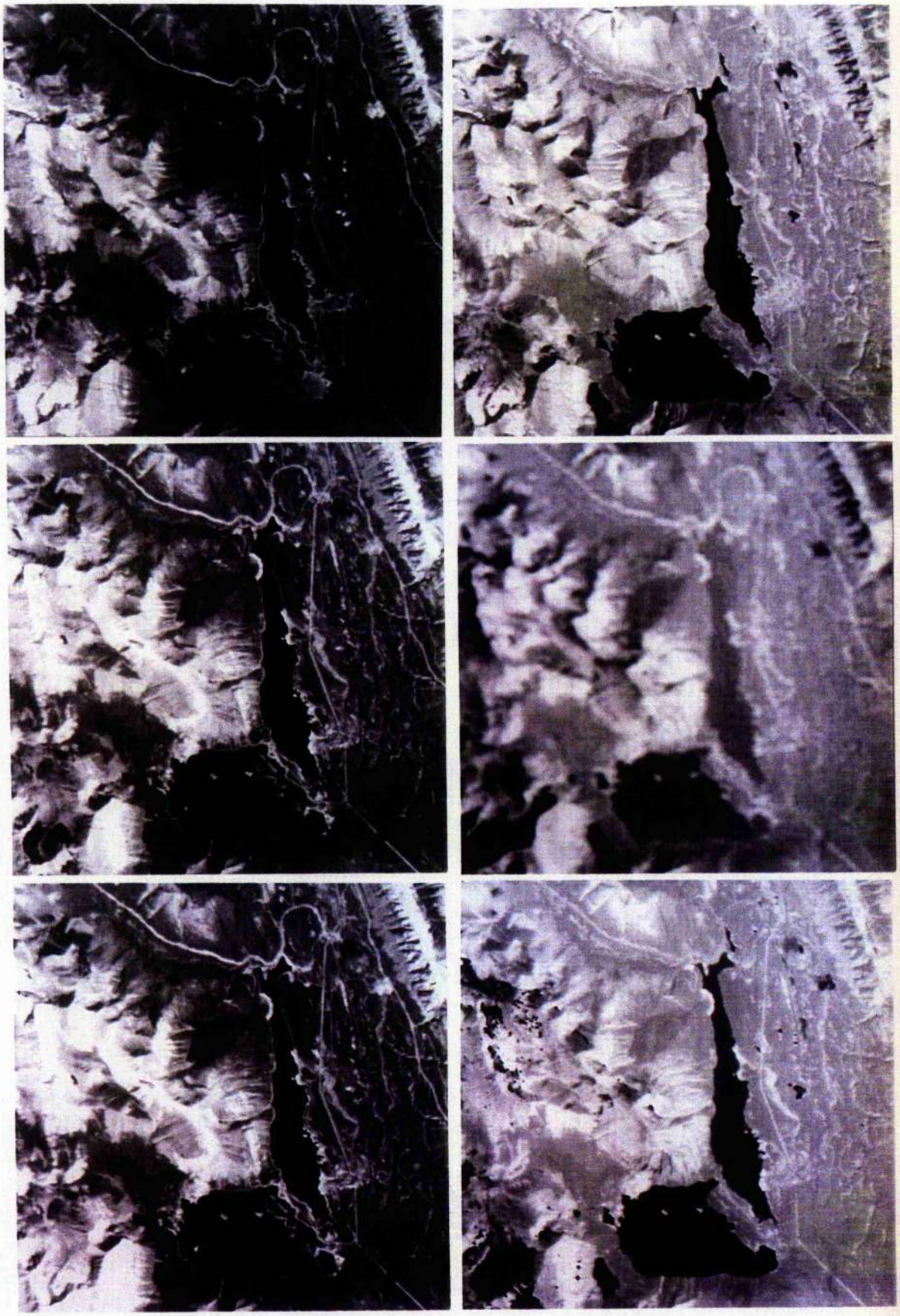

Figure 4.7 Principal components (continued)
Top: PC3 and PC4, Middle: PC5 and PC6
Bottom: PC7 and colour composite of PC1, PC2 and PC3.

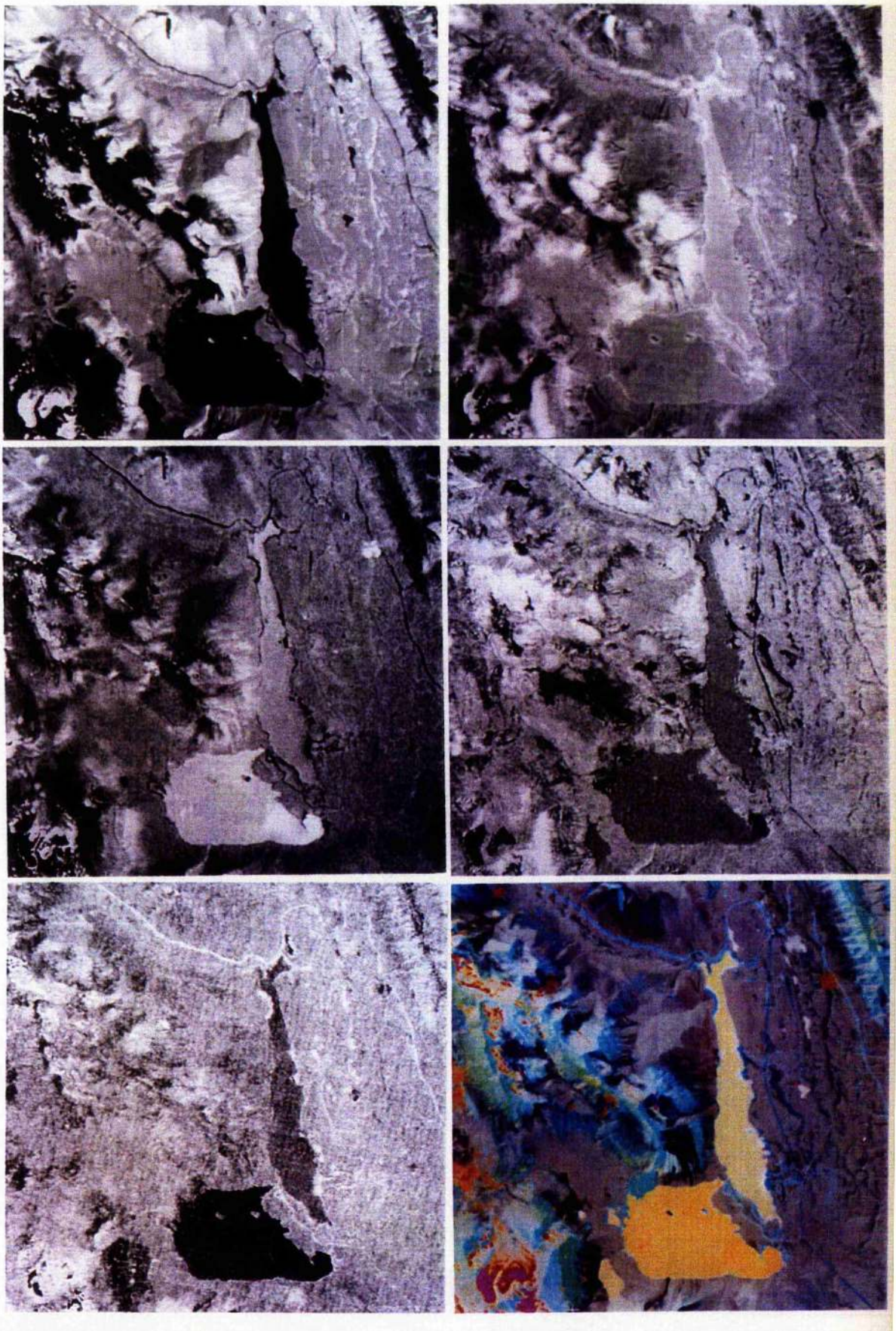

Table 4.9 PCA factor loadings, significant values in component in bold

Band	PC1	PC2	PC3	PC4	PC5	PC6	PC7
TM1	**.867**	**-.478**	-.082	.013	**-.091**	-.010	-.001
TM2	**.851**	**-.518**	.038	.011	**.084**	-.001	**-.063**
TM3	**.885**	**-.456**	.022	.010	**.076**	-.004	**.035**
TM4	**.678**	.098	**.722**	-.024	-.022	.030	.001
TM5	**.930**	.364	-.033	-.013	.003	**-.031**	-.001
TM6	.295	.595	.263	**.699**	.000	-.006	.000
TM7	**.937**	.245	.261	.001	.000	**.076**	.000
Summary	All bands	Vis. v IR	Near IR	Thermal	1 v 2,3	5 v 7	2 v 3

B. INTERPRETATION OF COMPONENT IMAGES (figures 4.5 to 4.7)

First principal component: PC1 (brightness)

This is simply the weighted sum of all the bands and explains almost 80% of the total scene variance. The bands contribute approximately the same to PC1, though the weighting from the longer infrared bands is slightly higher than from the visible bands. This is probably due to the predominance of the forest cover because this balance was reversed in a previous study for an overlapping area that contained more bare rock (Wheate and Franklin, 1991). This component image emphasises topography and geologic structure: the strata boundaries are particularly evident west of Hidden Lake, but lakes, shadows and forest vegetation are not clearly separated from each other, nor are vegetation classes clearly distinguished.

Second principal component: PC2 ('swirness')

This component, containing just under 15% of the scene variance is loaded by the difference between the visible and longer infrared bands (5-7), referred to as 'swirness' by Ahearn and Horler (1986). In their study area, which was completely forested, this was the third component which is the general case in non-alpine environments. Here this component appears primarily to highlight snow and glacier areas, as a result of their low reflection in longer wavelengths; this feature has been shown to be useful to map and inventory glacier areas (Sidjak and Wheate, 1996). In contrast, vegetation, hydrologic and geologic features are poorly represented, but the suppression of topography allows clear distinction between lakes and shadows.

Third principal component: PC3 ('greenness')

Greenness was the second principal component with MSS data, describing the difference between the visible and infrared bands. For TM data, it is primarily loaded by band 4, and indicates the contribution made by this band to the scene that is not present in the other bands, visible or mid infrared. This component looks to have the greatest amount of vegetation information, conforming with similar studies in other areas. Coniferous and deciduous stands are easily discriminated, as are the differences between avalanche slopes and alpine meadows, pine and spruce stands. Bare rock and soil show as darker areas, highlighting adjacent meadows and snow patches. The roads appear as dark strips running through vegetated areas. However the 1967 burn, northwest of the Upper Lake, can be more readily distinguished in PC1 and PC2 while geologic and topographic features have been visually suppressed.

Fourth principal component: PC4

PC4 is loaded almost entirely by the thermal channel, but maintains resolution equivalent to the other channels. Most researchers have excluded TM6 because it has such different properties, but it seems to exhibit some potential information pertaining to high soil moisture and high organic content, which in summer daytime have relatively lower temperatures than surrounding areas. This could also be a factor in identifying sedge and grass dominated valley environments which have similar spectral qualities to other deciduous areas, but have much lower slope gradients than alpine meadows and sub-alpine gully flanks. The image however retains a fair amount of topographic related information since the slopes are differentially heated according to slope and aspect.

Fifth principal component: PC5 ('blueness')

PC5 represents the difference between TM1 (blue) and the other two visible bands (green and red) and accounts for .27% of scene variance. It repeats some features identified on higher components, such as roads and unvegetated shorelines, as well as sediment patterns in the upper lake, also evident on TM1. However, feature recognition is becoming affected by noise, which is usually the case when the percentage of scene variance for a component drops below 1%.

Sixth principal component: PC6

The table indicates that PC6 presents the difference between the two longer infrared bands 5 and 7 and accounts for .11% of the scene variance. This image appears to be almost 'topography-free' and small lakes can be discriminated from shadows as on PC2. Visual noise, mostly in the striping seen also on PC5 is becoming more pronounced.

Seventh principal component: PC7

PC7 is loaded by the difference between bands 2 and 3 ('redness'). While being dominated by noise which is contributed to by sensor scan patterns, the most noticeable feature is the distinction between the Upper and Lower lakes, also visible on PC5. This may be related to a difference in sediment load in the two lakes, the upper being fed by glacier meltwater streams.

Principal component colour composite

Since the first three components explain more total scene variance, a colour composite composed of PC1, PC2 and PC3 technically contains more information than a colour composite of any three original bands. However, this is negatively compensated by the unfamiliarity of the image as seen in figure 4.7 (bottom right). Replacing PC1 with a lower component reduces the topographic effect but is likely to introduce a significant noise element and an even greater degree of unfamiliarity.

C. EFFECT OF OMITTING TM BAND 6

Omitting the thermal band from a principal components analysis in accordance with similar contemporary research, primarily eliminates one component, here PC4, which accounts for about half a percent of the scene variance, which by logic reverts back mostly into the first component. In addition, the contribution of band 6 to PC2 and PC3 has been removed. Interpretation of other components remains unchanged from the analysis using all seven bands, as loadings involving the other six bands are not substantially changed in value, only in sign (positive or negative), which is not by itself significant in principal components analysis.

Table 4.10 PCA eigenvalues and variances excluding Band 6 (thermal)

Eigenchannel	Eigenvalue	Standard Deviation	%Variance
1	4046.77	63.61	78.20
2	750.74	27.40	14.51
3	354.45	18.83	6.85
4	15.39	3.92	0.30
5	5.52	2.35	0.11
6	2.03	1.42	0.04

Table 4.11 Factor loadings (with thermal band excluded)

Band	PC1	PC2	PC3	PC4	PC5	PC6
TM1	**.869**	**-.474**	-.094	**-.091**	-.008	-.001
TM2	**.853**	**-.516**	.029	**.084**	-.001	**-.063**
TM3	**.887**	**-.454**	.013	**.076**	-.004	**.035**
TM4	**.677**	.086	**.735**	-.023	.024	.001
TM5	**.929**	.366	-.036	.004	**-.029**	-.001
TM7	**.936**	.253	-.230	.000	**.073**	-.000

D. USE OF PRINCIPAL COMPONENTS IN LAND COVER CLASSIFICATION

PCA has reduced the dimensionality of the seven band data set, down to three channels that between them contain more information than any three original TM bands, but they are not necessarily any better for land cover classification. PC1 as the weighted average of bands 1 to 7 offers few advantages in classification, but its isolation from the remaining components has similarly removed the topographic information contained within, as well as some obvious land cover information. PC2 is of limited interest except in hydrologic studies and it too has retained some topographic elements. PC3 however appears to be almost

topography free, displaying bare rock surfaces on opposite mountain sides in even tones, and enhancing contrast in the forested valley floors. Some vegetation differences however are not evident, such as the 1967 burn. All the other components are adversely affected by a low signal-noise ratio or continue to carry the effects of topography.

4.4 Selective principal component analysis

Continued investigation sought additional channels for the generation of topography-free image data for interpretation via the technique of 'directed principal component analysis'. Chavez and Kwarteng (1989) used this technique to enhance mineral deposits in a semi-arid environment by isolating the second principal component of selected band pairs, (which should be correlated to the ratio between those two bands). The second and subsequent components contain information that is otherwise overwhelmed by the contents of the first component. Hence instead we choose the second principal component from each combination of two from three of the major TM band groupings. These are:

Visible and Near IR:	Bands 1,2,3,4
Near and Short Wave IR:	Bands 4,5,7
Visible and Short Wave IR:	Bands 1,2,3,5,7

The following analyses were performed twice: once on the whole image and once using the vegetated areas as a 'mask' in order to maximise vegetation differences, which are of more interest than in non-vegetated areas (figure 4.4). This technique has been used effectively to map glacier surfaces in an alpine environment by selecting a mask covering glacier regions only and hence ignoring the influence of the dominant surrounding vegetated areas (Sidjak and Wheate, 1996). However in this

case, the use of the mask seemed to make only cosmetic differences, possibly because vegetated areas cover more than 50% of the study area, whereas in the former study area, glacier areas formed a smaller percentage of the total area subjected to analysis. However, it is felt that such a mask may play a role in other image analysis operations in a varied environment.

A. VISIBLE AND NEAR INFRARED

The first component is once again a weighted average of all the bands included in the task and thus resembles the contributing TM bands. The second component is closely equivalent to PC3 using all six or seven bands, being the difference between band 4 and the three visible bands and like the overall PC3 is largely free of topography, but fails to identify all land cover types, and to distinguish water from snow and ice (figure 4.8a). This image is slightly preferred over PC3 for its slightly higher detail and thus will be retained and subsequently referred to as PC-X. Eigenvalues and loadings are shown below:

Table 4.12 Eigenvalues from selective PCA for bands 1,2,3,4

Eigenchannel	Eigenvalue	Std deviation	%variance
1	2168.4	46.57	84.56
2	376.9	19.39	14.66
3	16.5	4.06	0.64
4	3.6	1.89	0.14

Figure 4.8 Selective principal component images
Above: second component of bands 1,2,3,4 ('PC-X')
Below: second component of bands 4,5,7 ('PC-Y') 'B' marks the 1967 burn

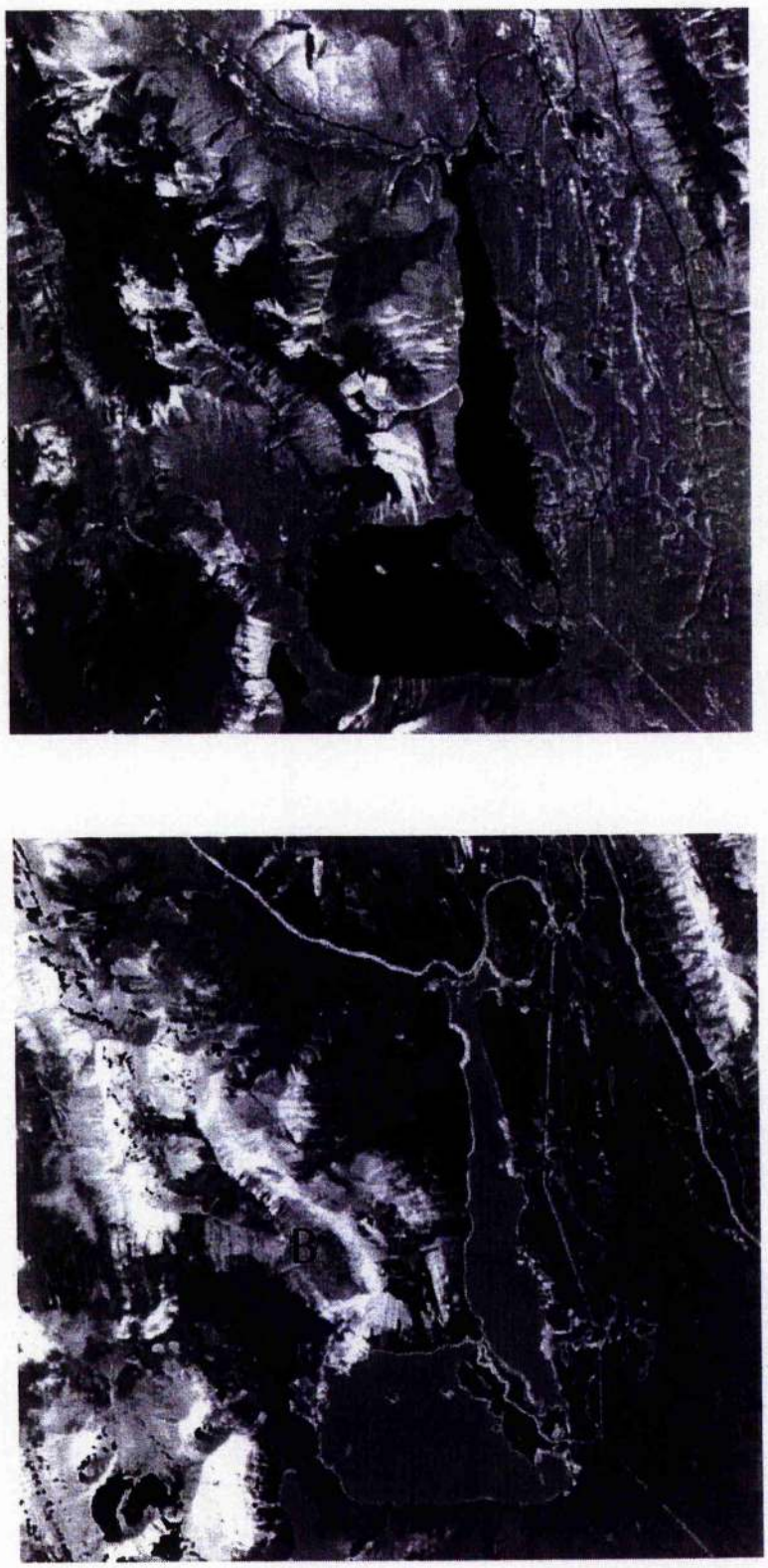

Table 4.13 Loadings from selective PCA for Bands 1,2,3,4

TM band	PC1	PC2
1	.974	-.204
2	.996	-.086
3	.991	-.085
4	.639	.769

B. NEAR AND MIDDLE (SHORT WAVE) INFRARED

This component, similar to a 5/4 or 7/4 ratio, does not have an equivalent in the seven band analysis, where it is likely subdivided and hidden within PC2 and PC3 if one scrutinises their eigenvectors and loadings back in tables 4.8 and 4.9. The image (figure 4.8b) is largely visually topography-free and highlights some vegetation classes omitted by the visible versus near infrared component. In particular the 1967 burn (marked 'B') is clearly seen as an intermediate light gray between the lightest tones of bare rock and medium grays denoting forest cover. Ice and snow patches show as dark, as do grass and shrub covered avalanche slopes as well as fens. Forest types however are poorly distinguished. This image channel will be retained and subsequently referred to as PC-Y. Its eigenvalues and loadings are shown in tables 4.14 and 4.15.

Table 4.14 Eigenvalues from selected PCA for bands 4, 5 and 7

Eigenchannel	eigenvalue	std. deviation	%variance
1	2801.8	52.93	88.43
2	349.7	18.70	11.04
3	17.0	4.13	0.54

Table 4.15 Loadings from selective PCA for bands 4, 5 and 7

TM Band	PC1	PC2
4	.673	.737
5	.997	-.058
7	.970	-.233

C. VISIBLE AND MIDDLE (SHORT WAVE) INFRARED

This analysis yielded a second component that was closely correlated to the overall PC2, with both of them loading bands 123 against bands 5 and 7, but both equally retaining a considerable residual topographic effect (figure 4.9a). This component is the equivalent of 'wetness' and displays hydrologic features more clearly than fundamental vegetation units. The third component features the contrast between the highly correlated bands 5 and 7 versus bands 2, 3 and 5. It exhibits some good ground cover discrimination, but is adversely affected by noise, as indicated by the low loading values and is unsuitable for further consideration.

Table 4.16 Eigenvalues from selective PCA for bands 1,2,3,5,7

Eigenchannel	eigenvalue	std. deviation	%variance
1	3816.1	61.77	82.65
2	748.5	27.36	16.21
3	36.7	6.06	0.80
4	13.7	3.69	0.30
5	2.0	1.43	0.04

Figure 4.9 Selective principal component and ratio image
Above: second component of bands 1,2,3,5,7 Below: 5/2 ratio ('PC-Z')

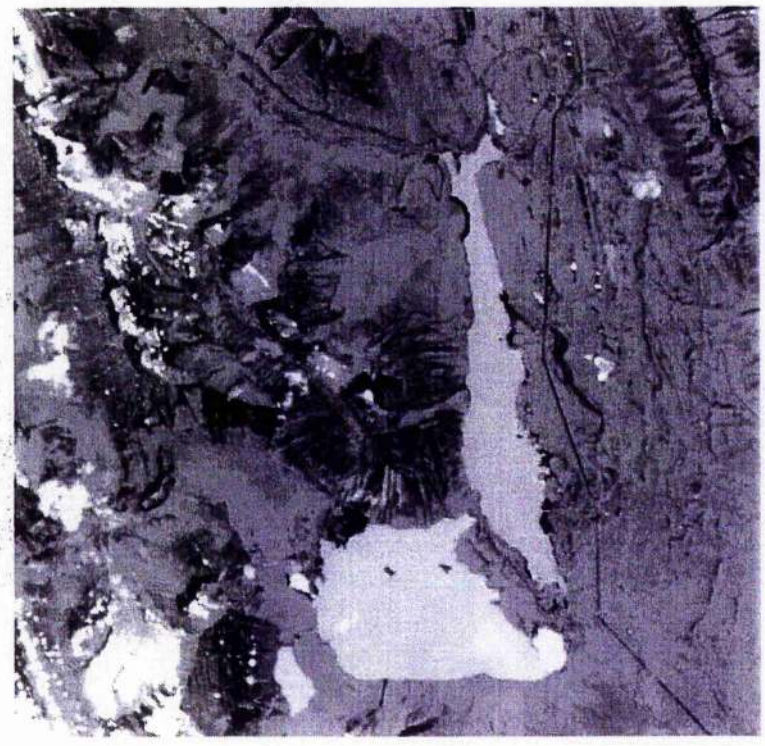

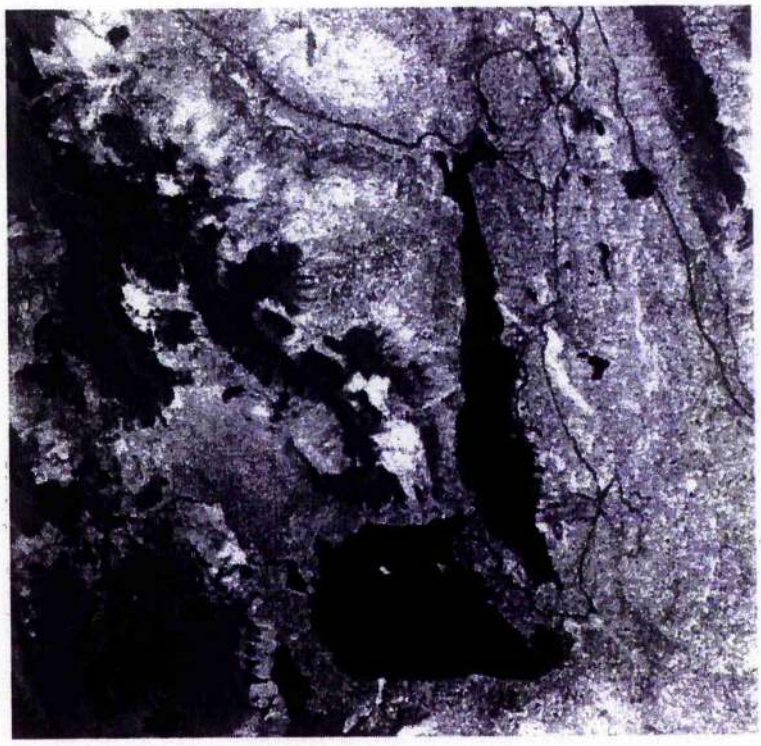

Table 4.17 Loadings from selected PCA for bands 1,2,3,5,7

TM Band	PC1	PC2	PC3
1	.877	. 468	.012
2	.852	.514	-.026
3	.888	.450	-.028
5	.934	-.370	-.061
7	.954	-.261	.173

In its place to represent the contrast between the visible bands and the middle infrared wavelengths, the ratios representing this relationship were examined. These were: 5/1,5/2,5/3,7/1,7/2 and 7/3. The best ratio image in this case was deemed to be 5/2, which was topography free and represents the ratio between the two strongest contributing bands from each spectral region in the PC2 channel above (table 4.17 and figure 4.9b). This image will be retained and subsequently referred to as PC-Z.

How do we know these selected image channels do have topography removed or at least subdued, other than by visual inspection and intuition? We can get some indication by cross-checking them against the aspect image. If an image were independent of topography, we might expect that all areas regardless of their initial topographic orientation now have approximately equal mean values, compared to the TM bands which exhibited the topographic effect and would carry higher values on slopes facing southeast, and lower values on northwest slopes. The median values for the three selected channels, PC-X, PC-Y and PC-Z, along with TM bands 3,4 and 5 and also the incidence channel have been tabulated against aspect in table 4.18, over thirty degree increments.

Table 4.18 Average values for selected image channels according to aspect

Aspect	PC-X	PC-Y	PC-Z	TM3	TM4	TM5	INC
0-30	60	44	67	20	43	39	38
30-60	63	47	66	22	48	49	44
60-90	69	47	68	24	57	59	52
90-120	*72*	*44*	*71*	*25*	*60*	*61*	*61*
120-150	*71*	*49*	*71*	*27*	*62*	*70*	*69*
150-180	*72*	*47*	*73*	*25*	*58*	*63*	*65*
180-210	68	24	71	24	54	57	53
210-240	66	34	65	29	55	71	45
240-270	63	52	65	25	49	57	36
270-300	**66**	**42**	**76**	**20**	**44**	**38**	**44**
300-330	**60**	**47**	**70**	**19**	**41**	**35**	**37**
330-360	**54**	**49**	**65**	**19**	**38**	**34**	**30**

At the time the imagery was captured, solar azimuth was 138 degrees; the three thirty-degree sections around that value have been highlighted in italics and the three sections directly opposed are in bold. On the TM bands, we expect the values in bold to be lower than those in italics and indeed they are by approximately 6 for band 3, 19 for band 4 and 29 for band 5. This last figure was even greater than that for incidence, which was on average 28 lower. In contrast, there is little difference between the two sets for PC-Y and PC-Z and a difference of about 12 for PC-X.

This last value is a little suprising as it was this image that seemed to be the most impressive for vegetation discrimination. One might surmise that this is a reflection of the bias of highly reflective deciduous communities towards south facing habitats, and for lower reflecting coniferous forests towards north facing habitats. Since this component image emphasises such vegetation differences, then it would not be surprising to find this contrast between these aspects, based now not on greater illumination, but rather on different vegetation communities that develop on such sites.

CHAPTER 5

DATA PROCESSING AND IMAGE ANALYSIS II: EXTRACTION OF TOPOGRAPHY AND ALBEDO

The two generated three-channel data sets described in chapter 4 will now be used in an attempt to separate the brightness variations due to the intrinsic spectral reflectance of the surface cover and the brightness variations due to topography. This will be done first for the ratio channels and then for the components channels, each using the following steps:

a. produce clusters using unsupervised classification;
b. determine the average value of pixels under each cluster for each band;
c. replace the cluster number with the average value for each band;
d. compare the result with the original TM band.

5.1 Topographic extraction using ratios

A. PRODUCE CLUSTERS USING UNSUPERVISED CLASSIFICATION

Clustering or unsupervised classification is a standard option in image processing. With minimal input from the user, the algorithm breaks down the data set, which in this case has three image channels, each with digital values from 0-255, and clusters the 262144 ground pixels into groups based on their similarity. If we consider the three channels to be x, y and z, then the groups can be visualised as clusters of data points in three-dimensional space. Several iterations were attempted and the procedure produced a total of 23 clusters, whose mean positions relative to the three ratio channels is shown in table 5.1.

Table 5.1 Clusters produced by unsupervised classification and their mean values for the three ratio channels

Cluster	Pixels	4/3 mean	5/4 mean	7/1 mean
(1)	6322	11	1	1
(2)	2302	11	13	13
(3)	9006	20	60	6
(4)	7210	12	17	56
(5)	7076	19	2	73
(6)	11192	19	38	92
(7)	12370	43	26	149
(8)	29308	18	98	55
(9)	13707	28	42	69
(10)	13917	52	29	154
(11)	14517	69	219	17
(12)	24183	90	171	53
(13)	25436	107	137	81
(14)	23974	103	207	65
(15)	19474	119	101	114
(16)	9005	129	83	160
(17)	5924	136	48	185
(18)	2438	152	53	222
(19)	679	170	66	251
(20)	116	200	113	167
(21)	8994	115	91	211
(22)	1437	102	158	116
(23)	13557	83	153	156

B. DETERMINATION OF AVERAGE VALUE UNDER EACH CLUSTER

Clustering or unsupervised classification makes the assumption that the resulting clusters are comprised of groups of pixels that represent a single cover type with uniform colour or albedo. The clusters have been defined according to pixel values in three derived ratios. We now want to know what are the original TM band average pixel values for these same clusters. These will be taken to represent the predicted brightness of the uniform groups or cover types in that band if there were no variation due to differential illumination, i.e. the surface was flat.

This is achieved by using each cluster bitmap (1-23) as a mask, overlaying these bitmaps on each of the original TM bands in turn and computing the mean and standard deviation of values for the pixels that have membership in that cluster. This was done for cluster bitmaps 1-23 acting on TM bands 3, 4 and 5, and the results presented in table 5.2. The mean value represents the reflectance of a uniform cover type with the topographic effect removed; the magnitude of the standard deviation gives an indication of the topographic effect within that cover class for that wavelength (band). This might be expected to be lowest for water surfaces and classes that exist only on flat surfaces such as fens, and highest for bare rock, since the highest elevations also contain the steepest slopes and are above the tree line. The results are given below:

Table 5.2 Average values for each cluster of pixels, in similar three-dimensional space, defined by ratios 4/3, 5/4, 7/1

Cluster Number	TM3 mean	Standard deviation	TM4 mean	Standard deviation	TM5 mean	Standard deviation
1	156	62.8	106	47.4	29	24.1
5	6	3.0	2	2.4	2	3.5
7	9	2.0	39	9.7	25	6.9
9	22	21.5	16	18.6	15	17.3
10	77	40.0	60	31.9	84	42.9
11	53	21.4	48	19.9	105	43.7
12	32	22.5	47	26.5	61	37.0
13	11	3.4	42	11.1	33	10.4
14	9	1.7	46	8.9	29	6.3
15	10	2.1	47	10.4	35	9.1
16	31	13.8	57	17.3	83	32.3
17	13	3.8	54	14.9	48	15.8
18	26	9.4	62	15.9	84	25.9
19	18	6.1	69	19.8	76	26.0
20	11	3.4	58	18.7	46	17.2
21	59	18.4	57	17.8	141	44.8
22	36	10.5	55	14.9	112	27.7
23	22	3.1	61	21.7	42	17.5

C. REPLACE CLASS ID WITH AVERAGE VALUE FOR EACH BAND and
D. COMPARE WITH ORIGINAL TM BAND

This operation is performed either by using a 'reclass' operation within a geographic information system software, such as IDRISI in which the operator simply replaces the cluster ID number with the appropriate average pixel value for each band, calculated in the previous stage. Alternatively, one could use a 'modelling' function in an image processing system such as PCI that allows a sequence of commands as below, where the routine is performed for every pixel and TM3, TM4, and TM5 are the 512 x 512 matrices designed to contain the predicted image data.

IF CLUSTER = 1 THEN TM3 = 156
IF CLUSTER = 5 THEN TM3 = 6

.

.

IF CLUSTER = 23 THEN TM5 = 42

By this procedure, pixels belonging to the cluster with ID number 1 receive the average values of 156 for the simulated band 3, 106 for the simulated band 4 and 29 for the simulated band 5. The resulting images for bands 4 and 5 can be seen in figure 5.1.

It became clear at this point that the procedure has met with limited success due to the amount of noise that has resulted from band ratioing of forested areas and further work switched to the use of the component channels.

Figure 5.1 Estimate of average image brightness if topography was removed, for bands 4 (above) and 5 (below), based on 3-ratio combination

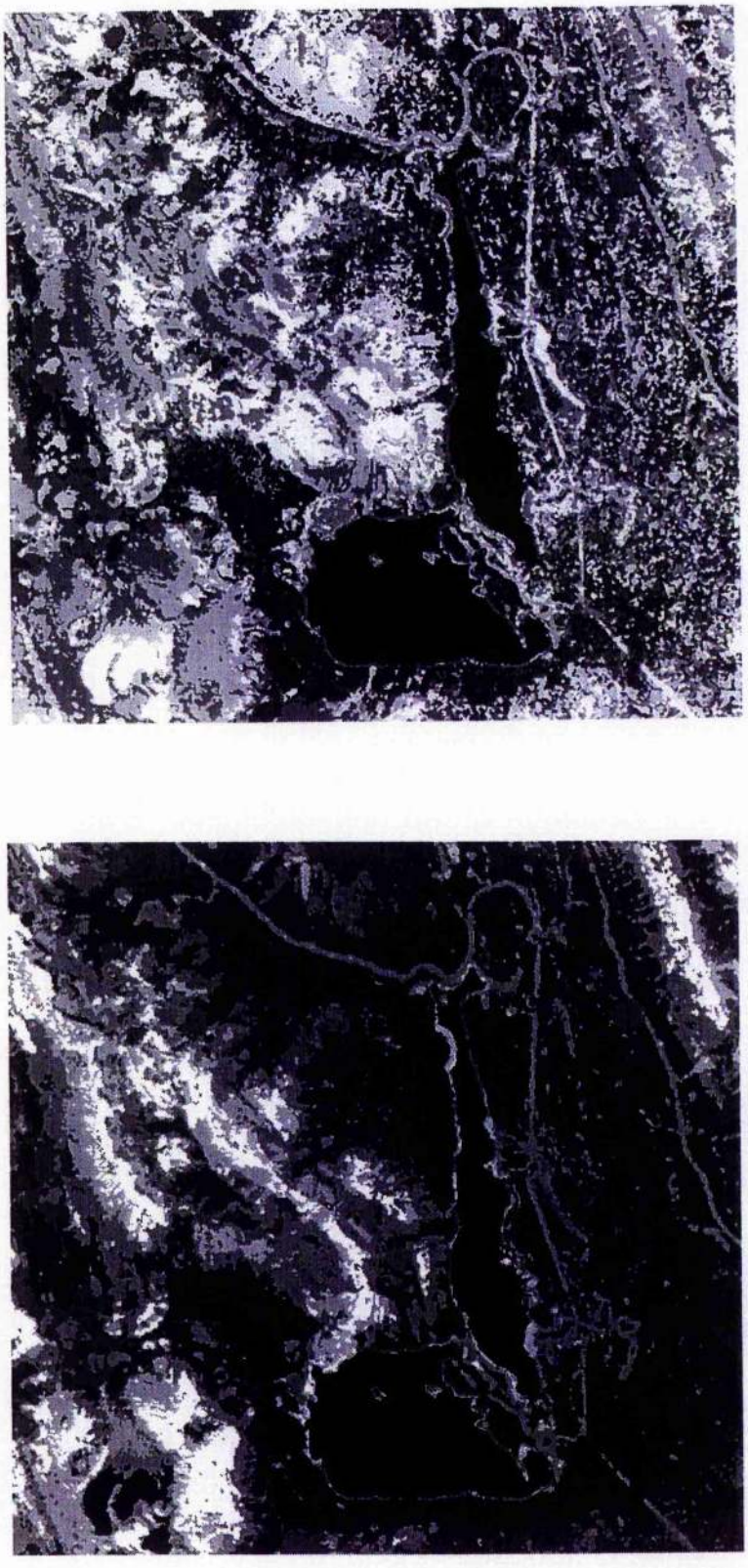

5.2 Topographic extraction using principal components

A. PRODUCE CLUSTERS USING UNSUPERVISED CLASSIFICATION

The channels considered optimal for surface cover classification, which were derived from principal components analysis and selected in the previous chapter, are now used as input for unsupervised classification in the same manner as the three ratio channels in section 5.1 and will be referred to as PC-X, PC-Y and PC-Z. These were previously derived and defined in chapter 4 as follows:

PC-X: the second component of bands 1,2,3,4
PC-Y: the second component of bands 4,5,7
PC-Z: the 5/2 ratio

The clustering procedure again produced 23 clusters which visually seemed to have reasonable correspondance to the known vegetation classes described in chapter 3. The cluster mean values are given in table 5.3, along with the likeliest vegetation class. It was noted that some of these clusters could immediately be combined to reduce processing time, notably 1 to 4 which are all snow and ice, the distinction between them being unimportant in this study. The algorithm has attributed several clusters to snow and ice, as there are few other features at the spectral extremes occupied by this cover, low in two channels, low to medium in the third. The validity of combining clusters can be checked by individually 'turning on' each cluster one at a time and consecutively to see whether groups of clusters are spatially contiguous or contained one within the other, as for example might be groups of pixels that represent snow and ice.

Table 5.3 Clusters generated from component channels PC-X, Y and Z

Cluster number	Number of pixels	Mean Value PC-X	Mean Value PC-Y	Mean value PC-Z	Cover class -see section 3.5
(1)	773	2	15	0	1
(2)	1107	0	27	0	1
(3)	445	1	56	1	1
(4)	550	85	14	1	1
(5)	472	2	108	4	1
(6)	22205	1	144	1	2
(7)	5111	6	163	45	3
(8)	8697	50	168	70	3
(9)	14052	77	209	125	3
(10)	14864	77	172	104	12
(11)	16072	103	130	73	5
(12)	24572	133	99	97	6
(13)	18155	159	74	110	4
(14)	28637	119	124	125	5
(15)	15897	95	179	153	13
(16)	25648	149	103	152	4
(17)	13650	116	136	175	5
(18)	10442	190	62	142	9
(19)	14922	170	139	154	7 - 8
(20)	7099	207	67	181	10
(21)	7841	193	124	195	11
(22)	8203	144	153	201	10
(23)	2730	185	155	221	14

B. DETERMINATION OF AVERAGE VALUE UNDER EACH CLUSTER

The procedure was as outlined in section 5.1 for the ratio channels, and the results are shown in table 5.4. The averages represent the predicted reflectance at that wavelength if the surface were flat, i.e. the variations due to differential illumination as a result of topography, have been removed. The standard deviations again indicate to what degree the pixels belonging to each cluster are influenced by topography in the original TM bands 3, 4 and 5.

Table 5.4 Average values for each cluster of pixels in similar 3-dimensional space, defined by component channels PC-X, PC-Y and PC-Z.

Cluster Number	TM3 average	Standard deviation	TM4 average	Standard deviation	TM5 average	Standard deviation
1	154	17.8	95	25.4	39	18.0
5	16	7.2	2	5.0	7	5.8
7	66	34.3	46	30.0	81	29.3
9	80	16.4	66	13.6	16	19.8
10	50	18.3	43	17.1	88	19.7
11	27	10.3	39	17.8	22	15.6
12	19	5.6	45	5.9	34	3.9
13	20	6.3	53	6.2	39	3.0
14	21	5.5	41	8.3	39	8.1
15	50	12.3	52	15.7	109	21.4
16	20	4.5	50	5.9	42	3.2
17	23	7.5	40	9.0	48	11.8
18	23	4.5	72	12.0	57	4.9
19	34	8.5	69	11.6	86	14.5
20	25	12.5	86	18.0	75	6.6
21	29	6.3	78	13.5	86	9.9
22	34	9.8	58	9.5	89	17.0
23	37	10.5	78	10.0	112	11.6

C. REPLACE CLASS ID WITH AVERAGE VALUE FOR EACH BAND and
D. COMPARE WITH ORIGINAL TM BAND

The new average values for bands 3, 4 and 5 are now replaced into new channels that describe predicted average brightness, were the surface flat. This is done using the same procedure described for the ratio combinations in section 5.1., replacing the class numbers (ranging from 1 to 23) with the computed average reflectance values. These new 'flat' images are illustrated in figures 5.2, 5.3, 5.4; in each case the average brightness image channel is compared with the respective TM band. Figure 5.5 combines the three flat channels into a colour composite which is compared with the original TM colour composite for bands 3, 4 and 5.

Figure 5.2 Band 3 (above) and the constructed average brightness image for band 3 if the terrain were flat (below), created from PC-X, PC-Y and PC-Z

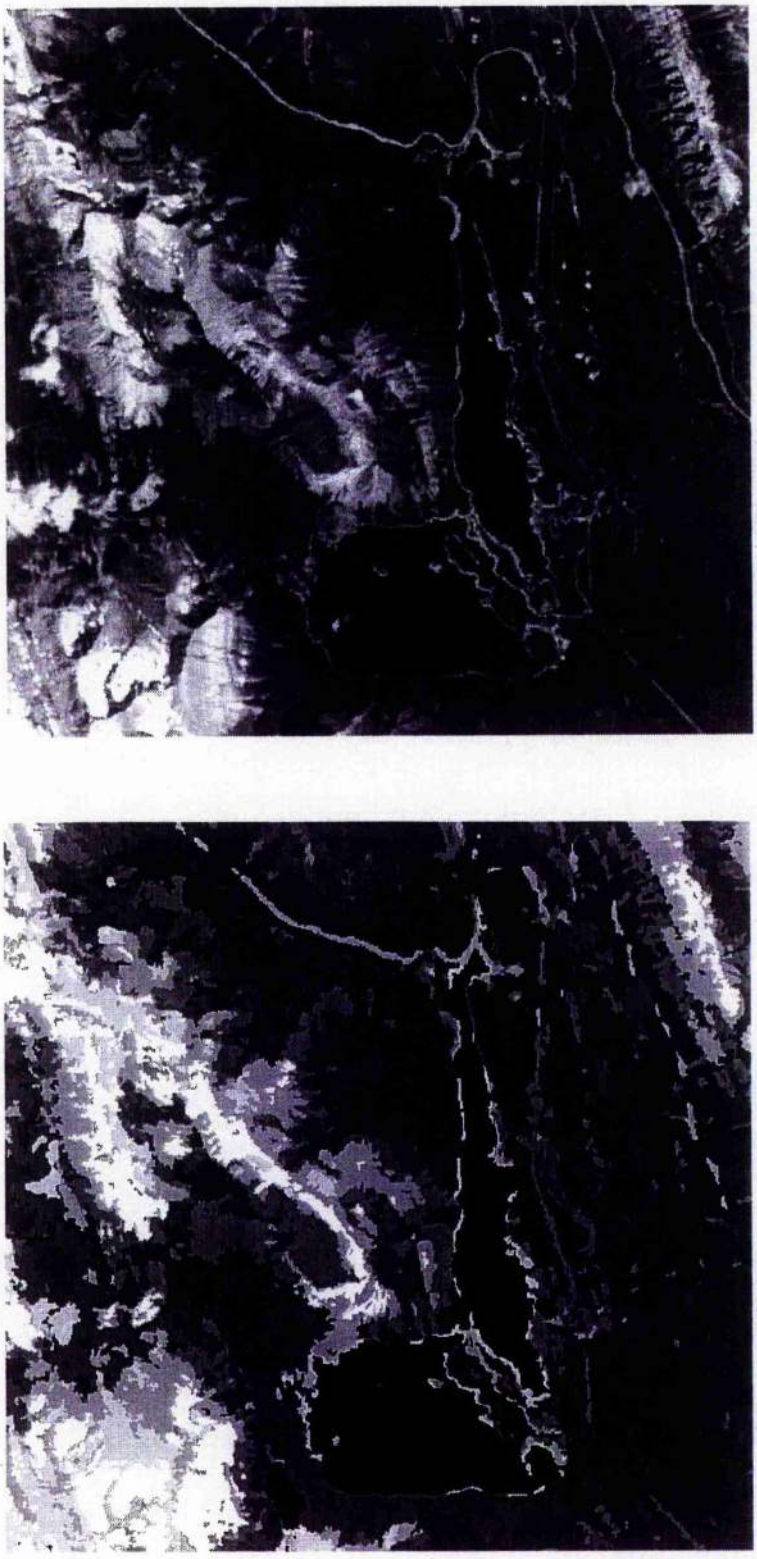

Figure 5.3 Band 4 (above) and the constructed average brightness image for band 4 if the terrain were flat (below), created from PC-X, PC-Y and PC-Z

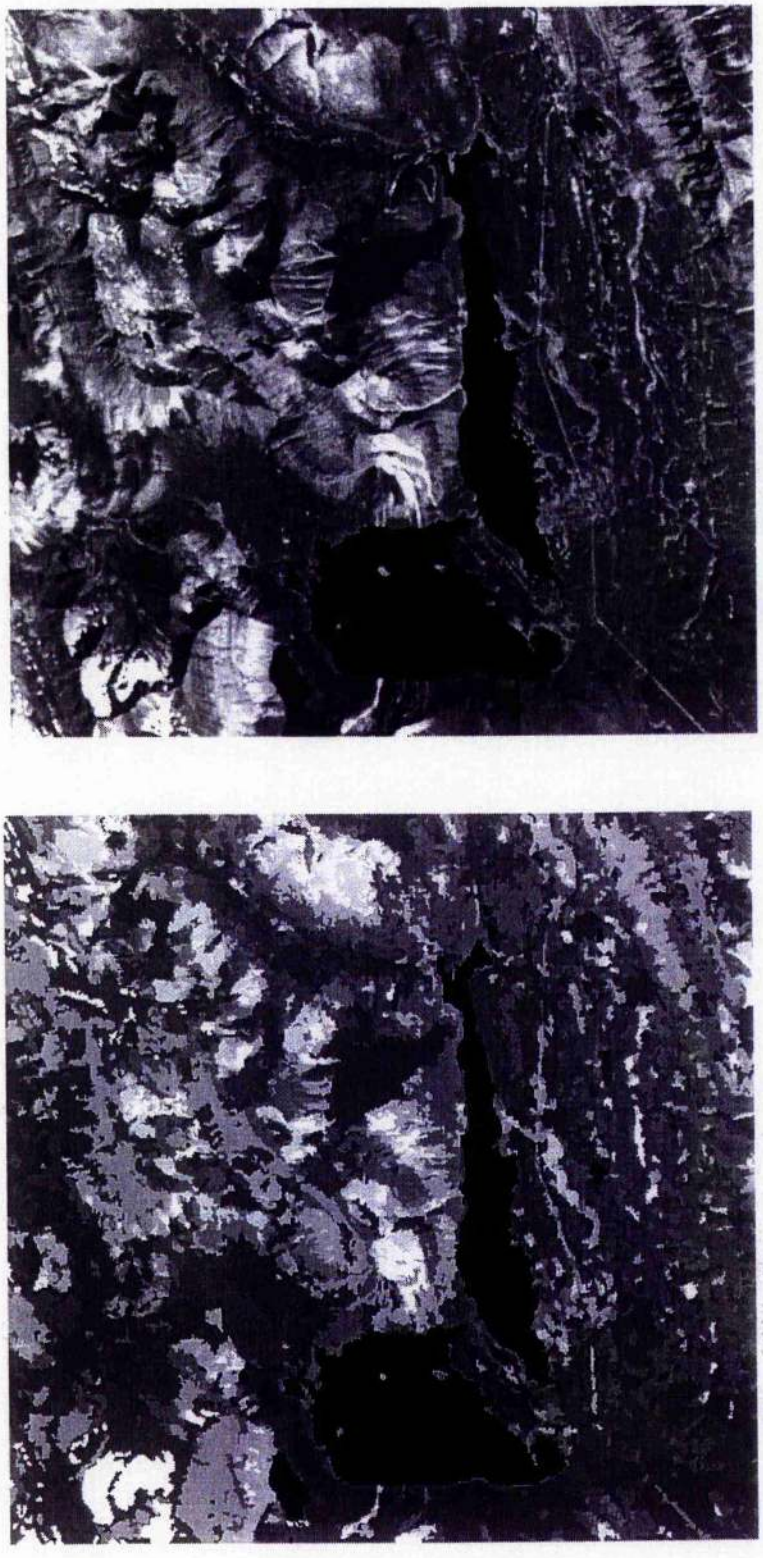

Figure 5.4 Band 5 (above) and the constructed average brightness image for band 5 if the terrain were flat (below), created from PC-X, PC-Y and PC-Z

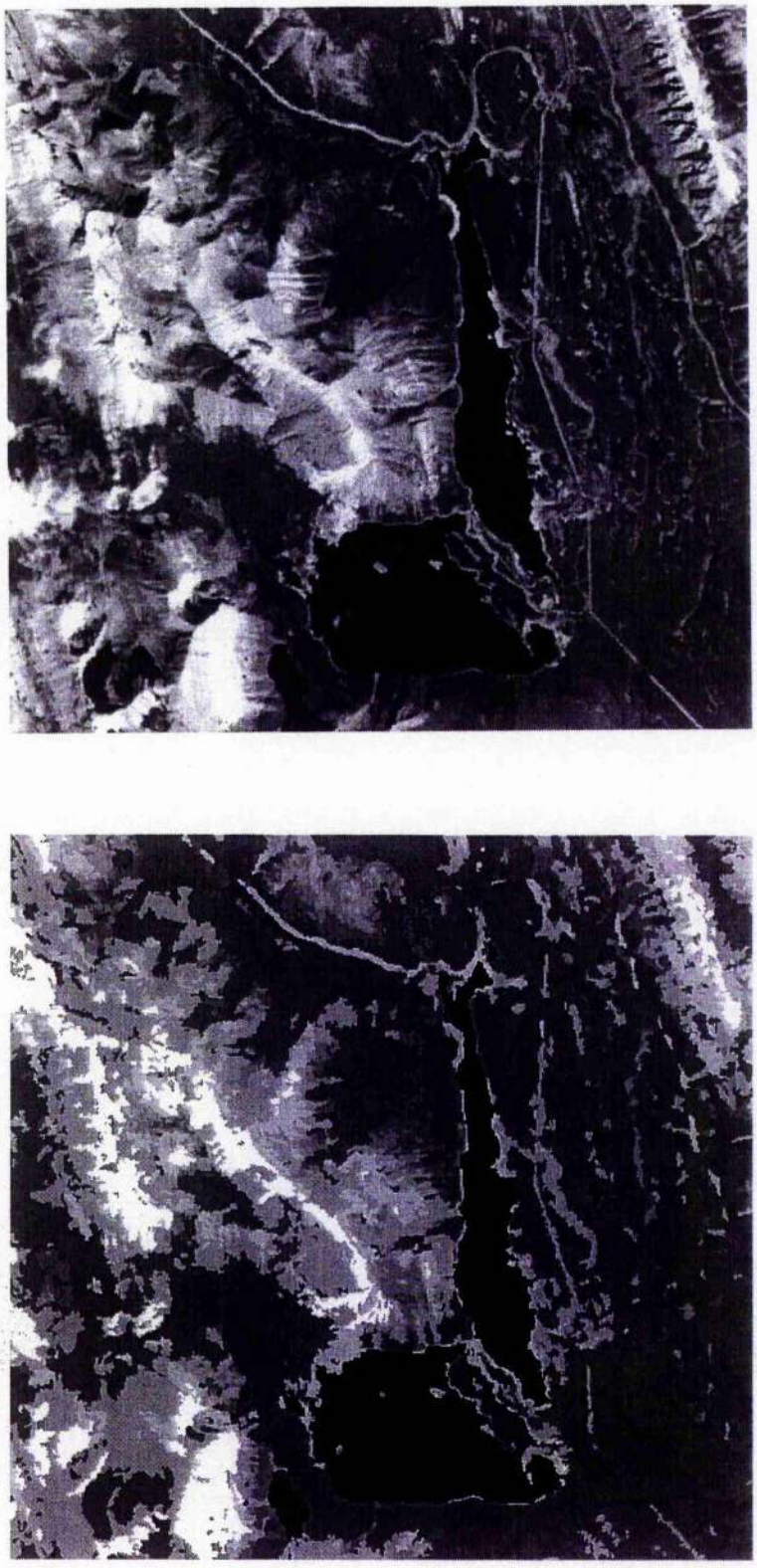

Figure 5.5 Colour composite -3,4,5 (above), and constructed average brightness colour composite (below), created from PC-X, PC-Y and PC-Z

We can also compute the difference between the average band and the original TM band to assess the size of the topographic effect, tabulated in table 5.5. Although the majority of pixels fall within ten digital numbers of zero difference, it should be noted that with the differences being signed either positive or negative, corresponding to areas that are illuminated and shaded respectively, the magnitude of the variations can be twice as large as they may first appear. The average effect is calculated to be 7.6, 9.4 and 16.5 in recorded digital number. The higher number for band 5 is a function of its higher natural variance; the extreme values which are few in frequency may partly be attributed to noise. However, for each band, there are several thousand pixels with an apparent difference (or variation from the average due to the effects of topography) of more than 60 pixels, bearing in mind that 1% of the image represents 262144 / 100 ground pixels or 2621.

Table 5.5 Difference between TM band and the generated average channel

DN difference	TM 3	TM 4	TM 5
> 60 (+)	0.54	0.39	2.22
50-60	0.33	0.32	1.49
40-50	0.60	0.75	2.40
30-40	1.18	1.70	3.55
20-30	2.95	3.95	5.23
10-20	7.22	9.75	8.61
0-10 (positive)	40.35	28.40	18.95
0-10 (negative)	37.18	40.07	33.18
10-20	5.60	9.37	11.85
20-30	1.83	3.22	6.07
30-40	0.81	1.30	2.75
40-50	0.68	0.54	1.67
50-60	0.32	0.07	1.05
>60 (-)	0.13	0.27	1.40
Minimum	-152	-101	-140
Maximum	162	144	141
Mean diff	7.6	9.4	16.5

5.3 Generation of topographic modulation image

Having seemingly produced a 'flat version' of the selected TM bands, mathematically, the topographic modulation component can be derived by dividing the estimate of the average scene brightness into the original scene (Eliason *et al.*, 1981). The result however (figure 5.6) bears only a passing resemblance to the incidence image and statistically, they have a low correlation of 0.23.

The topographic component can also be re-introduced to create a simulated TM band by combining the new topography-free TM 'albedo' band with the incidence channel. This can be modelled very simply by:

$$B_n = (A_n + I) \ / \ 2$$

where:

B_n is the simulated TM band

A_n is the generated average or albedo TM channel

I is the incidence channel

The resulting image is shown in figure 5.7 for band 4 and a simulated colour composite in which the process was repeated for the three bands.

By the same token, we might have produced a modelled version of the topography, as seen in the incidence image, by reversing the equation above:

$$I \text{ (incidence)} = 2 * B_n - A_n$$

However the resulting image is essentially the same as Figure 5.6.

Figure 5.6 Topographic modulation image channel produced by dividing the average brightness image into the original TM band

Figure 5.7 Simulated images created by adding the incidence channel to the average brightness image for band 4 (above) and colour composite (below)

5.4 Use of topographically corrected channels to classify cover

While the main goal of this study was to show the multispectral potential of TM data to generate image channels in which the signal component related to topography can be separated from the signal component related to surface albedo, these derived channels can also be used as input towards a surface cover classification. The clustering or unsupervised classification process generates signatures for each cluster containing the average or cluster mean and standard deviation of the member pixels. These signatures can now be used to refine the classification, assuming that we can associate each cluster with a vegetation cover type. They are fed back into the classifier in what has been termed a 'hybrid' approach as it combines aspects of unsupervised and supervised classification techniques. The result can be seen in figure 5.8. These classified pixels can be compared with known 'seeded' pixels as well as established field sites.

CLASSIFICATION SUMMARY

Non-vegetated

Water, snow and ice and rock separated well from other cover types with near to 100% accuracy. Bare rock included the lake shores and road beds. There is minor confusion between water and rock along lake edges, due to fluctuating water levels and between remnant snow patches and ponds.

Forest

There is some confusion within the forest types; areas of less dense pine were mixed with spruce-pine-fir and spruce-pine. This is not surprising given the variation within the forest groups. Crown density can vary from

5 to 100%, height from two to over 30 metres, composition from pure pine stands, to pine dominated, spruce sub-dominant, fir sub-dominant, as there can also be stress due to windburn and pest infestation. However the basic pattern maintains the identity of spruce-fir over pine in areas that have escaped recent fire.

Alpine

Buffaloberry-herb slopes, alpine slopes and herb-dominated avalanche slopes are distinguished fairly well, though further refinement is need to distinguish the heather and dryas-dominated meadows. The fir avalanche slopes are defined on the west shores of Hidden Lake and south shore of Upper Lake. The burn is identifiable though not distinct from all alpine areas.

Wetlands

The fens and lowland meadows are recognised when the area is fairly wide, but on the edges are mixed with coniferous forest, which dominates the response when the fen is narrow. In places they are confused with the deciduous alpine complex.

Overall accuracy was estimated at 76.3%. This may seem low compared to other types of landscapes, but it is above the average for studies in natural areas of similar complexity, using TM data alone in a supervised classification: 66% (Connery, 1992) and 62.0% (Williams, 1992). When these studies also used topographic variables, their accuracy increased to 76.4% and 75.3% respectively. Hence the unsupervised approach by 'removing' topography may produce better discrimination between communities than using a supervised approach and comparable even when the DEM variables were added as extra logical channels.

Figure 5.8 Classified image by hybrid technique

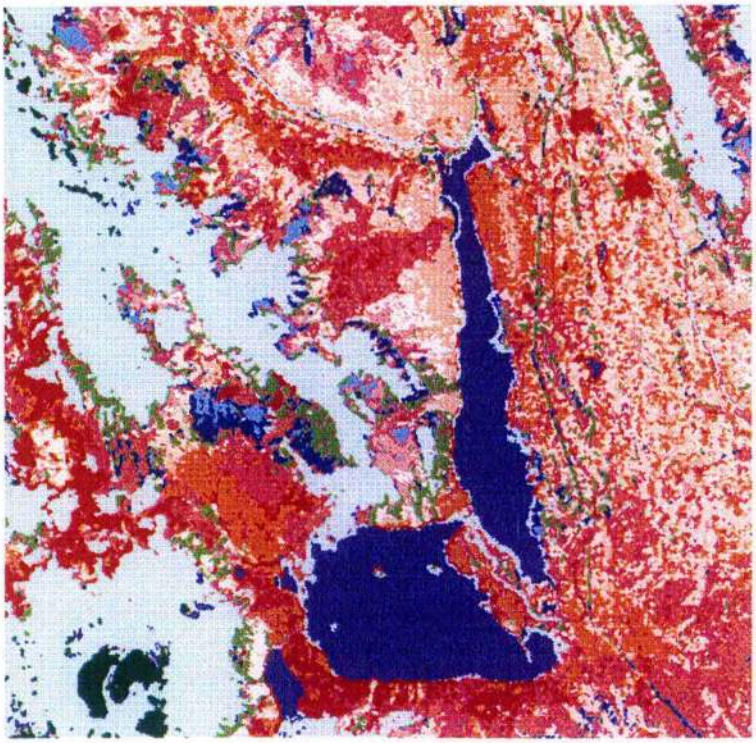

Indigo	water
Light blue	bare rock (includes lichen)
Dark green	ice / snow
Dark blue	burn
Lime green	herb and shrub-dominated avalanche slopes
Dark - medium red	spruce-fir (and clouds!)
Orange	pine / spruce-pine-fir
Salmon	pine and spruce-pine
White	fir avalanche track

CHAPTER 6

SUMMARY AND CONCLUSIONS

6.1 Existing research on correcting or compensating for topographic information

As indicated in the literature review, there has been considerable research in two areas, known as the logical channel approach and topographic correction. They are both based on the acquisition of a DEM at a resolution or scale appropriate to the image data. They have generally yielded improvements in classifiers over procedures that did not incorporate topographic data, in the order of 5 to 15%, but nevertheless they remain in the hands of the researcher and not the practitioner. This is due partly to the lack of availability of digital elevation models in the past and also to continuing concerns with how well they describe the terrain and can be integrated or registered with other types of digital data. They also require considerable *a priori* information relating to the surface cover characteristics, which ultimately is the purpose of remote sensing analysis.

6.2 Using band ratios to reduce the topographic effect

Spectral band ratioing as a technique is almost as old as digital imagery (Robinove, 1982). Creating a band ratio results in the loss of most or all of the topographic component in an image, because the act of division nullifies the common element in the numerator and denominator, that is, differential illumination from topography. A ratio image can show pure reflectance information without the effects of topography. In some

applications, by removing this previously dominant element from the image, we can see lesser features that were previously overwhelmed. Such is the case with remote sensing for geological applications: variations in reflection caused by different mineral accumulations are no longer disguised by differences in brightness due to topography. However in some environments, this process can over-emphasise the variations in the remaining elements, resulting in disturbing and undesirable noise.

Eliason *et al.* (1981) used band ratios both to create a 'topography-free' surface cover layer and by dividing that back into the original MSS bands to generate a topographic image, with brightness variations due to different surface materials removed. This worked in two landscapes, one in a lightly vegetated semi-arid landscape, the other on a non-vegetated extraterrestrial surface (we assume that Mars is non-vegetated!).

This thesis also succeeded in producing a topography-free layer but with some major differences. Ratioing was again tested as a procedure, this time with more band selections available from the TM sensor. However it was found lacking due to the noise generated mostly in forested areas, while areas above the treeline were not as adversely affected. The conclusion is that while ratioing is capable of separating major surface groups, such as bare rock versus deciduous versus coniferous cover, it cannot deal with the complex variations that occur in forested areas.

This might not be the case if all forests had a uniform tree height and consistent and high canopy density. However forest cover varies in these ways and more. The changing mixture of leaves, branches and shadows in a canopy helps create a mosiac of variable textures, akin to noise. If the canopy is not continuous, then the signal received by the sensor is inevitably also influenced by the sub-storey, whether it be shrubs, herbs,

lichens or bare ground. This explains why a ratio image is noisy in forests but less so for bare rock or deciduous herb and shrub communities. The latter may vary, but they do not have the magnitude of variation between a closed canopy and a sub-storey. The lower the canopy density in a forest stand, the greater the variability can be.

6.3 Using principal components to compensate for topography

In place of band ratios, therefore, the technique of principal component analysis was utilised. This was not realistically available for MSS data, which consists of only two pairs of highly correlated bands. PCA has some very similar principles to band ratioing, since the second component from a two band analysis is correlated to their ratio. But it surpasses band ratioing by being able to input any combination of bands, whereas ratios are usually limited to two, thereby losing information that may be in the other bands. In so doing, PCA can generate more noise-free images and depict new elements, hidden in the original bands by the overwhelming response to topographic variation. Other researchers have recognised this superiority of principal components analysis over band ratioing in classification performance (Conese *et al.*, 1988).

Previously principal components analysis has been used in four types of applications: to reduce the dimensionality of a data set, to allow the generation of more informative colour composites, for detecting and assessing surface change with multi-temporal data and finally to allow the recognition of subtle variations in image scenes by examining lower components. This thesis has explored a fifth type of application, which is surface cover discrimination by removing or reducing topographic features that are a cause of interference in automatic classification of digital imagery. Certainly this has some commonality with the use of PCA to

identify features on lower components, but in these, the extraction of topographic representation is incidental rather than the central goal.

The surface cover representations generated here certainly appear to have separated topographic variations from surface cover. This impression was particularly powerful when the software was used to 'flick' between the original TM band and the generated average brightness channel on the screen. Unlike the logical channel and topographic correction methods, PCA uses a 'closed system' to compensate for topographic information, requiring only multispectral data, avoiding the cost and problems associated with ancillary data sets.

6.4 Extraction of topographic information

The ability to create a representation of topographic relief by dividing the generated 'average' channel back into the original TM band did not materialise, at least not satisfactorily. To explain this, we need to go back again to the complexity of forest cover stands. There are many environmental variables affecting the reflection that is recorded by the sensor: soil type, moisture conditions, percentages of trees and shrubs, surface roughness, as well as slope and aspect. If the surface type is removed, however, it is not just slope and aspect that are left, but all the variability due to the other factors. The estimate of topography was unsatisfactory for the same reason that band ratioing was inadequate. There is much scope for future research to study the complex integrated role of all these variables in influencing the pixel values received in digital satellite image data.

Distinguishing natural vegetation communities is no easy task, compared to those well influenced by human activity. The former are generally much more complex and variable, containing great irregularity in species height, density, composition and spatial patterns. Boundaries are in many cases open to extreme subjectivity, as to where to draw any line. This has led researchers to conclude that classification of natural and semi-natural upland or montane vegetation based solely on spectral information will never be entirely satisfactory (Jones *et al.*, 1988).

6.5 The question of PCA and scene-dependence

Some researchers have limited confidence in PCA as a global procedure because it has been described as scene-dependent. This arises primarily from the uniqueness of component images and their associated eigenvalues and eigenvectors, which have only general similarities between scenes. Although the first component is a weighted average of all the bands, subsequent components may follow a general pattern, but vary considerably in the characteristics and the contrasts they display.

The key difference in this study was the use of selective principal components, by which the second components from each of the three pairings of spectral regions represented in the TM bands, produced three new and independent channels of data, based not on the scene itself, but on the actual spectral structure of TM data. These fundamentally displayed the difference between the visible and near infra-red, between the visible and the middle infra-red and between the near and middle infra-red wavelengths. The first is equal to 'greenness' which is usually the second component when the whole data set is used. The second is visually and structurally similar to PC3 for the whole data set and is usually described as wetness. The third however has no equivalent in

traditional principal component analysis and appears to be hidden within the first two when all bands are input.

6.6 Conclusions and directions for future research

A. EXTENSION OF THIS PROCEDURE TO OTHER AREAS

While this study has accepted the general applicability of the techniques developed, it is highly desirable to continue similar studies in other areas. For example we should examine whether the procedure is more or less successful in regions of lower complexity, more consistent forest cover, higher contrast boundaries, less non-vegetated areas and higher and lower local relief. It is likely to be particularly interesting to examine other climatological zones, both in different temperature and precipitation regimes, and the resulting relationships between topography and vegetation cover. Two variables which needed minimal manipulation in this research were the number of clusters selected by the unsupervised classification algorithm and the subsequent merging of clearly converging clusters, apparent visually by their spatial contiguity. Whether the procedure is perfectly transferable without modification may require that these conditions are common and not the exception.

B. DERIVATION OF NEW COMPONENTS

One point of frustration and considerable time investment was caused by the inability to generate a suitable image from selective PCA of the visible and middle infra-red bands and instead to have to rely on the 5 / 2 ratio as a substitute. This hybridises the procedure somewhat and would better be avoided. Further research is required to verify that this was not a local problem and to examine the exact nature of the remaining topographic influence in that image.

C. ENVIRONMENTAL FACTORS AND SCENE VARIANCE

It has been presumed that the unsatisfactory image produced by dividing the average brightness channel into the TM band failed to cleanly depict topographic shading because the variables removed in the average channel were not simply topographic slope and aspect. Hence the difference between these two channels, or residual images, also included other environmental variables, such as soil moisture, canopy density, amount of bare soil and vegetation health. In order to be able to separate these albedo effects which occur within an otherwise homogeneous cover type completely from the differential illumination effects due to topography, a much fuller understanding of these factors contribute to the mosaic of surface spectral response is required. This work can incorporate existing environmental studies that examine the effects of site characteristics, for example, Jupp and Mayo (1982), Karaska *et al.* (1986), Walsh (1987) and Yool *et al.* (1986).

D. THE FACTOR OF SCALE IN REMOTE SENSING

The Thematic Mapper has been a standard remote sensing tool for medium scale mapping since 1984, but many users require improvements in spatial and spectral resolution. This resolution has proved inadequate in this study and others for clearly distinguishing some linear wetland communities (Williams, 1992). A new era may be on the horizon, as new satellites are planned for the last few years of this century by private enterprises, with increasing resolutions of ten, five and even one metre pixels. These will however, come with a price, measured in increased variance which must be resolved before ground information can be extracted (Woodcock and Strahler, 1987).

REFERENCES

Avery T.E. and Berlin G.L. (1992), *Fundamentals of remote sensing and airphoto interpretation,* 5th edition, MacMillan Publishing Company.

Barry R.G. and Van Wie C.C. (1974), Topo- and microclimatology in alpine areas. In *Arctic and alpine environments,* editors: Ives J.D. and Barry, R.G.. Methuen Press.

Batson R.M., Edwards K. and Eliason E.M. (1976) Synthetic stereo and Landsat pictures. *Photogrammetric Engineering and Remote Sensing,* 42, 10, 1279-1284.

Bernstein R., Lotspiech J.B., Myers H.J., Kolksky H.G. and Lees R.D. (1984), Analysis and processing of Landsat 4 sensor data using advanced image processing techniques and technologies. *IEEE Transactions on Geoscience and Remote Sensing,* 22, 3, 192-221.

Bian L. and Walsh S.J. (1993), Scale dependencies of vegetation and topography in a mountainous environment of Montana. *Professional Geographer,* 45, 1-11.

Boresjo L. (1989), Landsat TM and SPOT data for medium-scale mapping of Swedish vegetation types. *National Swedish environmental protection board report 3571.*

Campbell J.B. (1987), *Introduction to remote sensing,* first edition, Guildford Press.

Carlatto M.J. (1986), Extracting surface features in multispectral imagery. *Proceedings of IGARSS '86 Symposium,* Zurich, September 1986, 283-287.

Carter J.R. (1992), The effect of data precision on the calculation of slope and aspect using gridded DEM's, *Cartographica,* 29,1, 22-34.

Chavez P.S., Berlin G.L. and Sowers L.B. (1982), Statistical method for selecting Landsat MSS ratios. *Journal of Applied Phorographic Engineering,* 8, 23-30.

Chavez P.S. and Bowell J.A. (1988), Comparison of the spectral information content of Landsat Thematic Mapper and SPOT for three different sites in the Phoenix, Arizona area. *Photogrammetric Engineering and Remote Sensing,* 54, 12, 1699-1708.

Chavez P.S. (1989), Radiometric calibration of Landsat Thematic Mapper multispectral images, *Photogrammetric Engineering and Remote Sensing,* 55, 9, 1285-94.

Chavez P.S. and Kwarteng A.Y. (1989), Extracting spectral contrast in Landsat Thematic Mapper image data using selective principal component analysis. *Photogrammetric Engineering and Remote Sensing,* 55, 3, 339-348.

Cibula W.G. and Nyquist M.O. (1987), Use of topographic and climatological models in a geographical data base to improve Landsat MSS classification for Olympic National Park. *Photogrammetric Engineering and Remote Sensing,* 53, 1, January, 67-75.

Civco D.L. (1989), Topographic normalization of Landsat Thematic mapper digital imagery. *Photogrammetric Engineering and Remote Sensing,* 55, 9, 1303-1309.

Colby J.D. (1991), Topographic normalization in rugged Terrain. *Photogrammetric Engineering and Remote Sensing,* 57, 5, 531-540.

Collins J.B. and Woodcock C.E. (1996), An assessment of several linear change detection techniques for mapping forest mortality using multitemporal Landsat TM data. *Remote Sensing of Environment,* 56, 66-77.

Colwell R.N. (1983), editor, *Manual of remote sensing,* 2nd Edition, American Society of Photogrammetry, 1058-1059.

Conese C., Maracchi G., Miglietta F., Maselli F. and Sacco V.M. (1988), Forest classification by principal component analyses of TM data. *International Journal of Remote Sensing,* 9, 10-11, 1597-1612.

Connery D.R. (1992), Avalanche vegetation classification using Landsat imagery and a digital elevation model in southwest Alberta (Canada), *Unpublished M.Sc. thesis,* University of Calgary.

Crippen R.E., Blom R.G. and Heyada R.H. (1988), Directed band ratioing for the retention of perceptually-independent topographic expression in chromaticity-enhanced imagery. *International Journal of Remote Sensing,* 9, 749-765.

Crippen R.E. (1988), The dangers of underestimating the importance of data adjustments in band ratioing. *International Journal of Remote Sensing,* 9, 4, 767-775.

Crist E.P and Cicone R.C. (1984), A physically-based transformation of Thematic Mapper data - The TM tasseled cap. *IEEE Transactions on Geoscience and Remote Sensing,* GE-22, 3, 256-263.

Crist E.P. and Kauth R.J. (1986), The tasseled cap de-mystified. *Photogrammetric Engineering and Remote Sensing,* 52, 1, 81-86.

Davis J.C. (1986) *Statistics and data analysis in geology,* second edition, Wiley, chapter 6: analysis of multivariate data.

Eastman J.R. and Fulk M. (1993) Long sequence time series evaluation using standardized principal components. *Photogrammetric Engineering and Remote Sensing,* 59, 8, 1307-1312.

Ekstrand S. (1996), Landsat TM based forest damage assessment: correction for topographic effects. *Photogrammetric Engineering and Remote Sensing,* 63, 2, 151-158.

Eliason P.T., Soderbloom L.A. and Chavez P.S. (1981), Extraction of topographic and spectral albedo information from multispectral images. *Photogrammetric Engineering and Remote Sensing,* 48, 11, 1571-1579.

Erner H. (1987), Digital elevation models for high mountains. *Mountain research and development,* 7,4, 353-356.

Eyton J.R. (1989), Low-relief topographic enhancement in a Landsat snow-cover scene. *Remote Sensing of Environment,* 27,105-118.

Fiorella M. and Ripple W.J. (1993), Determining successional stage of temperate coniferous forests with Landsat satellite data. *Photogrammetric Engineering and Remote Sensing,* 59, 2, 239-246.

Fontanel A., Blanchet C. and Lallenand C. (1975), Enhancement of Landsat imagery by combination of multispectral classification and principal components analysis. *Proceedings, United States National Aeronautical and Space Administration Earth Resources Survey Synposium,* Texas. NASA TM X-58168, 991-1012.

Forster B.C. (1985), Principal and rotated component analysis of urban surface reflectances. *Photogrammetric Engineering and Remote Sensing,* 51, 4, 475-477.

Forsythe W.K and Wheate R.D. (1995), Using Landsat and digital elevation models to map avalanche slopes in Yoho National Park, B.C.. *Proceeedings of the 17th Canadian Remote Sensing Symposium,* Saskatoon, 258-264.

Frank T.D. (1988), Mapping dominant vegetation communities in the Colorado Rocky Mountains front range with Landsat Thematic Mapper and digital terrain data. *Photogrammetric Engineering and Remote Sensing,* 54, 12, 1727-1734.

Fraser S.J. and Green A.A. (1987), A software defoliant for geological analysis of band ratios. *International Journal of Remote Sensing,* 8, 3, 525-532.

Fung T. and LeDrew E. (1987), Application of principal components analysis to change detection. *Photogrammetric Engineering and Remote Sensing,* 53, 12, 1649-1658.

Gadd B.J. (1990), *Guide to the Rocky Mountains,* Maligne Press.

Gillespie A.R. (1980), Digital techniques in image enhancement, in *Remote Sensing in Geology,* Wiley, editors: Siegel B.S. and Gillespie A.R., 139-226.

Gillespie A.R., Kahle, A.B. and Walker R.E. (1986), Color enhancement of highly correlated images: I. Decorrelation and hue-saturation-intensity contrast stretches. *Remote Sensing of Environment,* 20, 209-235.

Gillespie A.R., Kahle A.B. and Walker, R.E. (1987), Color enhancement of highly correlated images: II. Channel ratio and chromaticity transformation techniques. *Remote Sensing of Environment,* 22, 343-365.

Gould P. (1967), On the geographical interpretation of eigenvalues. *Transactions, Institute of British Geographers,* 42,53-86.

Hall-Konyves K. (1987), The topographic effect on Landsat data in gently undulating terrain in southern Sweden. *International Journal of Remote Sensing,* 8,2, 157-168.

Haralick R.M., Campbell J.B. and Wang S. (1985), Automatic inference of elevation and drainage models from a satellite image. *Proceedings of the IEEE,* 73, 6, 1040-1054.

Holben B.N. and Justice C.O. (1980), The topographic effect on spectral response from nadir-pointing sensors. *Photogrammetric Engineering and Remote Sensing,* 46, 9, 1191-1200.

Holben B.N. and Justice C.O. (1981), An examination of spectral band ratioing to reduce the topographic effect on remotely sensed data. *International Journal of Remote Sensing,* 2, 2, 115-133.

Horler D.N.H. and Ahern F.J. (1986), Forestry information content of Thematic Mapper data. *International Journal of Remote Sensing,* 7, 3, 405-428.

Horn B.K. (1981), Hill shading and the reflectance map. *Proceedings of the IEEE,* 69, 1, 14-47.

Huber T.P. and Casler K.E. (1990), Initial analysis of Landsat TM data for elk habitat mapping. *International Journal of Remote Sensing,* 11, 5, 907-912.

Hugli H. and Frei W. (1983), Understanding anisotropic reflectance in mountainous terrain. *Photogrammetric Engineering and Remote Sensing,* 11, 5, 907-912.

Hutchinson C.F. (1982), Techniques for combining Landsat and ancillary data for digital classification improvement. *Photogrammetric Engineering and Remote Sensing,* 48, 2, 123-130.

Ingebritsen S.E. and Lyon R.J.P (1985), Principal components analysis of multitemporal pairs. *International Journal of Remote Sensing,* 6, 5, 687-696.

Itten K. I. and Meyer P. (1993), Geometric and radiometric correction of TM data of mountainous forested areas. *IEEE transactions on geosciences and remote sensing,* 31,4, 764-770.

Jensen J.R. (1986), *Introductory digital image processing: a remote sensing perspective,* first edition, Prentice-Hall.

Jones A.R., Settle J.J. and Wyatt B.K. (1988), Use of digital terrain data in the interpretation of PSOT-1 HRV multispectral imagery. *International Journal of Remote Sensing,* 9, 4, 669-682.

Jupp D.L.B. and Mayo K.K. (1982), The use of residual images in landsat image analysis. *Photogrammetric Engineering and Remote Sensing,* 48, 4, 595-604.

Justice C.O., Wharton S.W. and Holben B.N. (1981), Application of digital terrain data to quantify and reduce the topographic effect on Landsat data. *International Journal of Remote Sensing,* 2, 3, 213-30.

Karaska M.A., Walsh S.J. and Butler D.R. (1986), Impact of environmental variables on spectral signatures acquired by the Landsat Thematic Mapper. *International Journal of Remote Sensing,* 7, 1653-1667.

Kauth R.J. and Thomas G.S. (1976) The tasseled cap: a graphic description of the spectral-temporal development of agricultural crops as seen by Landsat. *Proceedings of the Symposium on machine processing of remotely sensed data,* Purdue University, Indiana, 4B41-4B51.

Kimes D.S. and Kirchner J.A. (1981) Modeling the effects of various radiant transfers in mountainous terrain on sensor response. *IEEE Transactions on Geoscience and Remote Sensing,* 19, 2, 100-108.

Knepper D.H. and Rames G.L. (1985), Determining stretch parameters for lithological discrimination on Landsat MSS band ratio images. *Photogrammetric Engineering and Remote Sensing,* 51, 1, 63-70.

Kowalik W.S., Lyon R.J.P. and Switzer P. (1983) The effects of additive radiance terms on ratios of Landsat data. *Photogrammetric Engineering and Remote Sensing,* 49, 5, 659-669.

Leprieur C.E., Durand J.M. and Peyron J.L. (1988), Influence of topography on Forest Reflectance Using Landsat Thematic Mapper and Digital Terrain Data. *Photogrammetric Engineering and Remote Sensing,* 54, 4, 491-496.

Lodwick G.D. (1981), Topographic mapping using Landsat mapping. *Proceedings of the 15th International Symposium on remote sensing of the environment,* Ann Arbor, May 1981, 529-534.

Lodwick G.D. and Harrington R.D. (1985), Deriving sediment information for Lake Athabasca using principal components analysis of Landsat Data. *Canadian Journal of Remote Sensing,* 11, 1, 4-16.

Lodwick G.D. and Paine S.H. (1985), A digital elevation model of the Barnes ice-cap derived from Landsat MSS data. *Photogrammetric Engineering and Remote Sensing,* 51, 12, 1937-1944.

Lodwick G.D., Paine S.H., Mepham M.P. and Colijn A.W. (1986), A comprehensive LRIS of the Kananaskis Valley using Landsat data. *Symposium on remote sensing and environmental management,* Enschede, Netherlands, August 1986, 927-932.

Lodwick G.D., Franklin S.E. and Wheate R.D. (1991), Research related to digital remote sensing of mountain areas at the University of Calgary. *Canadian Journal of Remote Sensing,* 17, 2, 156-160.

Loughlin W.P. (1991), Principal components analysis for alteration mapping. *Photogrammetric Engineering and Remote Sensing,* 57, 9, 1163-1169.

Mackiewicz A. and Ratajczak W. (1993), Principal components analysis (PCA). *Computers and Geoscience,* 19, 3, 303-342.

Mather P.M. (1987), *Computer Processing of Remotely-Sensed Images,* Wiley, chapter 6: Image transforms.

McCechan M.E. (1988), Geology of the Kananaskis Valley, *Geological Survey of Canada,* Report number 5341.

Meyer P., Itten K.I., Kellenberger T, Sandmeier S. and Sandmeier R. (1993), radiometric correction of topography induced effects on Landsat TM data in an alpine environment. *ISPRS Journal of Photogrammetric Engineering and Remote Sensing,* 48, 4, 17-28.

Minnaert N. (1941), The reciprocity principle in lunar photometry. *Astrophysics Journal,* 93, 403-410.

Moulton J.E. (1989), Terrain classification using Landsat thematic mapper and digital topographic data in the Burash uplands, southwest Yukon. *Unpublished M.Sc. thesis,* Memorial University of Newfoundland.

Naugle B.I. and Lashlee J.D. (1992), Alleviating topographic influences on land-cover classifications for mobility and combat modelling. *Photogrammetric Engineering and Remote Sensing,* 58, 8, 1217-1221.

Niemann K.O. (1991), Landscape Drainage Modelling to Enhance Landsat classification accuracies. *GeoCarto International,* No. 1, 13-30.

Paine S.H. (1984), Using Landsat imagery for position-based surface cover mapping in the Rocky Mountains. *Canadian Journal of Remote Sensing,* 10, 2, 190-200.

Paine S.H. (1987), Information extraction from digital Landsat imagery for integration into an LRIS. *Unpublished Ph.D thesis,* University of Calgary.

PCI User's manual (1995), PCI Toronto.

Pinter P.J., Zipoli G, Maracchi G. and Reginato R.J. (1987), Influence of topography and sensor view angles on NIR/red ratio and greenness vegetation indices of wheat. *International Journal of Remote Sensing,* 8, 6, 953-957.

Robinove C.J. (1982), Computation with physical values from Landsat digital data. *Photogrammetric Engineering and Remote Sensing,* 48, 5, 781-784.

Rowan L.C., Goetz A.F.H. and Ashley R.P. (1977), Discrimination of hydrothermally altered and unaltered rocks in visible and near infrared multispectral images. *Geophysics,* 42, 3, 522-535.

Qari M.Y.H.T. (1991), Application of Landsat data to geological Studies, Al-Khabt Area, Southern Arabian Shield. *Photogrammetric Engineering and Remote Sensing,* 57, 4, 421- 429.

Richards J.A (1984), Thematic mapping from multitemporal image data using the principal components transformation. *Remote Sensingof Environment,* 15, 35-46.

Sheffield C. (1985), Selecting band combinations from multispectral data. *Photogrammetric Engineering and Remote Sensing,* 51, 6, 681-687.

Sidjak R.W and Wheate R.D. (1996), Mapping the Illecillewaet Glacier, B.C., using Landsat and digital elevation data. *Proceedings of the 4th Circumpolar Symposium on remote sensing of the environment,* Lyngby, Denmark (in press).

Siegal B.S. and Abrams M. (1976), Geologic mapping using Landsat data. *Photogrammetric Engineering and Remote Sensing,* 42, 3, 325-337.

Siegel B.S. and Gillespie A.R. (1980), *Remote Sensing in Geology,* Wiley.

Singh A and Harrison A. (1985), Standardised principal components. *International Journal of Remote Sensing,* 6, 6, 883-896.

Sjoberg R.W. and Horn B.K. (1983), Atmospheric effects in satellite imaging of mountainous terrain. *Applied Optics,* 22, 11, 1702-1716.

Smart A.J. (1992), Multiple hazard research in Kananaskis Country, Alberta: a geographical systems approach. *Unpublished M.Sc. thesis,* Wilfrid Laurier University.

Smith J.A., Lin T.L. and Ranson K.J. (1980), The Lambertian assumption and Landsat data. *Photogrammetric Engineering and Remote Sensing,* 46, 9, 1183-1189.

Strahler A.H., Logan T.L. and Bryant N.A. (1978), Improving forest cover classification accuracy from Landsat by incorporating topographic information. *Proceedings of the Twelfth International Symposium on Remote Sensing of Environment,* 927-942.

Switzer P., Kowalik W.S. and Lyon R.J.P. (1981), Estimation of atmospheric path-radiance by the covariance matrix method. *Photogrammetric Engineering and Remote Sensing,* 47, 10, 1469-1476.

Teillet P.M., Guindon B., Goodenough D.G. (1982), On the slope-aspect correction of multispectral scanner data. *Canadian Journal of Remote Sensing,* 8,2, 84-102.

Thomas J., Kober W. and Leberl F. (1991), Multiple image SAR shape-from-shading. *Photogrammetric Engineering and Remote Sensing,* 57, 1, 51-59.

Thomson A.G. and Jones C. 1990, Effects of topography on radiance from upland vegetation in North Wales, *International Journal of Remote Sensing,* 11, 5, 829-840.

Townshend J.R.G, Gayler J.R., Hardy J.R., Jackson M.J. and Baker J.R. (1983), Preliminary analysis of Landsat - 4 Thematic Mapper products. *International Journal of Remote Sensing,* 4, 4, 817-828.

Townshend J.R.G (1984), Agricultural land-cover discrimination using thematic mapper spectral bands. *International Journal of Remote Sensing,* 5, 4, 681-698.

Vogelmann J. E. and Rock B.N. (1986), Assessing forest decline in coniferous forests of Vermont using NS-001 Thematic Mapper simulator data. *International Journal of Remote Sensing,* 7, 1303-1321.

Walsh S.J. (1987) Variability of Landsat MSS spectral responses of forests in relation to stand and site characteristics. *International Journal of Remote Sensing,* 52, 9, 1289-1299.

Walsh S.J., Cooper J.W., Von Essen I.E. and Gallager K.R. (1990), Image enhancement of Landsat Thematic Mapper data and GIS data integration for evaluation of resource characteristics. *Photogrammetric Engineering and Remote Sensing,* 56, 8, 1135-1142.

Wang S., Haralick R.M. and Campbell J. (1984), Relative elevation determination from Landsat imagery. *Photogrammetria,* 39, 193-215.

Wheate R.D. (1988), PC-based GIS and image processing systems. *Photogrammetric Engineering and Remote Sensing,* 54, 10, 1473-76 (reprinted from *Newsletter of the Canadian Cartographic Association,* 14, 2, 12-15).

Wheate R.D. and Franklin S.E. (1991), Principal component transformation of satellite imagery in mountainous areas. *Proceedings, 14th Canadian Symposium on Remote Sensing,* 452-456.

Wheate R.D. (1996), Re-examining the cartographic depiction of topography. Chapter 12 in *Cartographic design: theoretical and practical perspectives,* editors: C. H. Wood and C. P. Keller, Wiley.

Williams J.A. (1990), Vegetation inventory of the Spray, Opal and Kananaskis Ranges. *Unpublished report,* Province of Alberta.

Williams J.A. (1992), Vegetation classification using Landat TM and SPOT-HRV imagery in mountainous terrain, Kananaskis Country, southwestern Alberta. *Unpublished M.Sc. thesis,* University of Calgary.

Woodcock C.E. and Strahler A.H. (1987), the factor of scale in remote sensing. *Remote Sensing of Environment,* 21, 311-332.

Wolter P.T., Mladenoff D. J., Host G.E. and Crow T.R. (1995), Improved forest clasification in the Northern Lake States using multi - temporal Landsat imagery. *Photogrammetric Engineering and Remote Sensing,* 61, 9, 1129-1143.

Woodham R.J. (1989), Determining intrinsic reflectance in rugged terrain and changing illumination. *Proceedings of the Twelfth Canadian Symposium on Remote Sensing / IGARSS '89,* 1-5.

Woodham R.J. and Gray M.H. (1987) An analytical method for radiometric correction of satellite multispectral scanner data. *IEEE Transactions on Geoscience and Remote Sensing,* 25,3, 258-271.

Yool S.R., Star J.L., Estes J.E., Botkin D.B., Eckhardt D.W. and Davis F.W. (1986), Performance analysis of image processing algorithms for classification of natural vegetation in the mountains of Southern California. *International Journal of Remote Sensing,* 7, 5, 683-702.